On the investigation of alcohol synthesis *via* the Fischer Tropsch reaction

Thesis submitted for the degree of Doctor of Philosophy

by

Yanjun Zhao

Department of Chemistry

Cardiff University

April 2007

ProQuest LLC
789 East Eisenhower Parkway
P.O. Box 1346
Ann Arbor, MI 48106-1346

DECLARATION

This work has not previously been accepted in substance for any degree and is not being concurrently submitted in candidature for any degree.

Signed ..zhao yz.. (candidature) Date ..23/04/2007

STATEMENT 1

This thesis is being submitted in partial fulfilment of the requirements for the degree of PhD.

Signed ..zhao yz.. (candidature) Date ..23/04/2007

STATEMENT 2

This thesis is the result of my own independent investigation, except were otherwise stated. Other sources are acknowledged by footnotes giving explicit references. A bibliography is appended.

Signed ..zhao yz.. (candidature) Date ..23/04/2007

STATEMENT 3

I hereby give consent for my thesis, if accepted, to be available for photocopying and for inter-library loan, and for the title and summary to be made available to outside organisations.

Signed ..zhao yz.. (candidature) Date ..23/04/2007

STATEMENT 4 BAR ON ACCESS APPROVED

I hereby give consent for my thesis, if accepted, to be available for photocopying and for inter-library loans **after expiry of a bar on access approved by the Graduate Development Committee.**

Signed ..zhao yz.. (candidature) Date ..23/04/2007

Abstract

The Fischer Tropsch (FT) reaction is hydrogenation of carbon oxides (mainly carbon monoxide) to produce hydrocarbons and alcohols. The produced alcohols can be used as substitutes to motor fuel or as fuel additives to enhance the octane number. The use of alcohols significantly reduces the environment related pollution. This thesis was aimed to investigate the alcohol synthesis *via* the FT reaction.

Cobalt molybdenum based catalyst and cobalt copper based mixed oxide catalyst are two patented catalyst systems for alcohol synthesis. This study investigated the preparation and evaluation of these two catalyst systems. The highest activity (30% CO conversion) and alcohol yield (methanol: 8%; higher alcohols: 13%) was obtained with an operation condition of 580 K, 75 bar, GHSV = 1225 h^{-1} and syngas ratio of 2 for cobalt molybdenum based catalyst.

Carbon monoxide hydrogenation to synthesize alcohol was also investigated over gold containing catalyst. When ZnO was used as a support, it was found that the addition of gold could shift the alcohol distribution towards higher alcohol side.

The carbon monoxide and hydrogen used for the FT reaction is mainly generated by steam reforming reaction. This thesis investigated the possibility of combining the steam reforming reaction and the FT reaction together. Ruthenium supported catalysts were investigated for this purpose. The obtained results demonstrate that both steam reforming and the FT alcohol synthesis can be performed over the same catalyst in the same reactor.

Acknowledgements

I would like to thank the following people to make this project possible.

Firstly, I would like to thank my academic supervisors Professor Graham Hutchings for his support, guidance and encouragement throughout this project, and Dr. Stuart Taylor for always being there to help in the research as well as in many difficult situations with his optimism. Thanks to my industrial supervisor Dr. Martin Atkins (BP Chemicals), for his keen interest in the project and help in many occasions.

I also would like to thank Dr. Philip Landon and Dr. Dan Enache, two extraordinary scientists for their help in this project. Their help makes this project run smoothly.

Thanks to Dr. Nianxue Song for his help in my research. Thanks to Chunli, Hongmei for helping me at the beginning of my time in Cardiff. Thank to all the members of Professor Hutchings' research group (past and present) for sharing their knowledge and experience with me.

Thanks to Pat for her help in all occasions. Thanks to Rob Jenkins for the help in the GC-MS and to store staff Gary, Mal for always being so sensitive and happy.

Thanks to my parents, brother, sister in law and my niece for the encouragement, patience and endless love during all these years.

Finally, I would like to thank my boyfriend Pablo for sharing the beauty of life with me and for making my life full of happiness.

On the investigation of alcohol synthesis *via* the Fischer Tropsch reaction

Table of contents

Chapter 1 Introduction

1.1 General introduction of the Fischer Tropsch synthesis

The world economy as we know has a strong dependence on energy resources. A recent review [1] estimates that 80% of the global energy consumption proceeds from fossil fuels, which include oil, natural gas and coal. These fuels are unsustainable and estimated availabilities at current rate of production are: 40 years for oil, 65 years for natural gas and 155 years for coal. In contrast to the limited resources, world demands for energy, particularly for oil, are increasing markedly as a consequence of the growing population and the world development. More than 60% of oil is consumed in the transportation sector in the form of gasoline, diesel and jet fuel. The remaining oil is used mainly for the production of petrochemicals including plastics, solvents, fertilizers and pesticides, and the production of electricity. In the foreseeable future, the transportation industry is expected to remain highly dependent on oil.

The limited natural reserves of oil combined with the increasing demand will drive the world rapidly to peak production and consumption, after which a permanent

shortage of oil can be expected. Hence, an alternative route for generating transportation fuel is highly desirable. The Fischer Tropsch (FT) process is one of the processes that are being developed [2] to offer a solution to this problem.

The FT process is a method developed to utilize some types of fuel reserves other than oil, e.g. coal, natural gas and biomass, and transform them to synthetic fuels by passage over an appropriate catalyst. Synthetic fuels mainly include gasoline, diesel, wax and oxygenates. Among them, liquid fuels have significant application in transportation industry. Bearing this in mind, FT technology can be classified according to the syngas used as follows: coal to liquid (CTL), gas to liquid (GTL) and biomass to liquid (BTL).

1.2 FT technology

1.2.1 Historical background

The FT process was discovered by two German scientists, Franz Fischer and Hans Tropsch in 1923. The process was intensively investigated and widely employed to produce liquid hydrocarbons in Germany during World War II. By 1944, there were nine plants in operation using cobalt based catalysts in Germany with a capacity of 700,000 tonnes of hydrocarbons per year. In the mid 1950's, the plants in Germany were shut down. With plenty of cheap oil supply from middle-east, only marginal interest was left in the FT synthesis except in South Africa.

Strategic reasons led a world leading company, Sasol, to invest a considerable amount of resources in a project called 'Sasol I', consisting mainly of producing liquid fuel from coal over iron based catalysts. This project commenced commercially in 1955. Following the success of Sasol I, subsequent plants Sasol II and III came into

operation in 1980 and 1982 respectively, which enabled South Africa to be partially independent from oil imports.

The oil crisis and fear of oil shortages in mid 1970's revived interest in the FT process across the world. For example, Statoil (Norway) developed a Gas to Middle Distillates (GMD) process in the mid/late 1980's that has been in operation since then.

Recent major processes developed by companies, such as Sasol and Shell are focused mainly on the natural gas related FT technology, and this topic is addressed in a later section of this chapter.

In general, interest in the FT process and its development are strongly influenced by the price and the accessibility of petroleum oil.

1.2.2 Chemistry involved in the overall FT process

Syngas

The FT process, strictly speaking, consists of three steps which are syngas generation, the FT synthesis and product up-grade. Currently capital cost in syngas generation is the major contributor to the cost of the FT process.

Syngas, also called synthesis gas, which consists of a mixture of carbon oxides (mainly carbon monoxide) and hydrogen, is the starting material for FT synthesis. It can be obtained from different resources. For example, it can be derived from coal or biomass by gasification process. It also can be obtained from natural gas by several processes: steam reforming, dry (CO_2) reforming, partial oxidation (POX) or autothermal reforming (ATR). Reactions involved in generating syngas from coal and

natural gas are shown in Table 1.1. With proven reserves of coal and natural gas, the FT process could provide a solution for the oil crisis, at least in the short term.

The quality of syngas is normally closely related to its source. Syngas obtained from coal has a high percentage of sulfur which is detrimental to FT synthesis. Syngas produced from natural gas, however, is sulfur-free or has a relatively low content. Normally, a de-sulfurization unit is employed to remove sulfur compounds from syngas if necessary.

Table 1.1 Syngas generation processes

Process	Equation	ΔH^{Θ}_{298} (kJ·mol^{-1})	
Coal gasification	$C + H_2O \leftrightarrow CO + H_2$	131	(1.1)
Steam reforming of methane	$CH_4 + H_2O \leftrightarrow CO + 3H_2$	206	(1.2)
CO_2 reforming of methane	$CH_4 + CO_2 \leftrightarrow 2CO + 2H_2$	247	(1.3)
Methane partial oxidation	$CH_4 + \frac{1}{2}O_2 \leftrightarrow CO + 2H_2$	-38	(1.4)
Autothermal reforming	$2CH_4 + \frac{1}{2}O_2 + H_2O \leftrightarrow 2CO + 5H_2$	168	(1.5)

The FT synthesis

By definition, the FT synthesis is hydrogenation of carbon oxides (carbon monoxide and/or carbon dioxide) generating higher hydrocarbons and/or alcohols [3]. Small amounts of other oxygenates such as aldehydes, acids, ketones and esters may also appear in product stream. The main reactions involved in the synthesis of hydrocarbons and alcohols are shown in Table 1.2.

The enthalpies of formation per carbon of hydrocarbons and alcohols at different temperatures have high negative values (Table 1.3). This indicates that the FT synthesis of hydrocarbons and alcohols from syngas is highly exothermic. From

Table 1.3, it can also be seen that the formation of alcohols becomes more exothermic with increasing carbon number.

Table 1.2 Main reactions involved in the FT synthesis

Products	Equation	
1-paraffins	$(2n+1)H_2 + nCO \leftrightarrow C_nH_{2n+2} + nH_2O$	(1.6)
α-olefins	$2nH_2 + nCO \leftrightarrow C_nH_{2n} + nH_2O$	(1.7)
alcohols	$2nH_2 + nCO \leftrightarrow C_nH_{2n+1}OH + (n-1)H_2O$	(1.8)

Table 1.3 Enthalpies of formation of hydrocarbons and alcohols per carbon for reactions listed in table 1.2 (original data used for calculation from ref. 4)

Product	$\Delta rH^{\ominus}$ (kJ mol^{-1})			
	298 K	300 K	500 K	700 K
1-paraffins				
CH_4	-206	-206	-215	-221
C_2H_6	-174	-174	-181	-185
C_3H_8	-166	-166	-172	-176
C_4H_{10}	-163	-163	-169	-173
α-olefins				
C_2H_4	-105	-105	-111	-114
C_3H_6	-125	-125	-130	-133
C_4H_8	-131	-131	-137	-140
alcohols				
CH_3OH	-91	-91	-98	-102
C_2H_5OH	-128	-128	-134	-137
1-C_3H_7OH	-137	-137	-142	-146
1-C_4H_9OH	-140	-140	-145	-148

For exothermic reactions, great attention has to be paid to heat removal and thermal control. Poor heat removal and thermal control are often accompanied by local overheating of the catalyst, resulting in hot spots, catalyst deactivation and short catalyst lifetime. These factors can have a significant impact on the conversion of carbon oxide(s) and selectivity to final products. For example, excessive unwanted methane formation is one of the consequences of inadequate heat removal [3, 5].

Another feature of exothermic reactions is that lower temperature is preferred. This is because that by applying Le Chatelier's principle, lower temperature can drive the equilibrium towards products. However, the temperature required for the FT reaction can not be too low since the temperature has to be high enough to provide a sufficient reaction rate.

By following the Le Chatelier's principle, it can also be seen that the FT synthesis is favored by high pressure because this reaction involves a reduction in the number of molecules. However, too high a pressure could significantly increase the capital cost of the reactor system including reaction vessel, pipeline *etc.*

Side reactions

In most instances, FT synthesis is accompanied by side reactions which occur at different levels (Table 1.4). Carbon produced by some of the side reactions may have a detrimental effect on the catalyst performance by blocking the active sites of the catalyst, e.g. carbide formation.

Table 1.4 Possible side reactions accompanying FT synthesis

Process	Equation	
Water gas shift	$CO + H_2O \leftrightarrow CO_2 + H_2$	(1.9)
Methane decomposition	$CH_4 \leftrightarrow C + 2H_2$	(1.10)
Boudouard reaction	$2CO \leftrightarrow C + CO_2$	(1.11)
CO reduction	$CO + H_2 \leftrightarrow C + H_2O$	(1.12)
Metal carbide formation	$xM + C \leftrightarrow M_xC$	(1.13)

Product distribution

Hydrocarbons and alcohols produced by the FT process can be used as synthetic fuels. Hydrocarbon products cover a broad range of chemicals including fuel gas (C_1-C_2), LPG (C_3-C_4), gasoline (C_5-C_{12}), diesel oil (C_{13}-C_{17}), middle distillates

(C_{10}-C_{20}) and wax (C_{19+}). Alcohol products mainly consist of C_1 to C_6 alcohols. The composition of the FT product is dependent on the catalyst formulation as well as the operating conditions employed. FT diesel can be used in existing diesel engines and is also compatible with the existing infrastructure. FT alcohols, typically higher alcohols, can be used as fuel additives to boost the octane number.

Anderson [6] reported that the distribution of products follows the so-called Anderson-Schulz–Flory (ASF) equation which is based on the assumption that FT synthesis is a polymerization process.

$$\frac{W_n}{n} = \frac{(1-\alpha)^2}{\alpha}\alpha^n \tag{1.14}$$

Where n is the carbon number, Wn is the weight fraction of products with carbon number n, and α is the chain growth probability factor which can be defined as follows:

$$\alpha = \frac{r_p}{r_p + r_t} \tag{1.15}$$

Where r_p and r_t are the rate of chain growth and rate of chain termination respectively. Both rates are controlled by the reaction conditions and catalyst type. Typical ranges of α on Ru, Co and Fe catalysts were reported as 0.85 – 0.95, 0.70 – 0.80, and 0.50 – 0.70 respectively by Dry [7]. The higher the value of α, the longer the chain length is.

For practical reasons, equation (1.14) is often re-written as:

$$\log\frac{W_n}{n} = n\log\alpha + \log\frac{(1-\alpha)^2}{\alpha} \tag{1.16}$$

A plot of $\log\frac{W_n}{n}$~n is the well-known Schulz-Flory diagram. It gives a linear plot with a slope of $\log\alpha$.

Experimental data that deviates from the ASF distribution usually have C_1 yields that are higher than the predicted value and have $C_{>2}$ yield that are lower. Schulz and co-workers [8] explained the high methane yield by assuming that there was a different catalytic site for the methanation reaction, whereas Dry *et al.* [7] suggested heat and mass transfer limitations could result in thermodynamically favored products.

Product distribution is also affected when secondary reactions, such as hydrogenation, isomerization, reinsertion and hydrogenolysis are involved [9-13]. So far, there has been no single model that can explain all the observed catalytic results.

FT products are better able to meet the increasingly tighter demands of laws designed to protect the environment. Compared with conventional refinery fuel, the FT fuel is essentially sulfur and aromatic free (except for high temperature processes) and has low nitrogen content, releasing much lower emissions of principle pollutants, such as CO, CO_2, SO_2, and NO_x and with little or no particulate emission. FT alcohols have a higher octane rating than hydrocarbons and thus can burn more completely which dramatically decreases environmental pollution.

1.2.3 Reactors for FT synthesis

Reactor design in FT synthesis is very closely related to the highly exothermic nature of the reaction. Since poor heat removal leads to rapid temperature build up inside the reactor resulting in high selectivity towards unwanted methane, heat transfer is a priority in designing an FT reactor. Other considerations include capital cost for construction and operation, ease of loading/unloading catalysts, capacity/productivity, ease of product separation, and product selectivity.

There are three main types of reactor that have been developed for FT synthesis: the tubular fixed bed reactor, the fluidized bed reactor and the slurry bed reactor.

(1) Tubular fixed bed reactor

The tubular fixed bed reactor is the simplest reactor type (Figure 1.1.a). Typically the catalyst is packed inside the reactor tube(s) with syngas flowing through from top to bottom. The reaction products are collected at the bottom. Heat removal is achieved by circulating cooling medium outside of the tubes. The fixed bed reactor is easy to operate and scale-up, however, it has a relatively low capacity. Catalyst replacement is very labor intensive. Pressure drop along the bed may be experienced as well as diffusion limitations. The first well studied commercial reactor, the Sasol Arge reactor belongs to the tubular fixed bed reactor type. Shell's Middle Distillate Synthesis (SMDS) process in Malaysia also employs this reactor type.

(2) Fluidized bed reactor

There are mainly two kinds of fluidized bed reactor: the circulating fluidized bed (CFB) reactor and the fixed fluidized bed (FFB) reactor.

In the circulating fluidized bed reactor (Figure 1.1.b), the catalyst is initially dropped down by gravity, and then mixed with feed gas and circulated through the reactor zone. The temperature of the reaction is maintained at the desired level by a cooling medium. Following the reaction zone, the mixture of feed gas, products and catalyst is passed to the hopper where products are separated out and lost catalyst is replaced. The operation of a CFB reactor is much more complicated than that of a fixed bed reactor. However, the CFB reactor provides better temperature control and a lower pressure drop compared to the fixed bed reactor. It also has the advantage of

online removal/addition of catalyst. A typical example of a CFB reactor is Sasol's Synthol reactor.

The fixed fluidized bed (FFB) reactor (Figure 1.1.c) is simpler than the CFB reactor. Feed gas is introduced to the reactor from the bottom of the reactor and flows upwards through catalyst bed. The catalyst bed and heat exchanger are 'suspended' inside the reactor. The products are collected from the top of the reactor. An FFB reactor was used at Brownsville (Texas) by Hydrocol. A recent example is Sasol's SAS (Sasol Advanced Synthol) reactor which is based on this technology.

The fluidized bed reactor has a much higher capacity than that of a fixed bed one. However, both the CFB reactor and the FFB reactor are more difficult to scale-up than the fixed bed reactor due to the complexity of gas-solid contacting as a function of reactor diameter. Furthermore, they require the desired products to have low molecular weight and volatility.

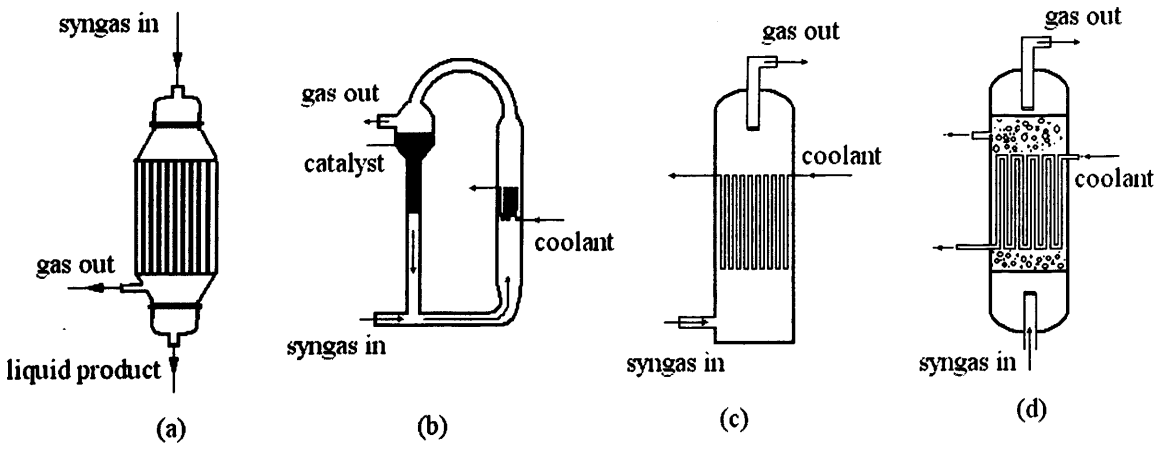

Figure 1.1 Types of FT reactors a) Tubular fixed bed reactor; b) Circulating fluidized bed reactor; c) Fixed fluidized bed reactor; and d) Slurry reactor

(3) Slurry reactor

The slurry reactor (Figure 1.1.d) is similar to the FFB reactor except that syngas bubbles up through a suspended mixture consisting of catalyst and liquefied hydrocarbon wax. The slurry reactor has the advantage of large single reactor capacity. It also provides excellent heat transfer, which leads to better selectivity control. Most companies nowadays employ this type of reactor, such as Sasol's SSPD (Sasol slurry phase distillate) process and Exxon's AGC-21 project. Other companies using this reactor type include Rentech, Statoil and Conoco Phillips *etc.* In all these cases, the technology details have not been revealed to the public so far.

1.2.4 Thermodynamics for the FT synthesis

The thermodynamic constraints of these reactions are described in Figure 1.2 which shows Gibbs free energy as a function of temperature.

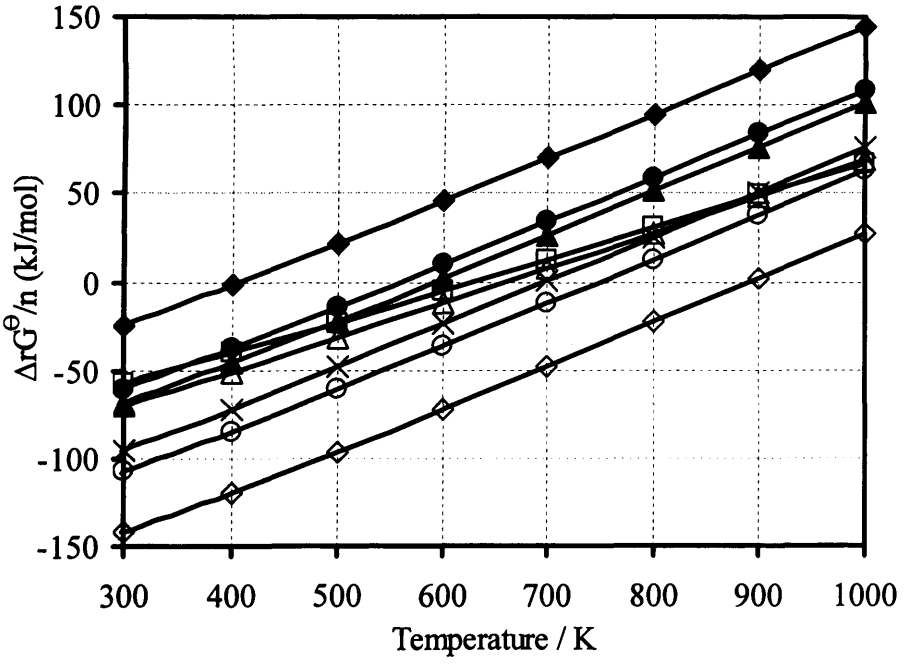

Figure 1.2 Standard free Gibbs energies of reaction per carbon of the product in equations (1.6-1.8) as a function of temperature ◊ Methane; □ Ethene; ○ Ethane; Δ Propene; × Butane; ♦ Methanol; ● Ethanol; ▲1-Propanol

The conversion of a reaction at equilibrium can be calculated according to the equilibrium constant obtained from equation (1.17). It can be seen that at a fixed temperature the conversion is directly related to the Gibbs free energy of reaction.

$$K = \exp\frac{-\Delta_r G^{\ominus}}{RT} \tag{1.17}$$

At a low temperature range (<400 K), most of standard Gibbs free energies of reactions are negative, which indicates the process is thermodynamically favorable at this condition. Unfortunately the reaction rate is so low that, as a consequence, the FT reaction does not spontaneously produce large amount of 'petroleum'. Industrial FT synthesis is carried out at certain temperatures over catalysts which accelerate the reaction rate by modifying the kinetics of the catalyzed system by opening alternative mechanistic pathways. FT synthesis involves a decrease in the number of moles of the system when the forward reaction proceeds, suggesting that the obtained equilibrium can be driven to the product side through the action of Le Chatelier's law by applying high pressure. In this sense, industrial FT synthesis is a highly regulated reaction to produce 'petroleum'.

From the thermodynamic data, it can be seen that in general, changes in the standard Gibbs free energy for the formation of methane are the most negative compared to the formation of other hydrocarbons and alcohols. Therefore, in most cases, methane is one of the major components of the FT product when the system reaches its equilibrium.

With increasing temperature, standard Gibbs free energy of reaction becomes less negative, leaving the reaction more kinetically than thermodynamically controlled.

A comparison of the Gibbs free energy of formation of hydrocarbons and alcohols at 600K is displayed in Figure 1.3. These data indicate that hydrocarbons are

more thermodynamically favored than alcohols. In order to obtain the thermodynamically un-favored alcohol product, an alternative reaction pathway for alcohol synthesis with lower activation barriers has to be created, which requires careful selection of catalyst and reaction parameters.

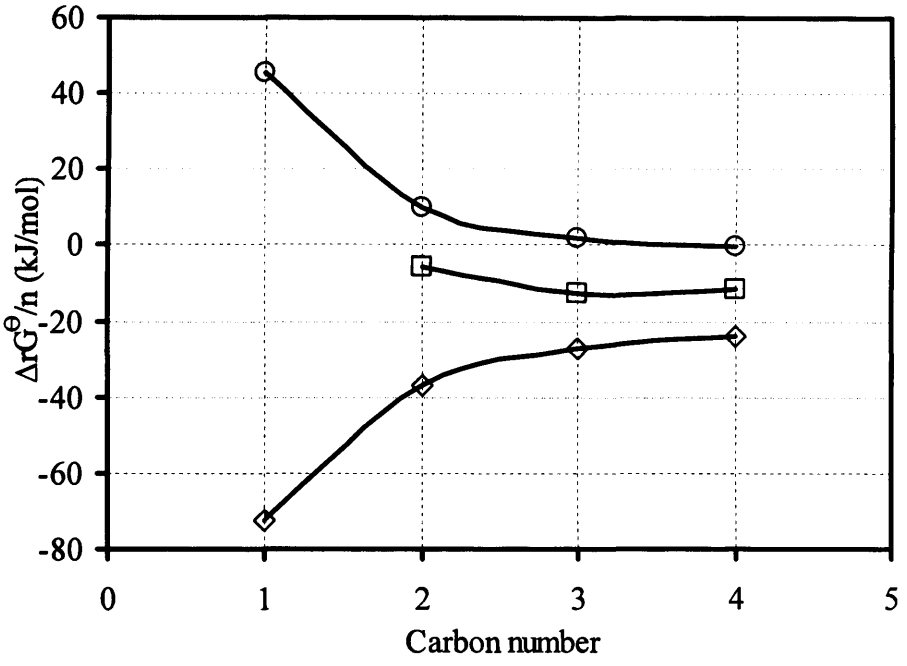

Figure 1.3 Standard free Gibbs energies of reaction per carbon of the product in equations [1.6-1.8] at 600K as function of carbon number. ○ Alcohols; □ α-olefins; ◊ 1-paraffins

1.2.5 Mechanism of the FT synthesis

Since the FT synthesis involves a wide range of products, the intrinsic mechanism is very complex. To date, the exact mechanism is still under debate. The mechanism of the synthesis of hydrocarbons and alcohols has been reviewed by several research groups [2, 3, 14-17].

The FT synthesis has been recognized as a polymerization process following these steps: reactant adsorption; chain initiation; chain growth; chain termination;

product desorption and re-adsorption for further reaction. With so many mechanisms suggested so far, this section describes the most popular mechanisms.

(1) Carbide mechanism

The carbide mechanism was first proposed by Fischer and Tropsch [18]. They suggested that the CO molecule was dissociated into carbon and oxygen and chemisorbed on the catalyst surface forming surface carbide. The surface carbide was then hydrogenated to M-CH_x species. The chain growth was realized by insertion of two adjacent CH_x species into the metal-carbon bond. The carbide mechanism was challenged when direct hydrogenation of metal carbide was investigated by Kummer *et al.*[19] using labeled ^{14}CO over reduced iron catalysts. Their results show that the carbide hydrogenation could be responsible for no more than 8 – 30% of the methane formed. Another limitation of the carbide mechanism is that it could not explain the formation of oxygenated products.

Development of surface science instruments led to a revival of the carbide mechanism. When CO adsorbs on a single crystal metal surface, it was found that carbon was produced on the catalyst surface but little oxygen. These findings indicated restricted carbide formation on the metal surface [20, 21].

(2) Hydroxy-carbene mechanism

The hydroxy-carbene mechanism was proposed by Storch *et al.*[22]. This mechanism assumes that CO chemisorbs on the metal atoms without dissociation. The adsorbed CO undergoes partial hydrogenation giving an M-CHOH species. Chain growth, carbon-carbon bond formation is achieved by condensation of two adjacent hydroxyl-carbene groups. One simple illustration of this mechanism is shown in Figure 1.4. This model successfully explains the formation of both hydrocarbons and alcohols and thus was supported by several research groups [23-27].

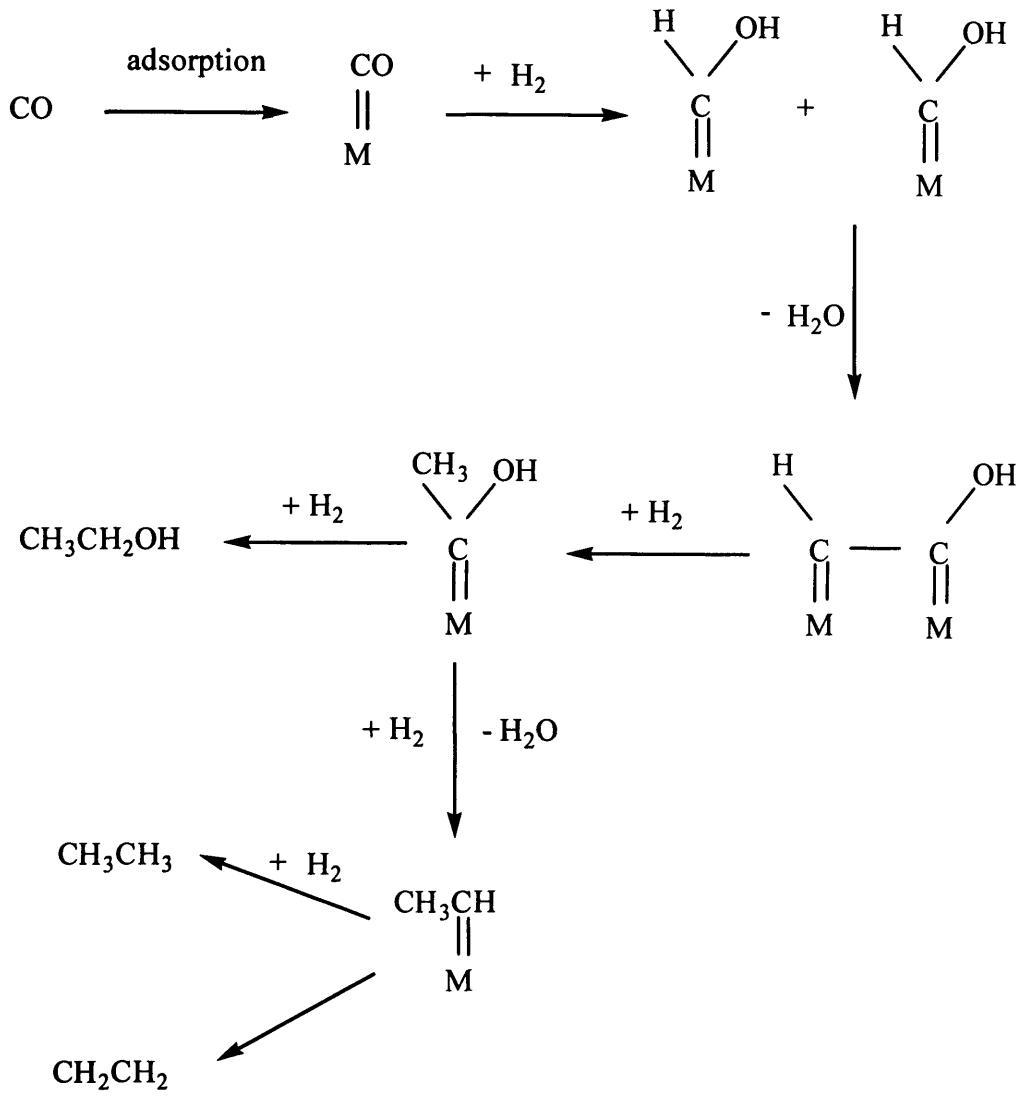

Figure 1.4 The hydroxy-carbene mechanism

(3) CO insertion mechanism

The CO insertion mechanism was proposed by Pichler and Schulz [28]. The mechanism suggests that the CO molecule does not dissociate but is incorporated into an M-H or M-C bond, forming a metal carbonyl which is the main intermediate involved in the FT synthesis. The metal carbonyl then reacts with hydrogen to form a metal-alkyl species. Chain growth is achieved by insertion of a CO molecule into the metal-alkyl bond and subsequent reduction of the acyl species. A variety of products including hydrocarbons and oxygenates can be obtained following desorption of the

intermediates. A scheme illustrating the CO insertion mechanism is shown in Figure 1.5.

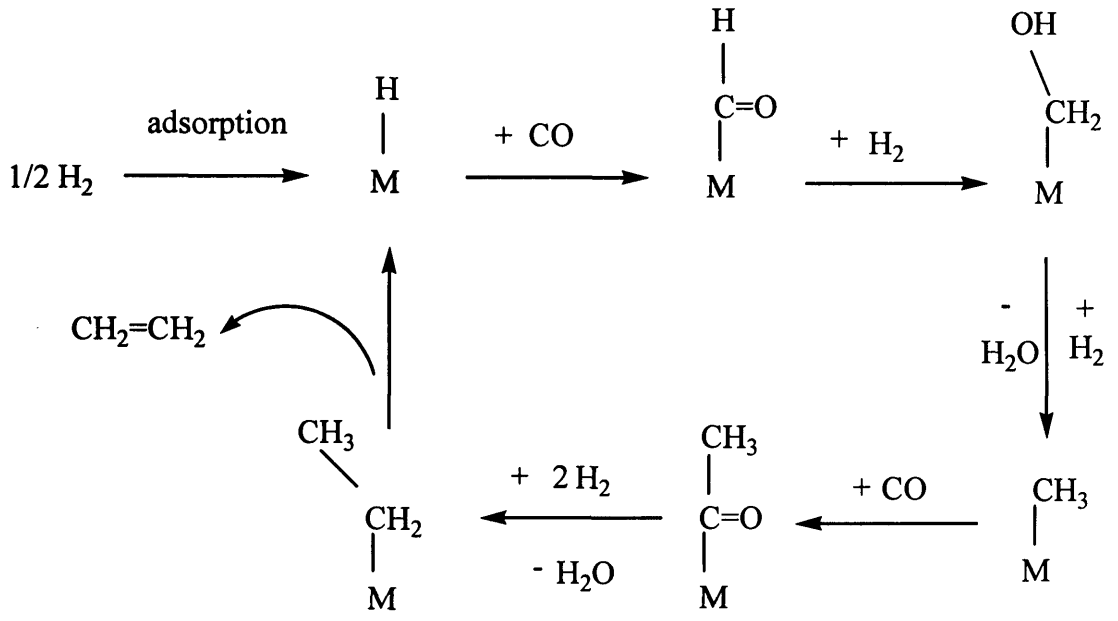

Figure 1.5 The CO insertion mechanism

Since the FT reaction is a very complicated catalytic reaction, the above presented mechanisms only provide some possible routes for CO hydrogenation. The 'real' intrinsic mechanism of the CO hydrogenation could be a combination of these routes or is possibly totally different. Identifying the 'real' mechanism is a task for the long term future.

1.2.6 FT Catalysts

The term catalyst, by definition, refers to a substance that alters the rate of a chemical reaction without being consumed by the process [29]. Catalysts are often referred as the 'heartbeat' of industrial processes. This is also true for the FT process.

Key features for measuring a successful catalyst are activity, product selectivity, lifetime and application of the commercial process.

The main components of a catalyst are normally active metal, support and promoters. The active metal plays a key role in activity/product selectivity, although the support and the promoter can influence the performance of the catalyst. The main function of the support is to maximize the surface area of the active phase. Generally, for catalysts with the same composition, higher surface area leads to higher activity. The support could also influence the morphology and mechanical properties (e.g. attrition resistance) of the final catalyst. Promoters are referred to as substances that are not catalytically active, but help to improve the activity of the active phase [29]. Other factors, such as the shape of the final catalyst, pellet size *etc.* may also contribute to the performance of a catalyst. Since all these factors are not isolated, catalyst design tries to find a combination of these factors that results in optimal performance for the target reaction.

The FT synthesis is a polymerization process with a wide range of products. To synthesize specific products with proper chain length requires careful catalyst choice.

In the FT synthesis, the active metals used are mainly group VIII transition metals. The activity of a series of group VIII transition metal was reported to decrease in the order: Ru > Fe > Ni > Co > Rh > Pd > Pt, Ir [30]. For commercial applications, selection of the metal for the catalyst is not only related to the activity, but also resources and cost. Ru was identified as being highly active, especially for the synthesis of high molecular weight waxes at high pressures. With a price of $3*10^4$ times more than Fe [31], its application is largely limited. Ni is active mainly as a methanation catalyst. Cobalt and iron are the earliest and most well-developed

catalyst systems. Cobalt catalysts are normally used at a low temperature range for producing diesel and have the advantage of a long life time (>5 years), whereas iron catalysts are used at relatively high temperature for synthesizing gasoline products and the life time is relatively short (~8 weeks). Compared with iron catalyst, cobalt is 230 times more expensive [31].

The supports used in the FT process are mainly silica, alumina and titania. Typically, silica and alumina have large surface areas in the range 150 – 250 m^2/g. They were widely used in patented commercial catalysts, e.g. Shell (silica) [32,33], Gulf/Chevron (alumina) [34,35] and Statoil (alumina) [36,37]. Compared with silica, alumina has a better attrition resistance. Titania was chosen for Exxon patented catalysts [38-41]. In fact, the surface area of titania in its rutile form is rather low (10 – 15 m^2/g), and titania in its anatase form has very low attrition resistance. Both are disadvantageous for a support. However, it is known that under certain pretreatment conditions titania is able to undergo structural changes which are responsible for the so called strong metal-support interaction (SMSI). The SMSI could be responsible for the catalytic activity.

There are normally two types of promoter in the FT synthesis. One is a reduction promoter which typically includes noble metals, such as Pt, Ru, Pd and Re. The main function of reduction promoters is to facilitate reduction of the active metals. The other type of promoter is an activity/selectivity promoter which normally comes from group A metals (e.g. alkaline). Their function is to stabilize the dispersion of the active metal on the catalyst surface.

1.2.6.1 Catalysts for alcohol synthesis

Catalysts used for alcohol synthesis can normally be classified into two main groups. One is for methanol synthesis and the other one is for higher alcohol synthesis (HAS).

(1) Catalysts for methanol synthesis

The zinc chromium oxide (ZnO/Cr_2O_3) catalyst was among the early systems developed for methanol synthesis. The active phase is ZnO, and Cr_2O_3 acts as structural promoter preventing the growth of ZnO crystals. Typical operation conditions involve high pressure (250 – 350 bar) and high temperature (623 - 723 K). This type of catalyst has the advantage of resistance to sulfur poisoning however the requirement of high pressure significantly increases the capital cost of the process. In the 1960's, benefiting from the development of gas purifying technology, interest in Cu catalysts was renewed. In 1966, ICI developed the so called low pressure methanol synthesis catalyst $Cu/ZnO/Cr_2O_3$ which was later replaced by $Cu/ZnO/Al_2O_3$. The active phase is Cu which is stabilized on ZnO/Al_2O_3. The low pressure methanol synthesis catalyst could be operated at 50 – 100 bar and 523 – 573 K approximately [42-44]. By using this type of catalyst, the required pressure for operation decreased dramatically. The temperature for this type of catalyst has to be limited to under 573 K to avoid sintering of the copper. Klier [45] suggested that a composition of $Cu/ZnO/Al_2O_3$ = 60/30/10 was good for methanol synthesis. Later on, in a review by Bart and Sneeden, a composition of $Cu/ZnO/Al_2O_3$ = 60/35/5 was recommended [46]. At present, low temperature and low pressure Cu based catalysts are employed for all commercial production of methanol from syngas.

(2) Catalysts for higher alcohol synthesis

Depending on the active metal involved, catalysts used for HAS can be roughly classified into 4 categories: a modified methanol synthesis catalyst, the IFP (Institut Français du Pétrole) mixed oxides catalyst, an alkali modified cobalt molybdenum catalyst and a rhodium based catalyst.

Modified methanol synthesis catalyst

For higher alcohol synthesis, it is commonly accepted that higher alcohols can be synthesized by appropriate modification of methanol synthesis catalysts and catalytic reaction conditions [45, 47]. With the addition of alkali and alkaline-earth components, the methanol synthesis catalyst favors the formation of higher alcohols and other oxygenates. This type of catalyst includes alkali-doped ZnO/Cr_2O_3, alkali-doped $Cu/ZnO/Cr_2O_3$ and Co, Fe, or Ni modified $Cu/ZnO/Cr_2O_3$ catalysts. Alkali-doped ZnO/Cr_2O_3 catalysts are also called modified high pressure methanol synthesis catalysts. Typical process conditions for high pressure methanol synthesis catalysts are 573 – 698 K and 125 – 300 bar with branched primary alcohols as the main product. For this series of catalysts, methanol still remains the principle product and the main higher alcohol is isobutanol. The other two types of catalysts, alkali-doped $Cu/ZnO/Cr_2O_3$ and Co, Fe, or Ni modified $Cu/ZnO/Cr_2O_3$ catalysts are called modified low pressure methanol synthesis catalysts. Their typical process conditions are 548 – 583 K and 50 – 100 bar with primary alcohols as the major products. Comparing the modified higher pressure methanol synthesis catalyst with lower pressure one, there is a decrease in the average carbon number of the oxygenates produced using the modified low pressure methanol synthesis catalyst [48].

The IFP mixed oxide catalyst

The IFP mixed oxide catalyst is also called a modified FT catalyst which consists mainly of oxides of copper and cobalt and a series of elements such as aluminum, chromium, zinc and noble metals [49, 50]. The function of cobalt in the IFP catalyst is different from that in the modified methanol catalyst because small additions can significantly affect the catalytic activity.

The IFP catalysts are homogeneously mixed oxides containing mainly Co and Cu. Small amounts of Zn, Zr, Al and alkali metals are included as modifiers. A typical composition was given by Xiaoding *et al.*[44] as 10-50% Cu; 5-25% Co; 5-30% Al; 10-70% Zn; alkali/Al = 0-0.2; Zn/Al = 0.4-2.0; Co/Al = 0.2-0.75; Cu/Al = 0.1-3.0. Typical operation conditions for the IFP catalyst are 523 – 623 K, 60 – 200 bar, giving a carbon oxide conversion of 5 – 30% and C_{2+} alcohol selectivity of 30 – 50% with linear primary alcohols as major products.

Alkali modified molybdenum catalyst

Molybdenum sulfide based catalysts for alcohol synthesis were independently discovered by research groups at Dow Chemicals [51-53] and Union Carbide [54]. They reported that molybdenum sulfide catalysts promoted by cobalt and alkali compounds are active for higher alcohol synthesis. This type of catalyst is normally operated at 533 – 623 K and 30 – 175 bar. CO conversion of circa 10% and 75 – 90% higher alcohol selectivity were reported with a syngas ratio (H_2/CO) of 1 by Herman [55]. The products are primarily non-branched linear alcohols and follow a similar ASF molecular weight distribution.

Due to the nature of this type of catalyst, molybdenum sulfide based catalysts do not suffer from sulfur poisoning. In fact, the operation of sulfide based catalyst require 50 – 100 ppm H_2S in the syngas stream to maintain the sulfidity of the catalyst

[56]. Catalyst activity was also reported to be less sensitive to the presence of CO_2 in the syngas feed. However, inhibition of catalytic activity was observed with high amounts of CO_2 (>30%). Additionally, the selectivity towards higher alcohols is reduced in the presence of even low levels of CO_2 [55]. Hence, CO_2 is recommended to be removed for the operation of this type of catalyst.

Molybdenum carbide catalysts have also been reported for the formation of alcohols by Leclercq [57] and Woo [58]. They reported that the formation of alcohols is linked to the surface stoichiometry and to the extent of carburization. Potassium promotion can enhance the selectivity towards C_1-C_7 alcohols [58]. Xiang *et al.* [59, 60] investigated the addition of cobalt and potassium to the molybdenum carbide systems and reported that both additives lead to high activity and selectivity towards C_{2+} alcohols.

Reduced molybdenum based catalysts have also been studied for HAS [61-63]. Alumina or silica is the commonly used support for this type of catalyst. Operation at 523 K and 50 bar with a syngas (H_2/CO) ratio of 2 gave a CO conversion of 7.2% and circa 60% alcohol selectivity.

Rhodium based catalyst

Rhodium based catalysts are another category for higher alcohol synthesis [64]. Rhodium containing catalysts show good selectivity toward the synthesis of ethanol and other C_2 oxygenates [65]. However, its high price due to limited natural resources makes commercial application difficult. Hence, studies of rhodium containing catalysts are currently for academic purpose. The possibility of future commercialization relies very much on its performance (activity, selectivity) and catalyst lifetime against its cost.

The performances of the rhodium based catalysts are closely related to selected supports [66-68], alkali promoters [69, 70] as well as the rhodium precursor employed. It was found that alcohol selectivity over Rh catalysts increases in the following order depending on the support: TiO_2 < Al_2O_3 < SiO_2 < MgO [66]. Rhodium on silica was reported to have excellent selectivity towards oxygenated compounds [71, 72]. Alkali promoters were found to enhance the formation of higher oxygenates from syngas [69, 70]. The precursor Rh_4CO_{12}/La_2O_3 was reported to lead to the highest selectivity towards ethanol [73].

1.3 Recent interest in the FT process

Although the FT synthesis has more than 80 years of history, there is still progress to be made in the improvement of catalytic performance and the optimization of experimental conditions used to perform the synthesis of fuels. Recent interest in the FT process arises mainly from two areas. One is GTL technology, and the other one is higher alcohol synthesis.

1.3.1 Interest in GTL technology

World reserves of natural gas has been estimated at around 180 trillion cubic meters [1], which has an equivalent energy value of 630 billion barrels of synthetic oil. Most of these reserves are in remote places and the natural gas is normally flared, vented or re-injected back to the ground. The price is thus negative, which is advantageous in reducing capital costs of the FT process. Another advantage of GTL technology is that the products have high quality – higher diesel yield than conventional refining process. The third advantage is that the GTL process yields

products with zero/less sulfur and aromatic compounds, making them much cleaner than products from the conventional refinery process. This meets the increasingly stringent environmental fuel legislation. A lifecycle assessment has been performed on conventional refinery product and GTL fuels. The results obtained are shown in Figure 1.6. It can be clearly seen that the GTL system has advantages in all aspects (e.g. green house gas, air acidification, smog formation, particulate emission).

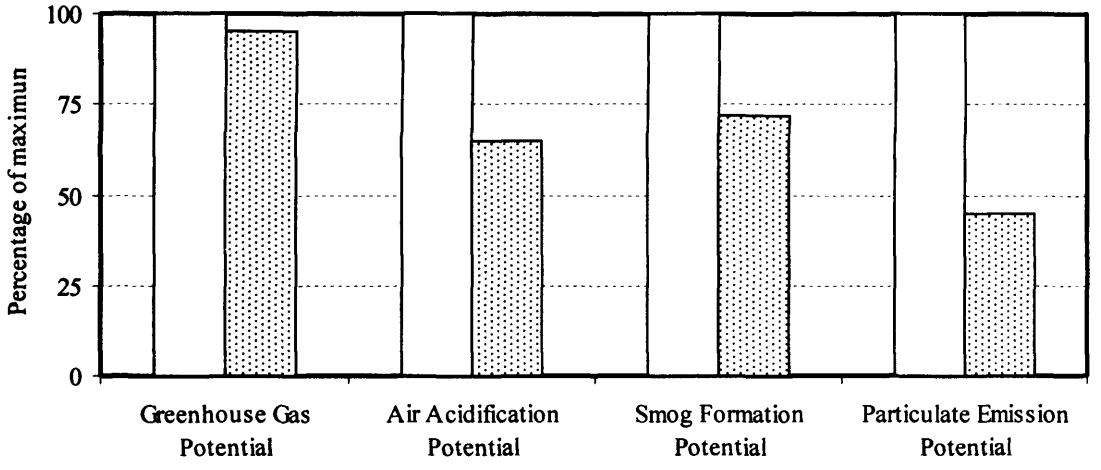

Figure 1.6 Lifecycle assessment results [74]; □ Refinery system ⁙ GTL system

The interest in the GTL is clearly demonstrated by the significant behavioral shift of world oil majors. These companies are researching or commercializing large-scale production of the FT fuels based on natural gas. In 1992, the world's first GTL plant was started up at Mossel Bay in South Africa by PetroSA. Currently it is producing 36,000 barrels per day (BPD) of synthetic and condensate based fuel. In 1993, Shell launched its GTL plant employing SMDS technology at Bintulu in Malaysia, producing 15,000 BPD. In 2004, Shell announced a $5 billion plant in Qatar as an expansion of its GTL operation. Sasol, the world's most experienced synthetic fuel firm based on coal, and Qatar Petroleum (QP) agreed on a $6 billion project to develop a 130,000 BPD upstream/downstream integrated GTL project

based on Sasol's Slurry Phase Distillate technology in 2004. Exxon Mobil signed a heads of agreement for a $7 billion GTL project based on the patented AGC-21 technology with QP in 2004. BP has successfully operated commercial pilot plants in Alaska and is now the front runner of GTL technology in the Far-East area. A detailed review on the global GTL development in industry up to 2002 was given by Fleich *et al.* [75].

1.3.2 Interests in the higher alcohol synthesis

Increasing attention has been paid to alcohol synthesis since last two decades ago. In the fuel industry, alcohol is considered as a potential substitute for motor fuel in modified engines and a fuel additive in gasoline to boost the octane number for use in conventional engines. Tetra-ethyl lead and methyl tert-butyl ether (MTBE) have been widely used as fuel additives to enhance the octane number. However, the use of lead in gasoline was found to have a damaging effect on the environment and health and thus was phased out in 1996 in the US and subsequently in many other countries. MTBE is now being phased out due to the difficulty of retrieving it from ground water and soil. On the contrary, alcohols when used as fuel additives, combust more completely than traditional fuels and do not have the negative impact on the environment that tetra-ethyl lead and MTBE exhibit. With increasingly tight environmental laws, the use of alcohol in the fuel industry is receiving much attention.

Methanol

Methanol is one of the most important chemicals ever developed. The majority of methanol is produced *via* the syngas route. The process is a very well developed commercial process with high activity and selectivity. Methanol is widely used as a primary raw material and solvent in laboratory as well as pharmaceutical industries.

When used in the fuel industry to blend with gasoline, methanol can cause problems due to its high blending vapor pressure, low water tolerance and low hydrocarbon solubility.

Ethanol

Ethanol is another important chemical. It has a long history of use in the food industry and the medical sector. It has also been used in the chemical industry as a solvent or as starting material to manufacture detergents, paint and cosmetic products.

When used in the fuel industry, ethanol can be blended up to 10% with gasoline without engine modification in any brand of today's automobiles with emissions reduced by up to 30%. The extensive application of ethanol as an automotive fuel started in the 1970's and is now the fastest growing sector among all applications. Currently around 30 million cubic metres per year are used in the fuel industry, which accounts for 70% of the world ethanol production. In the entire fuel market, ethanol only plays a minor role because it accounts for 2.5% of the total gasoline consumption that is 1.2 billion cubic meters per year.

There are various methods that can be used to produce ethanol. The two most widely employed methods are fermentation and catalytic synthesis. Fermentation (equation 1.18) uses food e.g. sugar cane or corn as feedstock to produce ethanol and has been commercially operated in Brazil (sugar cane) and the USA (corn).

$$C_6H_{12}O_6 \rightarrow 2CH_3CH_2OH + 2CO_2 \qquad (1.18)$$

Currently 95% of fuel ethanol is obtained from the fermentation process. The fermentation method is, however, time consuming and labor intensive. Due to its successful application in Brazil, a number of countries or firms are interested in this technology and are attempting its commercialization.

Another approach to produce ethanol is catalytic synthesis which can be further divided into ethylene hydration (equation 1.19) and the syngas route. The former route refers to ethylene gas reacting with extremely pure water over the surface of a catalyst support impregnated with phosphoric acid.

$$CH_2 = CH_2 + H_2O \rightarrow CH_3CH_2OH \qquad (1.19)$$

This process is operated commercially and the main manufacturers are Sabic in the Middle East, BP in the UK, Sasol and PetroSA in the South Africa and Equistar in the US.

Syngas routes to produce ethanol are similar to the mixed alcohol synthesis, and hence are covered in the following section.

Higher alcohols

Apart from the interest in ethanol synthesis, higher alcohol synthesis (also called HAS) has been receiving growing attention. HAS normally refers to the synthesis of a mixture of C_1-C_6 alcohols with the aim of obtaining high C_{2+} alcohol selectivity. The percentage of higher alcohols for blending to gasoline is estimated to be circa 30 – 45wt% [76]. In contrast to methanol, higher alcohols have the advantage of higher water tolerance, higher volumetric heating values and lower vapor lock tendency when used as fuel additives. The use of higher alcohols also improves the combustion efficiencies and reduces environmentally damaging emissions. The higher alcohols obtained can be used as mixtures as fuel additives in the fuel industry or can be separated into pure alcohols for use in the chemical industry.

Several processes have been developed to synthesize mixed alcohols: the FT synthesis, isosynthesis, oxosynthesis which includes the hydroformylation of olefins and the homologation of methanol and lower molecular weight alcohols. The potential

of the FT synthesis route via syngas is widely recognized especially with regard to the development of various GTL technologies.

Since the 1980's, there have been several technological developments on the HAS. Dow was the first company that developed HAS technology. Their catalysts were molybdenum sulfide based materials (as described in section 1.2.6.1). Snamprogetti and Haldor Topsoe developed an HAS process using a modified methanol catalyst and started a 12,000 ton/y pilot plant in 1982 [77]. Lurgi built 2 tonnes per day (TPD) demonstration plants in 1990 based on its HAS process with low pressure methanol synthesis [78]. IFP built its 20 BPD pilot plant in Chiba (Japan) [79]. Currently these companies have no further interest in commercializing their higher alcohol processes.

Several other companies/firms has shown interest in developing HAS technology. Power Energy Fuels Inc. (PEFI) developed the Ecalene^{TM} mixed alcohol process [80] which uses a modified MoS_2 catalyst based on Dow's process. The mixed alcohol product consists primarily of linear C_1 – C_6 alcohols. The targeted weight composition is 0% methanol, 75% ethanol, 9% propanol, 7% butanol, 5% pentanol and 4% hexanol & higher. Currently 2-3 pilot plants are being considered to produce mixed alcohol from biomass. The Standard Alcohol Company of America (SACA) is seeking funds to build a pilot plant based on their Envirolene^{TM} technology [81]. The Envirolene^{TM} process mainly produces a mixture of methanol through to octanol over a modified high pressure methanol synthesis catalyst. Pearson Technologies has built a 30 ton/day biomass gasification and alcohol production plant in Mississippi with an emphasis in producing ethanol product [81].

It is known that the core of catalytic synthesis is to find a catalyst with good conversion as well as high selectivity. Due to low conversions and poor selectivity,

commercial plants for the synthesis of higher alcohol have not yet been built. The final commercialization of HAS technology depends very much on the development and performance of its catalyst. Together with development in syngas generation technology, mixed alcohol synthesis could play an important role in the next generation of the fuel industry.

1.4 Aims of the research project

The aim of this project is to investigate alcohol synthesis *via* FT synthesis. The investigation was first performed on the two well-known catalytic systems for alcohol synthesis: (a) Cobalt molybdenum based catalyst and (b) the IFP mixed oxide catalyst. Their activity and selectivity towards higher alcohols was studied. The reaction conditions were identified for both catalyst systems.

The FT alcohol synthesis was also investigated over gold containing catalysts with the purpose of studying the possibility of using gold for alcohol synthesis by CO hydrogenation.

A combination of syngas generation and FT synthesis in a single reactor was investigated to evaluate the feasibility of combining steam reforming and the FT synthesis together whereby methane is first reacted with H_2O to form $CO + H_2$ which then further reacts to form hydrocarbons and alcohols.

Following this introduction, chapter 2 is the experimental section which is mainly focused on catalyst preparation, catalyst characterization, catalytic reaction procedures and data analysis. CO hydrogenation over cobalt molybdenum based catalysts and cobalt copper based mixed oxide catalysts for alcohol synthesis has been

investigated and is described in chapter 3. Chapter 4 presents the initial results of CO hydrogenation over gold containing catalysts. Studies of combined steam reforming and FT synthesis for alcohol synthesis are described in chapter 5. Finally, chapter 6 presents the conclusions of the investigated catalyst systems of this study.

References

[1] BP Statistical Review of World Energy (2006)

[2] Hindermann, J.P.; Hutchings, G.J.; Kiennemann, A., Catal. Rev. Sci. Eng., 35 (1993) 1

[3] Anderson, R.B., The Fischer-Tropsch Synthesis, Academic Press, London, 1983

[4] Stull, D.R.; Westrum, E.F.; Sinke, G.C., The Chemical Thermodynamics of Organic Compounds (Wiley, New York, 1969).

[5] Bochniak, D.J.; Subramaniam, B., AIChE Journal 44 (1998) 1889

[6] Anderson, R.B., Catalysts for the Fischer-Tropsch synthesis, vol. 4, Van Nostrand Reinhold, New York 1956

[7] Dry, M.E., J. Mol. Catal., 17 (1982) 133

[8] Schulz, H.; van Steen, E.; Claeys, M., in 'Selective hydrogenation and dehydrogenation', DGMK, Kassel, Germany, 1993

[9] Novak, S.; Madon, R.J.; Suhl, H., J. Catal., 77 (1982) 141

[10] Iglesia, E.; Reyes, S.C.; Madon, R.J.; Soled, S.L., in E.E. Eley; H. Pines; P.B.Weisz, eds., Advances in Catalysis, vol. 39, Academic Press, New York, 1993 pp. 221–302

[11] Kuipers, E.W.; Scheper, C.; Wilson, J.H.; Oosterbeek, H., J. Catal., 158 (1996) 288

[12] Kuipers, E.W.; Vinkenburg, I.H.; Oosterbeek, H., J. Catal., 152 (1995) 137

[13] Bianchi, C.L.; Ragaini, V., J. Catal., 168 (1997) 70

[14] Ponec, V., Catal. Rev. Sci. Eng. 18 (1978) 151

[15] Bell, A.T., Catal. Rev. Sci. Eng., 23 (1981) 203

[16] Adesina, A.A., Appl. Catal. A, 138 (1996) 345

[17] Davis, B.H., Fuel Process. Technol. 71 (2001) 157

[18] Fischer, F.; Tropsch, H., Brennstoff Chem. **7** (1926) 97

[19] Kummer, J.T.; de Witt, T.W.; Emmett, P.H., J. Am. Chem. Soc. 70 (1948) 3632

[20] Maitlis, P.M., Pure Appl. Chem. 61 (1989) 1747

[21] Davis, B.H.; Xu, L.; Bao, S., Stud. Surf. Sci. Catal. 107 (1997) 175

[22] Storch, H.H.; Golumbic, N.; Anderson, R.B., The Fischer –Tropsch and Related Synthesis, New York, John Wiley & Sons, (1951)

[23] Hall, W.K.; Kokes, R.J.; Emmett, P.H., J. Am. Chem. Soc. 79 (1957) 2983

[24] Hall, W.K.; Kokes, R.J.; Emmett, P.H., J. Am. Chem. Soc. 82 (1960) 1027

[25] P.H. Emmett, Lecture No. 4, Catalytic Processes Utilizing CO and H , Oak Ridge National Laboratory, 2 November 20–22, 1974.

[26] Ponec, V., Catalysis 5 (1981) 49

[27] Raje, A.; Davis, B.H., in: J.J. Spivey Ed., Catalysis. The Royal Soc. Chem., Cambridge, vol. 12 (1996) 52

[28] Pichler, H.; Schultz, H., Chem. Ing. Tech. **42** (1970) 1162

[29] Bond, G.C., Heterogeneous Catlaysts, Principles and Applications, Oxford University Press (1984)

[30] Vannice, M.A.; J. Catal., 37 (1975) 449

[31] Rao, V.U.S.; Stiegel, G.J.; Cinquegrane, G.J.; Srivastave, R.D., Fuel Process. Technol., 30 (1992) 83

[32] Reinalda, D.; Kars, J., European Pat. Appl., 0 421 502 A2 (1990)

[33] Reinalda, D.; Blankenstein, P.; Derking, A., European Pat. Appl., 0 510 771 A1 (1992)

[34] Beuther, H.; Kibby, C.L.; Kobylinski, T.P.; Pannell, R.B., U.S. Patent, 4,493,905 (1985)

[35] Beuther, H.; Kibby, C.L.; Kobylinski, T.P.; Pannell, R.B., U.S. Patent, 4,605,680 (1986)

[36] Eri, S.; Goodwin Jr, J.G.; Marcelin, G.; Riis, T., U.S. Patent, 5,102,851 (1992)

[37] Eri, S.; Goodwin Jr, J.G.; Marcelin, G.; Riis, T., U.S. Patent, 5,116,879 (1992)

[38] Iglesia, E.; Soled, S.; Fiato, R.A., U.S. Patent, 4,794,099 (1988)

[39] Iglesia, E.; Soled, S.; Fiato, R.A., U.S. Patent, 4,822,824 (1988)

[40] Pedrick, L.E.; Mauldin, C.H.; Behrmann, W.C., U.S. Patent, 5,268,344(1993)

[41] Soled, S.; Iglesia, E.; Fiato, R.A.; Ansell, G.B., U.S. Patent, 5,397,806 (1995)

[42] Natta, G., Columbo, U., Pasquon, I., Catalysis, Emmett, P. H., ed., (Reinhold, Volume 5, Chapter 3, New York: 1957).

[43] Herman, R., Studies in Surface and Catalyst, (Chapter 7, Elsevier, Amsterdam: 1990).

[44] Xiaoding, X., Doesburg, E., Scholten J., Catal. Today, 2 (1987) 125

[45] Klier, K., Adv. Catal., 31 (1982) 243

[46] Bart, J.C.J.; Sneeden, R.P.A., Catal. Today, 2 (1987) 1

[47] Smith, K.; Anderson, R. B., J. Catal., 85 (1984) 428

[48] Forzatti, P.; Tronconi, E.; Pasquon, I., Catal. Rev. Sci. Eng., 33 (1991) 109

[49] Surgier, A., US Patent 3787332, (1974)

[50] Surgier, A., US Patent 3899577, (1975)

[51] Quarderer, G. J.; Cochran, K. A., European Patent 0,119,609, 1984

[52] Stevens, R. R., European Patent 0,172,431, 1986

[53] Murchison, C.B.; Conway, M.M.; Stevens, R.R.; Quarderer, G.J., Proc. 9th Int. Congr. Catal., Calgary, 2 (1988) 626

[54] Kinkade, N. E., European Patents 0,149,255 and 0,149,256, 1985

[55] Herman, R. G., New Trends in CO Activation, L. Guczi, ed., Elsevier, New York, (1991) 265-349

[56] Courty, P., Chaumette, P., Raimbault, C., and Travers, P. (1990). Revue de l'Institut Francais du Petrole, 45(4), 561-78

[57] Leclercq, L.; Almazouari, A.; Dufour, M.; Leclercq, G., in: S.T. Oyama (Ed.), The Chemistry of Transition Metal Carbides and Nitrides, Blackie, Glasgow, 1996, p. 345

[58] Woo, H.C.; Park, K.Y.; Kim, Y.G.; Nam, I.; Chung, J.S.; Lee, J.S., Appl. Catal. 75 (1991) 267

[59] Xiang, M.; Li, D.; Li, W.; Zhong, B.; Sun, Y., Catalysis Commun. 8 (2007) 503

[60] Xiang, M.; Li, D.; Qi, H.; Li, W.; Zhong, B.; Sun, Y., Fuel 86 (2007) 1298

[61] Alyea, E.C.; He, D.; Wang, J., Appl. Catal. A: General 104 (1993) 77

[62] Storm, D.A., Top. Catal. 2 (1995) 91

[63] Fujimoto, K.; Oba, T., App., Catal. 13 (1985) 289

[64] Ichikawa, M. et al., (agency of Industrial Science and Technology), early disclosure, No. 85-32731, 2 (1985) 19

[65] Nirula, S. C. (1994). PEP Review no. 85-1-4, SRI International, Meno Park, CA.

[66] Katzer. J.R.; Sleight, A.W.; Gajarsdo, P.; Michel, J.B.; Gleason, E.F.; McMillian, S., Faraday Discussions of the Chemical Society, 72 (1981) 121

[67] Ichikawa, M., Chemtech, (November, 1982) 674

[68] Erdohelyl, A., and Solymosi, F., J.Catal., 84 (1983) 446

[69] Kagami, S.; Naito, S.; Kikuzono, Y.; Tamaru, K., J. Chem. Soc., Chem. Commun., (1983) 256

[70] Orita, H.; Naito, S.; Tamaru, K., Chem. Lett., (1983) 1161

[71] Arakawa, H.; Fukushima, T.; Ichikawa, M.; Takeuchi, K.; Matsuzaki, T.; Sugi, Y., Chem. Lett. (1985) 23

[72] Bashin, M.M.; Bartley, W.J.; Ellgen, P.C.; Wilson, T.P., J. Catal., 54 (1978) 120

[73] Ichikawa, M., J.C.S. Chem.Commun. (1978) 566

[74] Pricewaterhousecoopers, London, 2006

[75] Fleisch, T.H.; Sills, R.A.; Briscoe, M.D., Journal of Natural Gas Chemistry 11 (2002)1

[76] Slaa, J.C.; van Ommen, J.G.; Ross, J.R.H., Catal. Today, 15 (1992) 129

[77] Olayan, H. B. M., Energy Progress, 7(1987) 9

[78] Höhlein, B.; Mausbeck, D.; Supp, E.; König, P., International Symposium on Alcohol Fuels, Florence, Italy, 43-48

[79] El Sawy, A. H., NTIS. DE90010325. SAND89-7151, (1990) Mitre Corporation

[80] Lucero, A. J.; Klepper, R. E.; O'Keefe, W. M.; and Sethi, V. K., Preprints of Symposia -American Chemical Society, Division of Fuel Chemistry, 46(2001)413

[81] U.S. Department of Energy, National Renewable Energy Laboratory, NREL/SR-510-39947: Equipment Design and Cost Estimation for Small Modular Biomass Systems Synthesis Gas Cleanup, and Oxygen Separation Equipment, May 2006

Chapter 2 Experimental

2.1 Catalyst preparation

Numerous preparation methods have been developed to synthesize heterogeneous metal, metal oxide and metal sulfide catalysts. Co-precipitation and impregnation techniques are two widely used methods in industry [1]. In this thesis, catalysts were prepared mainly using these two methods. Relevant starting materials used for catalyst preparation in this study are listed in Table 2.1.

2.1.1 Co-precipitation

The co-precipitation technique is a commonly used catalyst preparation method. Two or more active metal compounds (when only one active metal compound is present, co-precipitation is simplified to precipitation) precipitate when solutions of the metal precursors are added together simultaneously into a precipitating solution with proper control of temperature, pH and flow-rates. The obtained precipitate then typically goes through the following processes: aging, washing, drying, calcination and reduction, giving a final catalyst with uniform distribution of active metal compounds.

Table2.1 Reagents used in catalyst preparation

Reagents	Grade	Supplier
$(NH_4)_6Mo_7O_{24}\cdot 4H_2O$	-	Sigma Aldrich
20% wt $(NH_4)_2S$ in H_2O	-	Aldrich
$Co(CH_3CO_2)_2\cdot 4H_2O$	98+%	Sigma Aldrich
CH_3COOH	>99%	Fischer
K_2CO_3	>99%	Fischer
bentonite clay	-	Aldrich
sterotex® lubricant	-	Abitec
$Cu(NO_3)_2\cdot 3H_2O$	99%	Aldrich
$Co(NO_3)_2\cdot 6H_2O$	98+%	Aldrich
$Zn(NO_3)_2\cdot 6H_2O$	98%	Aldrich
$Zr(NO_3)_2\cdot xH_2O$	-	Aldrich
$Nd(NO_3)_2\cdot 6H_2O$	99.9%	Aldrich
$(NH_4)_2CO_3$	-	Aldrich
Na_2CO_3	99.95%	Aldrich
Cs_2CO_3	99.9%	Aldrich
HNO_3	-	Fischer
natural graphite	-	Aldrich
$HAuCl_4\cdot 3H_2O$	-	Johnson Matthey
$Fe(NO_3)_3\cdot 9H_2O$	98+%	Aldrich
Au/Fe_2O_3	-	World gold council
ZrO_2	99%	Aldrich
MgO	GPR	BDH chemicals
MoO_3	99.5%	Avodado
TiO_2	99+%	Aldrich
ruthenium (III) nitrosyl nitrate solution in dilute nitric acid	-	Aldrich

Co-precipitation requires detailed control of every preparation variable and step. Variables include the order and rate of addition of different solutions, the speed of mixing, the variation of pH and the procedure for aging. All these factors influence the nucleation and growth of the precipitate, which then further affects the structure of the final catalyst. Consequently, catalysts prepared using this method may suffer reproducibility problems [2, 3].

Most of the metal catalysts used in this study were prepared by the co-precipitation method. A batch co-precipitation rig (Figure 2.1a) was employed unless otherwise indicated.

(1) Preparation of alkali-promoted cobalt molybdenum sulfide catalysts

Alkali-promoted cobalt molybdenum sulfide catalysts (Co-MoS_2/K_2CO_3) were prepared as follows. A solution of $(NH_4)_2MoS_4$ was prepared by dissolving $(NH_4)_6Mo_7O_{24}\cdot 4H_2O$ (15g) into $(NH_4)_2S/H_2O$ (106 ml, 20%) with stirring (340-343K, 1h). A solution of the cobalt compound was prepared by dissolving Co $(CH_3CO_2)_2$ (10.5g) in distilled water (200 ml). The two solutions were then added simultaneously, drop-wise into a well-stirred solution of aqueous acetic acid solution (30%) at 328K. The solution was vigorously stirred (1h, 328 K) and the resultant black solution was filtered and dried at room temperature in a fume cupboard overnight. The dried sample was heated under nitrogen (1h, 773 K ramping rate 25K/min), giving a grey-black product. This product was then ground and mixed with K_2CO_3, bentonite clay and sterotex® lubricant in a weight ratio of 66/10/20/4 (10% K_2CO_3) unless otherwise indicated.

(2) Preparation of Cu/Co/Zn/Zr mixed oxide catalysts

Preparation of Cu/Co/Zn/Zr mixed oxide catalysts was carried out in a continuous co-precipitation rig as shown in Figure 2.1b. Compared with the

conventional one, the continuous one has an additional out flow port which allows the precipitate to be released constantly. The flow rates of the two solutions were controlled by pH, measured in the turbulent zone of the stirring.

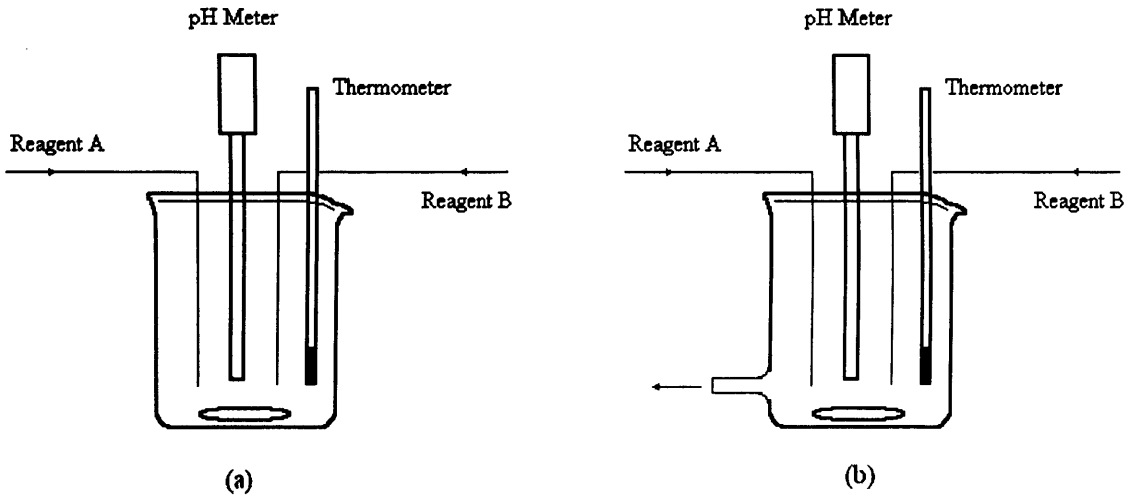

Figure 2.1 Co-precipitation technique. (a) batch co-precipitation rig (b) continuous co-precipitation rig

A mixed oxide containing the metals Nd and Zr was first prepared. Hexahydrated neodymium nitrate (4.4 g) and dehydrated zirconyl nitrate (8.1 g) were dissolved in nitric acid solution (7 v%, 100 ml) and then heated to 358K. A diammonium carbonate solution (18 g, 30%wt crystallized salt) was diluted in distilled water (100 ml) and was then heated to 338K. The two solutions were simultaneously introduced into the above mentioned co-precipitation rig in the pH range 6.5-6.8. The obtained precipitate was matured in its mother liquor overnight at room temperature, followed by washing with hot distilled water (2.7 l). A wet precipitate was obtained (53 g).

Separately, a mixed oxide containing the metals Cu, Co and Zn was prepared. Trihydrated copper nitrate (9.7 g), hexahydrated cobalt nitrate (8.7 g), hexahydrated zinc nitrate (7.4g) and dehydrated zirconyl nitrate (13.4 g) were dissolved in nitric

acid solution (7 v%, 200ml). This resultant solution was diluted to give solution A (300 ml). Meanwhile, anhydrous sodium carbonate (32 g) was dissolved in water (500 ml), giving solution B. The two solutions (A and B) were simultaneously introduced into the continuous co-precipitation rig at 348K in the pH range 6.95-7.04. The obtained precipitate was matured (313K 1h), cooled to room temperature and kept overnight in the presence of its mother liquor. The resultant material was washed with hot distilled water (1.8 l).

The two precipitates were mixed in a beaker with stirring (3 h). The obtained thixotropic solution was matured in a solution (5 ml) containing Na_2CO_3 (0.45 g) and Cs_2CO_3 (0.04 g) with stirring (6 h) at room temperature. The resultant material was dried overnight in an oven at 393K.

The dried product was calcined in flowing air for 5h at 673K. The obtained solid material was ground with natural graphite in a weight ratio of 39/1 to give a final catalyst before each catalytic reaction.

(3) Preparation of supported Au catalysts

5wt%Au/ZnO catalysts were prepared from $HAuCl_4 \cdot 3H_2O$ and $Zn(NO_3)_2 \cdot 6H_2O$. An aqueous mixture of the precursors ($HAuCl_4 \cdot 3H_2O$, 0.002 $mol \cdot l^{-1}$ and $Zn(NO_3)_2 \cdot 6H_2O$, 0.1 $mol \cdot l^{-1}$) was introduced at the rate of 7.5 ml/min into an aqueous solution of Na_2CO_3 (1 mol l^{-1}, pH 9-11.5) under vigorous stirring (~600 rpm) for 90-120 min. The precipitation temperature was maintained at 343-353K. The co-precipitated sample obtained was aged for 24h, filtered, washed several times with warm distilled water, and then dried overnight in oven at 393K. The resulting powder was calcined in air at 673K. A ZnO catalyst was prepared in a similar way without adding the gold source.

5wt%Au/Fe_2O_3 catalyst was used as obtained, as a standard catalyst provided by the World Gold Council [4]. A Fe_2O_3 catalyst was prepared by a precipitation method. An aqueous solution of Fe nitrate ($Fe(NO_3)_3 \cdot 9H_2O$, 0.25 $mol \cdot l^{-1}$) was heated to 353K. Na_2CO_3 solution (0.25 $mol \cdot l^{-1}$) was added drop wise to the nitrate solution until a pH of 8.2 was reached. The precipitate was washed with distilled water and then dried overnight in oven at 393K. The dried brown colour solid was calcined in air at 673K for 6h.

2.1.2 Impregnation

Impregnation is achieved by adding solutions of metal precursors to the pores of a preformed support, following by subsequent evaporation of solvent. Impregnation can be further classified as wet impregnation and incipient wetness impregnation according to the amount of added volume of the solutions. In the former case, the volume of the solution is significantly larger than the pore volume of the support. However, in the latter case, the amount of added solutions is equal or slightly less than the pore volume of the support [3]. For both cases, the resulting solid material goes through drying, calcination and reduction processes to give the final catalyst.

Compared with the co-precipitation technique, impregnation has the advantage of better control of metal loading, less waste of expensive metal components and simpler scale up.

(1) Preparation of supported Ru catalysts

3wt% Ru containing metal oxide catalysts were prepared by the impregnation technique. Metal oxide supports used were ZrO_2, MgO, MoO_3 and TiO_2. A calculated amount of ruthenium nitrosyl nitrate was impregnated onto a single oxide support at 353K. After evaporation of the aqueous solution, the material was dried overnight in

oven at 393K. The dried sample was then calcined in flowing air at 773K for 5h. The catalyst was reduced with hydrogen in the reactor at 673K for 10h before catalytic reaction.

2.2 Catalytic Tests

A schematic representation of the catalytic testing rig is shown in Figure 2.2. All catalytic reactions including Fischer Tropsch (FT) synthesis, steam reforming and Combined Steam Reforming and Fischer Tropsch (CRAFT) were carried out in this rig with slight variations. Three parallel lines were built in a similar manner for introducing gases to the system. Typically these lines were feed line (syngas in the FT or methane in the steam reforming), reduction line (H_2) and dilution line (methane). All or some of these lines were used depending on the nature of the investigated process. In addition, a fourth line for introducing water to the system was used when required.

For a typical run, gas passed through a filter, non-return valve with its flow-rate controlled by a mass flow controller (BROOKS 5850S). A 3-way valve was used to direct the gas through the reactor or by pass. A pressure relief valve was installed before the reactor to ensure safe operation of the system. Liquid products were collected in a gas liquid separator wrapped with copper coil and insulator jacket. Cold water (276K) was circulated inside the copper coil. High pressure in the system was achieved by a back-pressure regulator (TESCOM 26-1700) and indicated by a pressure gauge. Gaseous products and non-reacted syngas passed through an online gas chromatograph (GC) for analysis before venting to fume cupboard.

Variations were made concerning the manner of starting a catalytic test depending on the type of reaction. Detailed procedures are described in the experimental sections of relevant chapters.

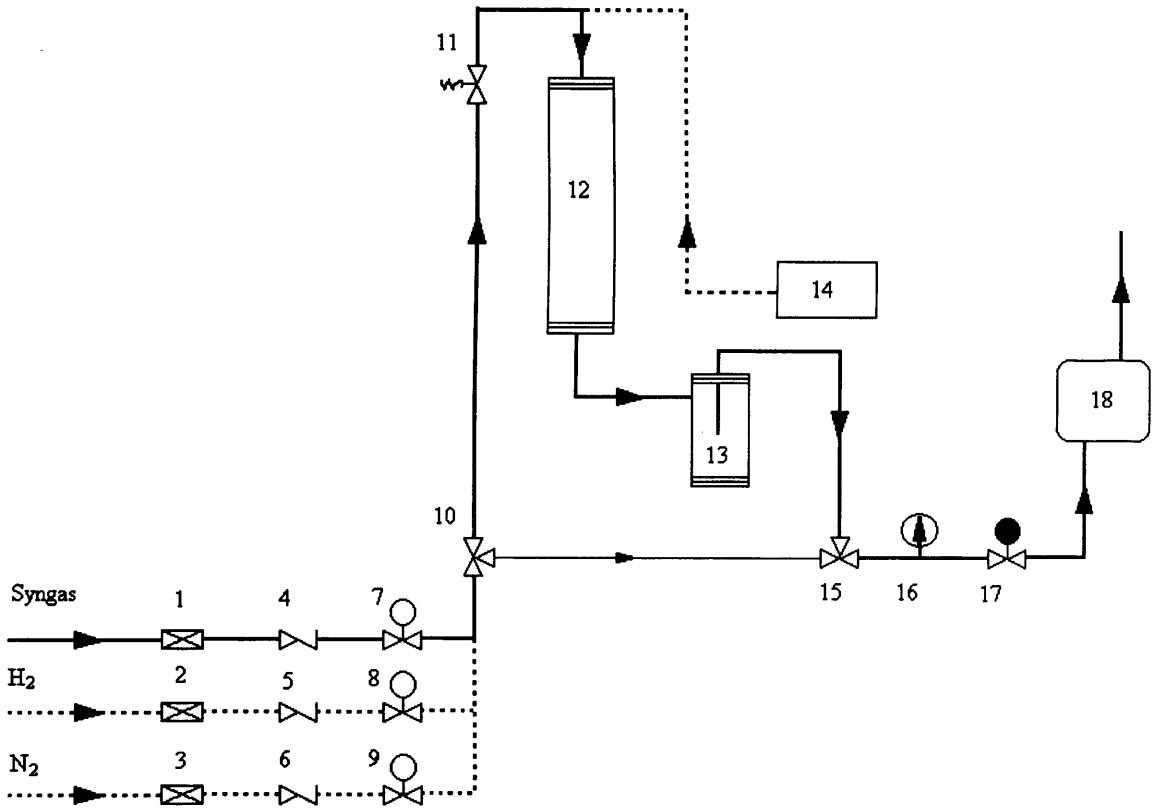

Figure 2.2 Flow diagram of catalytic reaction rig
1,2,3: filter; 4,5,6: non-return valve; 7,8,9: mass flow controller; 10,15: 3-way valve; 11: pressure relief valve; 12: reactor; 13: gas liquid separator; 14: HPLC pump; 16: pressure gauge; 17: back pressure regulator; 18: online GC.

2.2.1 Fixed bed reactors

Two fixed bed reactors were used for catalyst evaluation. One was a simple lab-reactor made of a stainless steel tube (3/16-in i.d.) housed within a single zone furnace. The furnace controlled the temperature of the reactor through a thermocouple dipped inside the catalyst bed. The other one was a sophisticated micro-reactor donated by BP. The micro-reactor consisted of a stainless steel tube (3/8-in i.d., 27-in length) and a thermo-well (3/16-in o.d.) fitted with an axial thermocouple. The reactor

fitted inside a three-heating-zone heated furnace. Temperature control of the furnace was achieved by a control panel that consisted of three Eurotherm controllers (2116). Each controller linked to a single zone. The micro-reactor was designed in such a way so as to ensure isothermal operation during reaction.

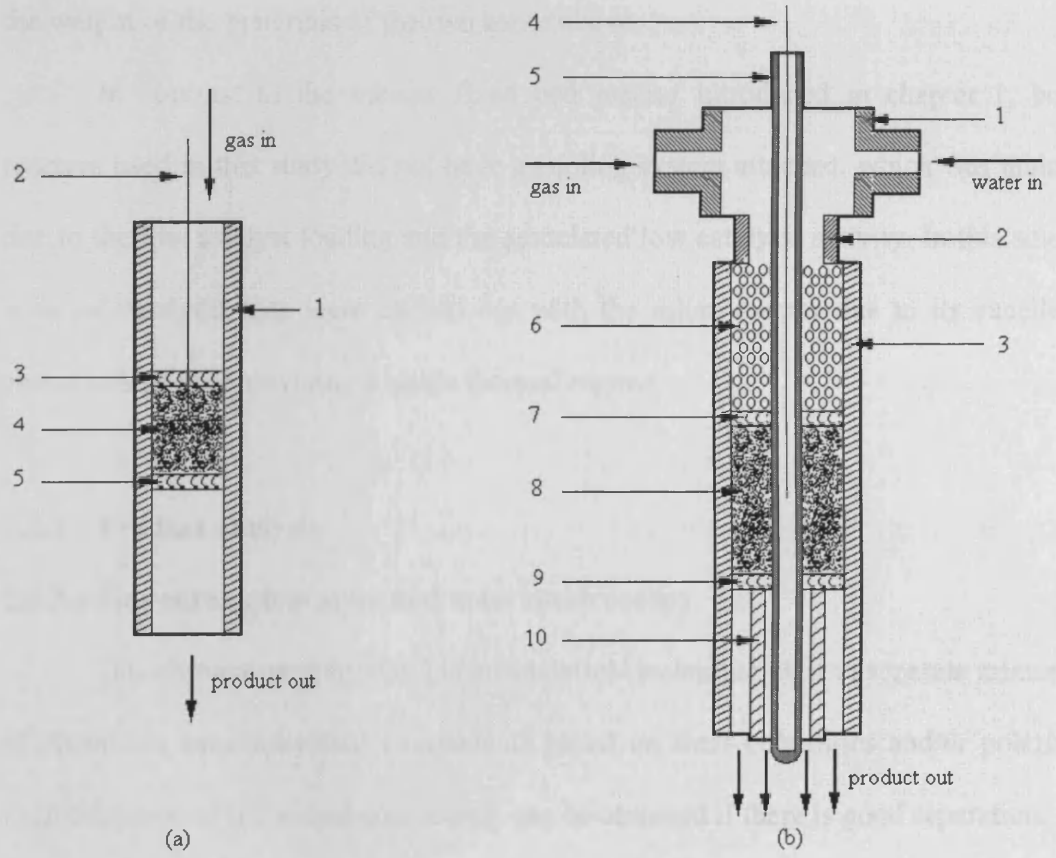

Figure 2.3 Schematic re-presentation of reactors (a) lab reactor. 1: reactor chamber; 2: thermocouple; 3,5: quartz wool; 4: catalyst bed. (b) micro-reactor. 1: cross fitting; 2: connector; 3: reactor chamber; 4: thermocouple; 5: thermowell; 6: glass beads; 7,9: quartz wool; 8: catalyst bed; 10: support tube.

Schematic diagrams of the two reactors are shown in Figure 2.3. In the lab reactor, the catalyst bed was sandwiched between quartz wools. For the micro-reactor, the reactor chamber had a cross fitting for introducing reactant gas as well as

water if necessary. The top zone of the reactor was normally packed with glass beads (2mm diameters, Sigma Aldrich), functioning as a pre-heater (and pre-mixer when more than one line was used in the system). The middle zone was the reaction zone and placed within it the catalyst bed which typically consisted of catalyst and SiC (80 grit, Fischer Scientific). The ratio of volume of catalyst and SiC is detailed in the experimental part of the relevant chapters. The bottom zone had a support tube to hold the weight of the materials of the two zones above.

In contrast to the tubular fixed bed reactor introduced in chapter 1, both reactors used in this study did not have a cooling system attached, which was mainly due to the low catalyst loading and the associated low catalytic activity. In this study, most of catalytic tests were carried out with the micro-reactor due to its excellent characteristics for providing a stable thermal regime.

2.2.2 Product analysis

2.2.2.1 Gas chromatography and mass spectroscopy

Gas chromatography (GC) is an analytical technique used to separate mixtures of chemicals into individual components based on their volatilities and/or polarity. Quantification of individual compounds can be obtained if there is good separation.

Mass spectroscopy (MS) is a technique used to identify a compound. The compound is first fragmented into small ions. According to their mass-to-charge ratios, the ions are sorted in a mass analyzer and then collected by a detector to produce a mass spectrum. For a given molecule, its mass spectrum is unique, which can be used to identify an unknown compound.

The combination of GC and MS provides a powerful tool to analyze unknown chemical mixtures. The mixtures can be first separated, then identified and finally quantified.

2.2.2.2 Experimental

Analysis of gaseous product was achieved by an online gas chromatograph (GC, Varian 3800). A 5m*1/8 inch stainless steel Porapak-Q column (mesh size 80-100) was used to separate the reactants and products. Concentrations of hydrogen, carbon monoxide, carbon dioxide and nitrogen were analyzed by a thermal conductivity detector (TCD). The TCD compares the conductivity of the analyzed gas to that of a reference gas. Conversion was determined using an internal standard, nitrogen. Organic compounds such as hydrocarbons and oxygenates were determined by a flame ionization detector (FID). By using a hydrogen and air flame, the FID burns the organic compounds into ions whose amounts are roughly proportional to the number of carbon atoms present.

Liquid products were identified by gas chromatography mass spectrometer (GC-MS, Perkin Elmer TurboMass). Quantification of liquid products was determined by an offline GC equipped with a Chrompack capillary column (CP-Sil 8CB, 30m, 0.32mm, 1μm) and an FID detector. Either 2-propanol or 3-pentanol was chosen as an internal standard for the quantification depending on whether it was absent from the product mixture or not.

2.3 Catalyst Characterization

2.3.1 Brunauer Emmett Teller (BET) method

In heterogeneous catalysis, gas diffusion, adsorption processes are very closely related with surface area and porosity of the solid catalyst. Surface area provides information about the porosity which helps to understand the structure of solid catalysts. Surface area can also be used in the measurement of the activity of a solid catalyst.

The BET method is the most commonly used technique for the determination of the surface area of a solid material. The concept of the BET method is an extension of Langmuir theory, which involves monolayer molecular adsorption, to multilayer adsorption. The following assumptions are used to derive the BET equation.

(1) The adsorption of the 1st layer takes place on a uniform solid surface.

(2) There is no interaction between molecules adsorbed in a given layer. The 2nd layer only adsorbs on the 1st layer, and the 3rd only on 2nd one, and so on.

(3) Langmuir model is applied to every layer.

(4) For layers ≥ 2, the heat of adsorption is equal to the heat of condensation.

The BET equation is expressed below as:

$$\frac{p}{V(p_0 - p)} = \frac{1}{V_m C} + \frac{C-1}{V_m C} \bullet \frac{p}{p_0} \qquad (2.1)$$

Where p and p_0 are the equilibrium and saturation pressure, V is the volume of gas adsorbed at pressure p, V_m is the volume of gas required to form a monolayer and C is a constant related to the heat of adsorption.

Based on experimental results, equation 2.1 can be plotted as $\frac{p}{V(p_0 - p)}$ versus $\frac{p}{p_0}$. The slope and y intercept of the BET plot are equal to $\frac{C-1}{V_m C}$ and $\frac{1}{V_m C}$ respectively. With the monolayer volume V_m known, the surface area can be obtained by:

$$A_s = \frac{V_m}{22414} N_A \sigma \tag{2.2}$$

Where N_A is the Avogadro number, and σ is the area of one nitrogen molecule (generally accepted as 0.162 nm^2).

Measurement of the BET surface area was achieved by N_2 physi-sorption at the temperature of liquid nitrogen. Prior to each measurement, the sample was degassed for 1 h at 393K under flowing N_2. Measurement was performed using Micromeritics ASAP2000 (Gemini). Sample tube (with sample) was first evacuated and the void volume of the apparatus measured using helium. Afterwards the sample tube was immersed into liquid nitrogen, followed by adding nitrogen to start adsorption. Data of pressure drop versus volume of nitrogen adsorbed were then recorded, which could be used to calculate the surface area according to the method described above.

2.3.2 X-Ray Diffraction

Solid materials can be divided into amorphous and crystalline depending on whether the atoms are arranged in a regular pattern. Approximately 95% of solids belong to the crystalline category. X-Ray Diffraction (XRD) is a technique which can reveal information about the structure of crystalline materials.

Diffraction occurs when electromagnetic radiation impinges on a material with a comparable length scale to the wavelength of radiation. The distances of crystal lattices are between 0.15-0.4 nm that is within the electromagnetic spectrum of X-ray, which allows diffraction to occur.

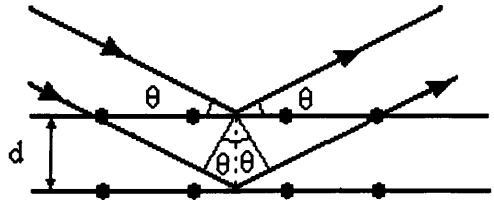

Figure 2.4 X-Ray beams on a crystal

Figure 2.4 shows a simple illustration of X-ray diffraction. Two X-ray beams with wavelength λ are reflected from two adjacent crystal planes. The resulting diffraction follows a mathematical correlation called Bragg's law:

$$d = \frac{n\lambda}{2\sin\theta} \tag{2.3}$$

Where d is the interplanar spacing, θ is the diffraction angle, n is an integer and λ is the wavelength of the radiation.

Powder XRD is one of the widely used XRD techniques. It offers information on the dimensions and content of the elementary cell, crystallite size and quantities of the phases present. In the powder XRD, a sample contains a large number of randomly oriented crystalline particles, of which those orientated at the Bragg angle θ produce a diffracted beam of angle 2θ.

The powder XRD method has used in this study to characterize catalysts. An Enraf Nonius PSD120 diffractometer with a monochromatic CuKα source operated at

40 keV and 30 mA was used to obtain intensity and 2θ values. Phase identification was performed by matching experimental patterns to the JCPDS data base.

2.3.3 Raman spectroscopy

Raman spectroscopy is a useful technique for fingerprint identification of substances according to their vibrational modes. It can be used for solids, liquids and gases. In this study, Raman spectroscopy was used for the characterization of solid catalyst, mainly metal oxide systems.

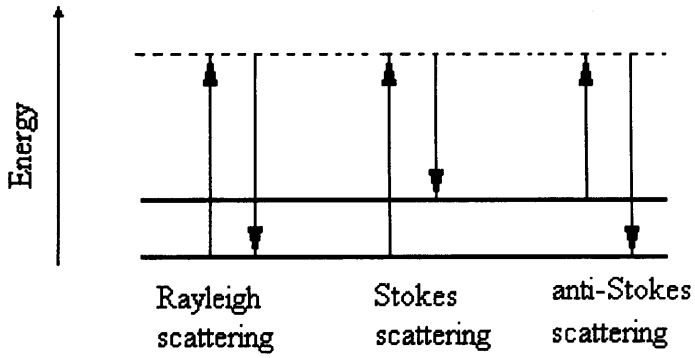

Figure 2.5 Rayleigh and Raman (Stokes and anti-Stokes) scattering

When a monochromatic light impinges on a sample at the molecular level some of photons are absorbed and some are scattered. If the scattered photons have the same frequency as those incident photons, the scatter is called Rayleigh scattering. If there is a frequency change, it is called a Raman shift. The shift towards higher frequency is referred to as anti-Stokes scattering, and to lower frequency as Stokes scattering. Figure 2.5 shows energy-level diagrams for Rayleigh scattering, anti-Stokes scattering and Stokes scattering.

Measurement of Raman spectra is achieved by analyzing scattered light from a sample when the sample is illuminated by a monochromatic light beam. Raman spectroscopy was performed using a Renishaw 1000 Raman microscope spectrometer. An argon ion laser was the photon source giving a monochromatic radiation of 514.5 nm. For each sample, typically 10 accumulations of scanning were performed over the range of 150 to 1200 cm^{-1}. The signal was detected by a charge-coupled device (CCD) with final processing by computer. The obtained spectra were compared with reference spectra from the literature for identification.

2.3.4 Temperature programmed reduction

Temperature programmed reduction (TPR) is a characterization technique used to gain information on the reduction behavior of metal oxide and sulfide catalysts. The direct information obtained includes the number of defined peaks in the TPR profile and the corresponding temperature at which these peaks occur. Characteristics including the ease with which species can be reduced, the state of metallic compounds, interactions of metal-metal and metal-support can be revealed. These characteristics can then be used for the optimization of catalyst pretreatment.

In a typical TPR measurement, a reducing mixture normally consisting of hydrogen and an inert gas passes through a catalyst bed at a constant flow rate. The rates of hydrogen adsorption and desorption were constantly monitored by a TCD which is highly sensitive to hydrogen concentration. The obtained TPR trace displays intensity as a function of temperature.

A TPDRO 1100 series (Thermo Electron Corporation) was used to perform the TPR measurements. Typical measurement was performed by sandwiching a sample (0.03 g) with quartz wool in a quartz reactor tube. The sample was out-gassed

by heating at 393K for 40 minutes in a stream of Ar (15 cm^3/min). After cooling down to ambient temperature, Ar was switched to a gas mixture made of 10% H_2/Ar. A cold trap containing a mixture of liquid nitrogen and iso-propanol was used to trap water that was produced from the reduction of the metal oxide. The gas mixture (20 cm^3/min) flowed through the reactor, followed by an increase of temperature at 5K/min from ambient to 773K and then returned to ambient. The consumption of hydrogen during the reaction was recorded by a TCD detector, giving intensity as function of temperature.

References

[1] M. V. Twigg, Catalyst Handbook, 2nd edition, Wolfe Publishing (1989)

[2] J. Haber, J.H. Block and B. Delmon, Pure & Appl. Chem., 87(8) (1995) 1257

[3] F. Pinna, Catal.Today, 41 (1998) 129

[4] World Gold Council: Gold reference catalysts, Gold Bull. 36 (2003) 1

Chapter 3 CO hydrogenation for higher alcohol synthesis over Co-MoS_2 based and Cu-Co based catalysts

3.1 Introduction

With the development of syngas technology, mixed alcohol synthesis or higher alcohol synthesis from syngas has attracted increasing attention which has been attributed to its wide application in fuel industry. When used as fuel additives to gasoline, mixed alcohols boost the octane number and reduce the environmentally related pollution.

Among the catalyst systems as described in Chapter 1, alkali-doped molybdenum sulfide based catalyst and the IFP catalyst have been paid much attention and this has been attributed to the high activity and selectivity.

Alkali-doped molybdenum sulfide based catalysts

Molybdenum sulfide based catalysts deserve special attention due to their high selectivity to C_{2+} alcohol synthesis and natural resistance against sulfur. This catalyst

was first discovered to be active for higher alcohol synthesis (HAS) by Dow [1, 2] and Union Carbide [3]. The catalyst system has been studied by several academic research groups [4-6].

Dow investigated alkali doped Co-MoS_2 catalysts prepared by a co-precipitation method to make higher alcohols. They reported that the alcohol selectivity could be increased by increasing pressure, space velocity and by decreasing H_2/CO feed ratio and temperature. Alkali doped Co-MoS_2 catalysts have also been investigated by Iranmahboob and co-workers [6-8]. The influence of cobalt, clay and potassium has been thoroughly studied. The highest oxygenates-productivity was obtained at 583 K and 135 bar for the catalyst with Co/Mo atomic ratio about 0.5 and K_2CO_3 about 12.5%. They also found that a temperature range of 563 – 583 K provided suitable condition for clay to act as modifier of the investigated catalyst, increasing the catalyst activity and higher alcohol selectivity [6]. For K and Cs promoted Co-MoS_2/clay catalyst, they found that the increase in reaction temperature led to increased alcohol yield however decreased alcohol selectivity [9].

The addition of potassium to the MoS_2 based catalyst was also investigated by other groups [1, 4, 10]. These authors found that the addition of potassium lowered the CO conversion and shift the products from hydrocarbons to alcohols.

The function of cobalt in Co-MoS_2 based catalysts was considered to modify the product selectivity mainly towards higher alcohols, which could be attributed to the capability of cobalt in promoting carbon chain growth [11-14].

The nature of cobalt atoms in MoS_2 catalysts was also investigated. Farragher suggested that cobalt atoms at the MoS_2 edges are located between adjacent MoS_2 layers [15]. Topsøe *et al.* proposed a model of 'Co-Mo-S' in which Co atoms were

located at MoS_2 edges in a 'decoration' mode [16, 17]. This model was generally accepted. The XRD analysis by Iranmahboob *et al.* [8] suggested that Co-MoS_2 is a primary phase in potassium doped cobalt molybdenum sulfide catalyst.

The IFP catalyst

IFP was granted a series of patents for its HAS catalyst which mainly consists of homogeneously mixed copper and cobalt oxides.

One patent granted in 1978 described catalysts with formula $Cu_1Co_1Cr_{0.8}K_{0.09}$, in which Cr could be replaced by Mn, Fe and V, and K could be replaced by Li or Na [18]. This catalyst was found to deactivate very fast. Another one in 1981 described the previous catalyst modified by the addition of rare earth and noble metal in a weight percentage of 0.005 and 0.5 [19]. Deactivation of this catalyst was not as severe as the previous one. In 1983, a further modification was made by introducing Al to the system replacing or adding to Cr and Re [20]. Catalyst described in the patent in 1987 comprised of 10 – 65% Cu, 5 – 50% Co, 1 – 50% Zn, 5 – 40% Al, alkali or alkaline earth metal [21]. For the last two catalysts in series, only little deactivation was observed during the start up stage of the reaction. The start up of the reaction for these two catalysts requires progress substitution of the syngas for the inert gas to avoid a transitory methanation reaction. The patent in 1988 described new catalysts with a composition of 15 – 55% Cu, 5 – 25% Co, 15 – 70% Zn, 0 – 55% Zr, 0.01 – 5% A (alkali or alkaline earth metals), 0 – 20% M (from La, Ce, Pr or Nd) and 0 – 1% N (from Rh, Pd or Pt) [22]. With this invention, the catalytic reaction only needs to be conditioned under hydrogen or syngas in a simple manner with reduced transitory methanation reaction.

For the IFP catalyst, the homogeneity of obtained catalyst is important to achieve high catalyst activity. Structural in-homogeneity and chemical segregation of more than 15% are detrimental for HAS [20, 23]. Co-precipitation technique was employed in preparation of the IFP catalyst. Various co-precipitation techniques including a continuous batch flow reactor (see Chapter 2) were reported by Courty *et al.* [24]. The continuous batch flow reactor is advantageous over traditional batch reactor because the former one could maintain equal residence time for any portion of the precipitate at a specific temperature and pH value, which ensures the homogeneity of final product.

The preparation of the IFP catalyst is a complicated procedure due to many steps and variables involved. These variables have to be carefully controlled [25]. So far, the results claimed by IFP have not been replicated by other researchers. The effect of catalyst preparation variables on the performance of Cu/Co/Al/Zn catalysts were investigated by Baker and co-workers [26]. They found the order of importance for preparation of dry precursors as: ageing of precipitate > precipitation temperature > pH > total metal ion concentration > drying temperature. They also found that thermal activation of the dry precursors is the single most important variable in the preparation of these catalysts. A similar conclusion on the importance of variables was drawn in a recent study by Mahdavi *et al.* [27].

For the above two catalyst systems, although so many investigations were reported and discussed, the detailed catalyst preparation procedure and catalytic data has not been fully disclosed so far. This chapter is aimed to explore the activation procedure and operation condition for the above two catalyst systems, demonstrating a high yield toward higher alcohols particularly over Co-MoS_2 based catalysts.

3.2 Experimental

Alkali-promoted cobalt molybdenum sulfide solid (Co-MoS_2/K_2CO_3) mixed with bentonite clay and sterotex® lubricant was used for the Co-MoS_2 based catalyst in this study. The Co-MoS_2 (Mo:Co = 2:1) solid was prepared by co-precipitation as described in Chapter 2.

As mentioned in Chapter 2, the ramping rate of calcinations (10 K/min or 25 K/min) and the weight percentage of K_2CO_3 (10% or 12.5%) were changed for different samples, which are detailed in the results section.

For Cu/Co based catalyst, mixed oxides containing mainly metals Cu, Co, Zr and Zn were used in this study. The mixed oxides were prepared by co-precipitation technique following the IFP patent in 1988 [22].

Catalytic tests were carried out using Lab reactor and Micro reactor which are described in Chapter 2. A neat catalyst bed was used in the Lab reactor with 0.3 ml catalyst loading. A diluted catalyst bed was used in the Micro reactor. The dilution was performed by intimate mixing of the catalyst with silicon carbide (4.8 ml/5.2 ml for Co-MoS_2 based catalyst and 1 ml/9 ml for Cu-Co based catalyst).

Prior to the catalytic run, system leakage test was carried out using nitrogen (Oxygen free, BOC). After the system was found safe and leak-free, syngas was gradually introduced to the system, replacing the nitrogen. Following the complete replacement, the system was brought up to the required pressure, followed by heating with a ramping rate of 1 K/min until it reached the desired temperature. Detailed reaction parameters were given in each specific catalytic test.

3.3 Results on Co-MoS_2 based catalyst system

3.3.1 Catalyst characterization

The physical adsorption and structural information about the Co-MoS_2 solid were obtained by the use of BET method and X-ray diffraction (XRD) technique (see Chapter 2 for details). Additionally, the temperature programmed reduction (TPR) technique was used in order to collect information about the reducibility of the metal sulfide precursor.

The analysis of metal content was given by Inductively Coupled Plasma Mass Spectroscopy (ICP-MS) (Earth department, Cardiff University). The obtained ratio of metal components is: Mo/Co = 2.2.

3.3.1.1 BET surface area

The surface areas of Co-MoS_2 solid obtained with different ramping rate were measured using BET method. For catalysts with calcinations carried out at 10 K/min, the obtained BET surface area was 16 m^2/g, whereas for those at 25 K/min, the BET surface area was 35 m^2/g. This is consistent with the findings on the reduction of MoS_3 to MoS_2 by Utz and co-workers [28]. They found that a rapid increase in temperature during the reduction causes an increase in the surface area.

3.3.1.2 X-ray diffraction results

Figure 3.1 shows the XRD pattern of the sample. The solid sample was identified as belonging to the MoS_2. This was concluded because of the characteristic reflections at $2\theta = 33.4°$, 39.4°, 50° and 59°.

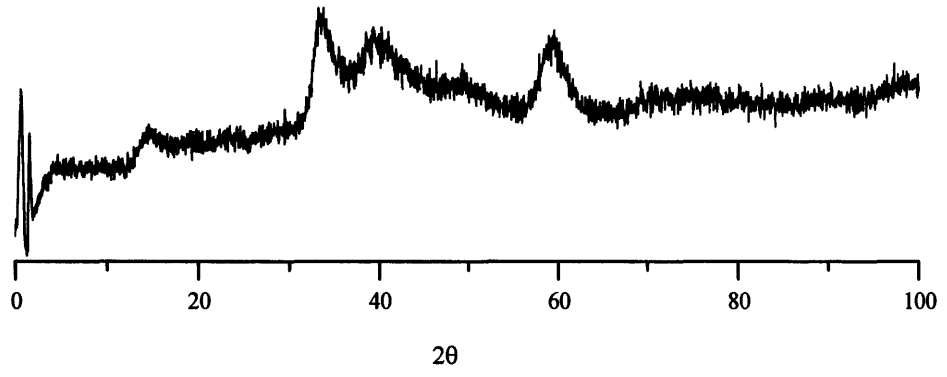

Figure 3.1 XRD patterns of Co-MoS_2 solid

3.3.1.3 Temperature programmed reduction

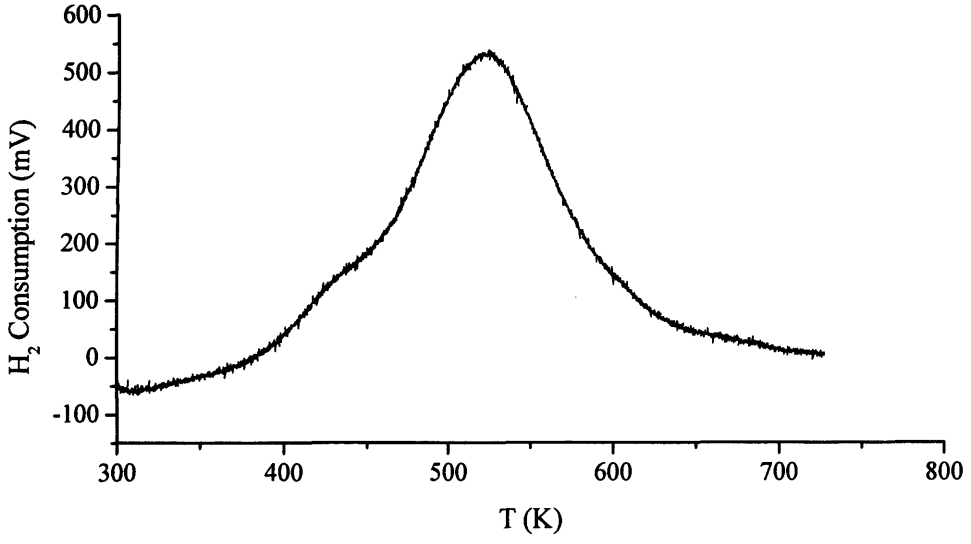

Figure 3.2 TPR profile for Co-MoS_2 solid

TPR technique was used to study the influence of hydrogen reduction on the investigated catalysts. The TPR profiles for the catalysts are shown in Figure 3.2.

A broad peak was observed at 350 – 650 K. It could be attributed to the hydrogenation of surface sulfur atoms [29]. This indicates that the surface sulfur could be removed as H_2S from the surface of the catalyst when hydrogen reduction was employed. As introduced in Chapter 1, one of the requirements for good performance of this catalyst is keeping sulfidity of the catalyst; hence the catalyst used in this study was without any pretreatment.

3.3.2 Catalytic results

The present section describes the CO hydrogenation activity of Co-MoS_2/K_2CO_3/clay/lubricant catalyst. Silicon carbide intimately mixed with catalyst was used when Micro reactor was employed for the catalytic reaction. Before catalytic test, a blank run with silicon carbide was carried out. There was no catalytic activity observed with the blank run. This suggests that silicon carbide is an inert material with respect to CO hydrogenation and hence can be used as diluent for catalytic test. Reasons of diluting the catalyst bed are: (1) to achieve and maintain an isothermal regime for the reaction; and (2) to avoid possible hot spots developing in the catalyst bed.

3.3.2.1 Catalyst aerial oxidation

As a preliminary test, catalytic reaction using the Lab reactor was carried out. Two catalytic runs were performed over the same batch of catalyst however with different life time. One was obtained by freshly grinding Co-MoS_2 solid with K_2CO_3, clay and lubricant for immediate use, hereafter denoted as fresh catalyst. The other

one was obtained by exposure to atmospheric air of the former catalyst for 1 week, hereafter denoted as old catalyst.

Alcohols including methanol, ethanol, 1-propanol, 2-methyl-1-propanol and 1-butanol were synthesized from the above two catalytic tests. A volume of 0.4 ml mixed alcohol was collected in the reaction involving the fresh catalyst, whereas 0.1 ml was obtained with the old catalyst. Figure 3.3 presents CO conversion and hydrocarbon yields.

In general, the conversions in both cases were very low (< 2%). This could be due to the low pressure employed in the catalytic reactions. According to the figures above, the CO conversion (Figure 3.3 a), hydrocarbon yields (Figure 3.3 c) and alcohol productivity decreased when the old catalyst was employed. A higher activity for the fresh catalyst was observed with respect to that of the old one, suggesting that the sulfided catalyst may become deactivated by exposure to atmospheric air. A similar finding was reported by Woo *et al.* over fresh and oxidized K_2CO_3/MoS_2 catalysts [30]. It is very likely that the presence of K_2CO_3, clay and lubricant may facilitate this oxidation.

This preliminary test demonstrated that fresh catalyst was more preferred for the synthesis of hydrocarbons and alcohols. This is the reason why fresh catalysts were employed in all the remaining catalytic tests.

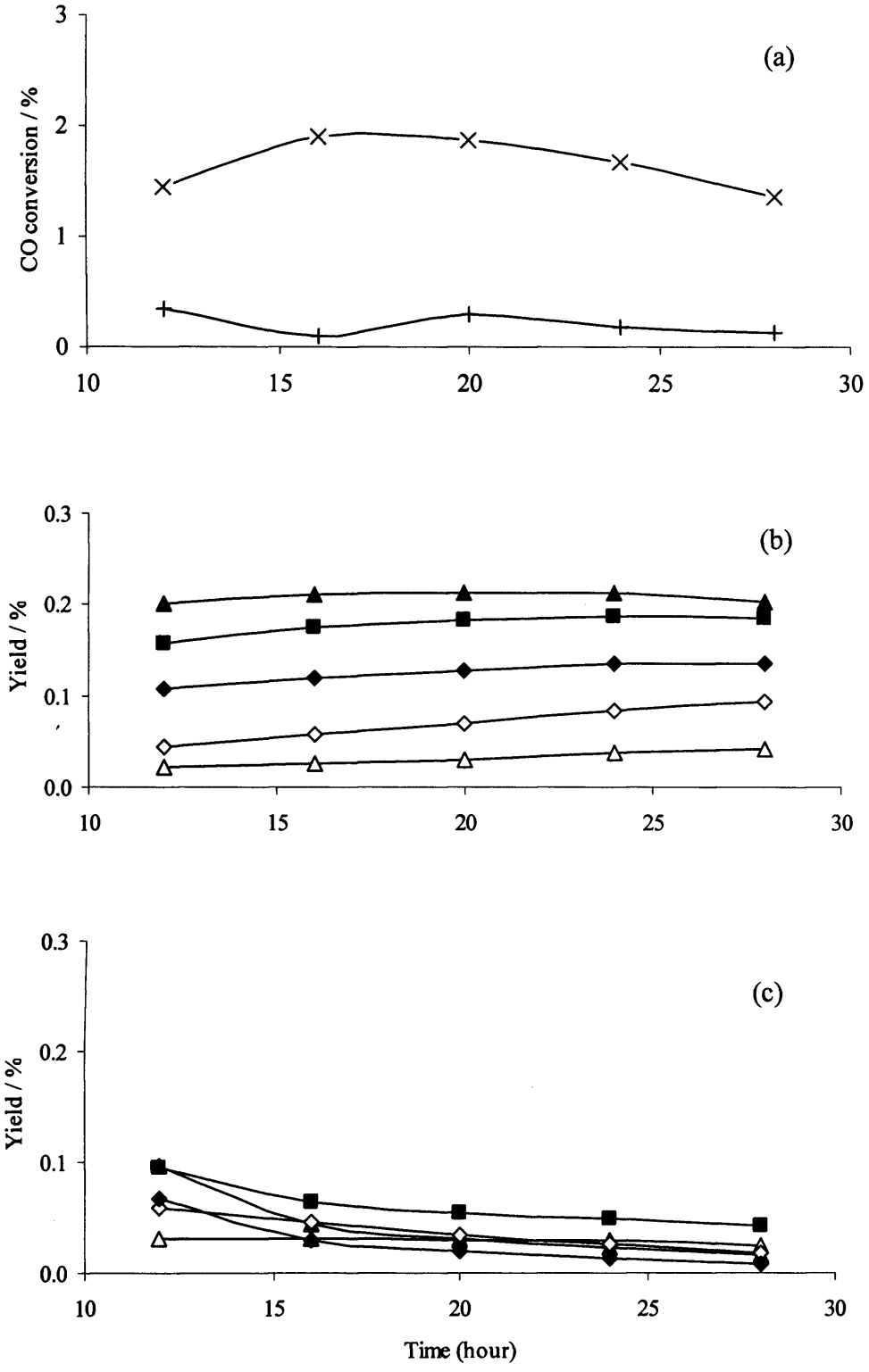

Figure 3.3 Gas phase time online data of CO hydrogenation over Co-MoS/K_2CO_3/clay/lubricant catalyst (a) CO conversion: × fresh catalyst, + old catalyst; (b) hydrocarbon yield over fresh catalyst; (c) hydrocarbon yield over old catalyst: ■ CH_4; Δ C_2H_4; ▲C_2H_6; ◊ C_3H_6; ♦ C_3H_8. Reaction conditions: 578 K, 20 Bar, CO/H_2 (1:1 mol ratio), GHSV (gas hourly space velocity) = 1200 h^{-1}

3.3.2.2 Effect of temperature ramping rate for catalyst calcination on the catalyst performance

Catalysts with different ramping rates of calcinations were tested. Table 3.1 shows the results of overall analysis. According to these results, the ramping rate had a clear effect on the performance of the catalyst, since the CO conversion obtained over catalyst calcined at higher ramping rate (denoted as $Catalyst_{HRamp}$) almost doubled the conversion obtained for the catalyst calcined at a lower ramping rate (denoted as $Catalyst_{LRamp}$). Additionally, the results presented in Table 3.1 suggest that the selectivity of the obtained products is strongly influenced by ramping rate of catalyst calcinations. Generally, compared with $Catalyst_{LRamp}$, $Catalyst_{HRamp}$ had a lower selectivity in alcohols and higher selectivity in hydrocarbon products.

Figure 3.4 illustrates the CO conversion, gas phase hydrocarbon yield for the hydrogenation of CO at various times on stream for these two catalysts. From the CO conversion data, it can be seen that there were circa 20 – 30 hours needed for the reaction to reach stable condition. This induction period was also observed by Woo *et al.* [30] and Iranmahbood *et al.* [31]. The induction period could be the time required for the alkali promoters and/or clay to spread onto the Co-MoS_2 surface. After this period, both catalytic systems show rather stable activities during entire catalytic run.

For hydrocarbons yield, methane follow similar trend as conversion. However, for higher hydrocarbons, the yield first reached a maximum and then started to decrease slowly, which is much more clearly demonstrated by C_2 hydrocarbons.

Table 3.1 CO hydrogenation over Co-MoS_2/K_2CO_3/clay/lubricant catalyst calcined with different ramping rate

	Run 1	Run 2
Ramping rate of catalyst calcination (K/min)	10	25
Conversion of CO (exclusive CO_2) /%	10.1	18.9
Products (mol%)		
CH_4	12.2	24.9
C_2H_4	0.39	0.24
C_2H_6	1.05	8.87
C_3H_6	0.44	1.03
C_3H_8	0.33	4.91
C_4H_8	0.05	0.15
C_4H_{10}	0.27	1.53
C_5H_{10}	0.00	0.12
C_5H_{12}	0.00	0.43
Methanol	53.1	26.7
Ethanol	27.3	23.3
1-Propanol	4.30	6.28
2-methyl-1-Propanol	0.00	0.55
1-Butanol	0.57	0.91
Carbon mole Selectivity (%)		
CH_4	8.81	14.1
$C_{>2}$	4.71	25.9
Methanol	38.4	15.2
Ethanol	39.5	26.5
1-Propanol	9.32	10.7
2-methyl-1-Propanol	0.00	1.26
1-Butanol	1.64	2.07
Yield (%)		
Methanol	3.85	2.86
Ethanol	3.97	5.00
1-Propanol	0.94	2.02
2-methyl-1-Propanol	0.00	0.24
1-Butanol	0.16	0.39

Reaction conditions: 580 K, 75 Bar, CO/H_2 (1:1 mol ratio), GHSV = 1225 h^{-1}

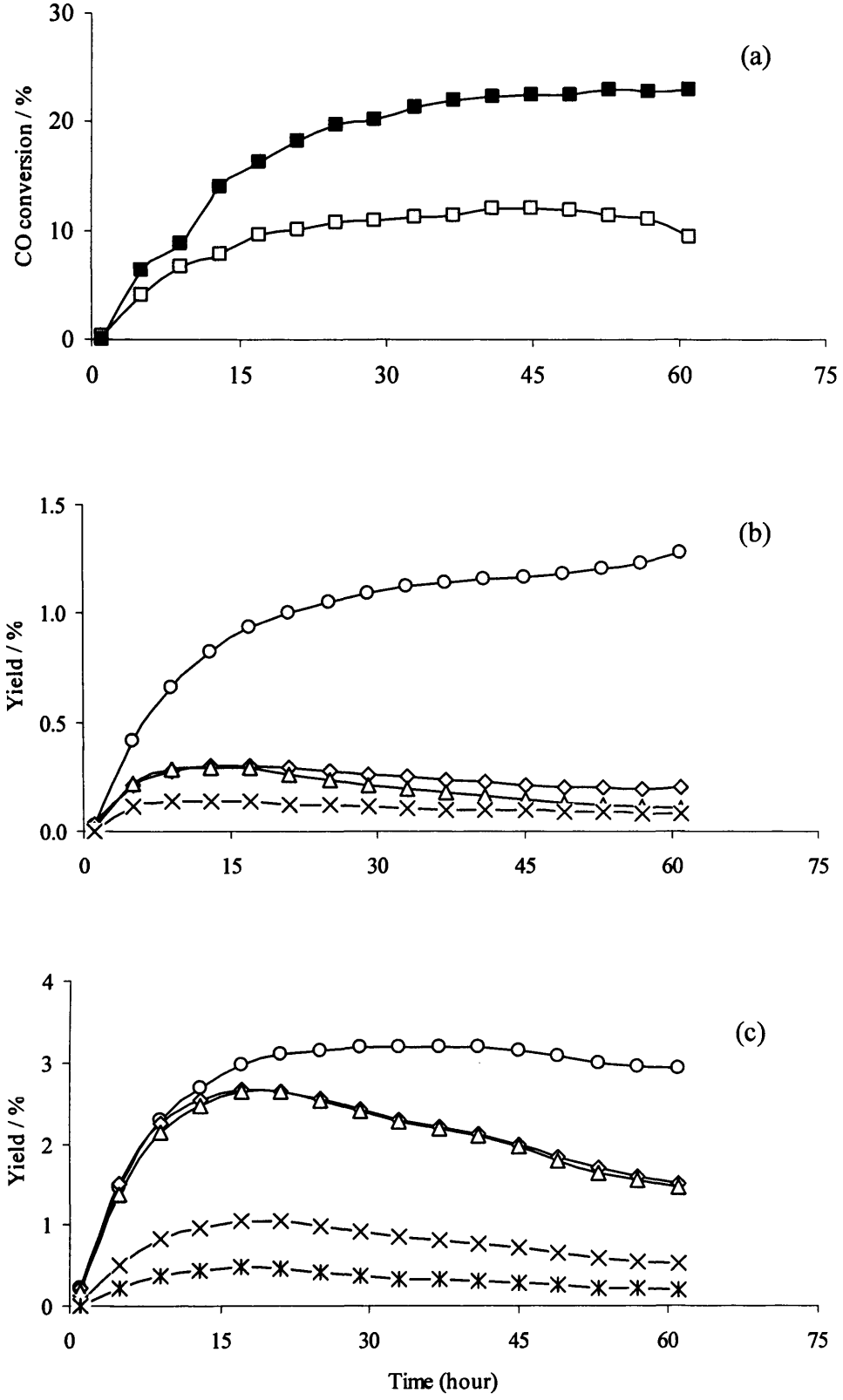

Figure 3.4 Gas phase time online data of CO hydrogenation over catalysts $Catalyst_{LRamp}$ and $Catalyst_{HRamp}$ (a) CO conversion: □ $Catalyst_{LRamp}$, ■ $Catalyst_{HRamp}$; (b) hydrocarbon yield over $Catalyst_{LRamp}$; (c) hydrocarbon yield over $Catalyst_{HRamp}$. ○ C_1; ◊ C_2; Δ C_3; × C_4; * C_5

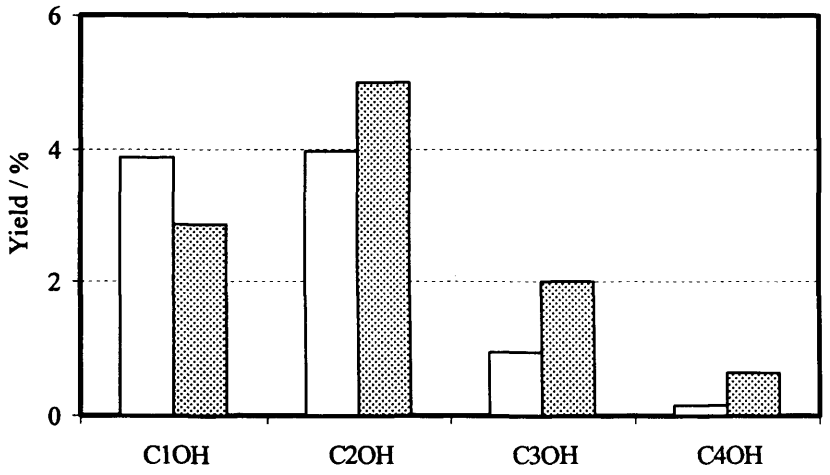

Figure 3.5 Effect of ramping rate of calcination on alcohol yield; □ $Catalyst_{LRamp}$ ⁙ $Catalyst_{HRamp}$

Due to the restriction of the current set-up, it was not possible to obtain online liquid analysis. All the liquid was analyzed together after the reaction completed. There was no hydrocarbon detected in the liquid product. Figure 3.5 compares the yields of alcohol products. Clearly, it can see that $Catalyst_{HRamp}$ had higher yield for $C_2 - C_4$ alcohols than that obtained from $Catalyst_{LRamp}$. A reverse trend was observed on methanol yield.

Since the only difference between these catalysts were the ramping rate of calcinations, the observed results could be very likely related to the change in surface area due to different calcination conditions. As can be seen from the BET results, the surface area was more than doubled for the catalyst calcined with higher ramping rate employed. This high surface area could be responsible for the high activity of catalyst and high yield towards higher alcohols. Since the investigation on Co-MoS_2/K_2CO_3/clay/lubricant catalyst was aimed at higher alcohol synthesis, the following tests were carried out over catalyst prepared by high ramping rate.

3.3.2.3 Performance of Co-MoS_2/K_2CO_3/clay/lubricant catalyst

Table 3.2 Results of CO hydrogenation over Co-MoS_2/K_2CO_3/clay/lubricant catalyst

	Run 2	Run 3	Run 4	Run 5	Run 6
Temperature, K	580	580	580	603	580
Pressure, Bar	75	75	75	75	75
GHSV, h^{-1}	1225	1225	2450	2450	1225
Feed ratio, H_2/CO	1	1	1	1	2
K_2CO_3, %	10	12.5	12.5	12.5	10
Conversion of CO (exclusive CO_2) /%	18.9	16.5	10.9	18.8	30.6
Products (mol%)					
CH_4	24.9	19.8	18.0	22.4	24.4
C_2H_4	0.24	0.34	0.56	0.44	0.08
C_2H_6	8.87	3.36	2.90	3.63	6.10
C_3H_6	1.03	0.67	0.67	0.96	0.32
C_3H_8	4.91	1.51	1.18	1.76	2.65
C_4H_8	0.15	0.07	0.06	0.15	0.03
C_4H_{10}	1.53	0.51	0.35	0.61	0.64
C_5H_{10}	0.12	0.04	0.00	0.06	0.05
C_5H_{12}	0.43	0.16	0.00	0.19	0.15
Methanol	26.7	36.0	46.9	34.0	37.9
Ethanol	23.3	29.5	25.9	28.4	23.2
1-Propanol	6.28	6.67	2.98	6.00	3.92
2-methyl-1-Propanol	0.55	0.56	0.26	0.64	0.22
1-Butanol	0.91	0.78	0.32	0.75	0.41
Carbon mole Selectivity (%)					
CH_4	14.1	13.0	12.7	13.4	17.0
$C_{>2}$	25.9	11.3	9.94	12.3	17.4
Methanol	15.2	23.7	33.0	20.4	26.5
Ethanol	26.5	38.8	36.4	34.0	32.4
1-Propanol	10.7	13.2	6.29	10.8	8.22
2-methyl -1-Propanol	1.26	1.46	0.73	1.53	0.62
1-Butanol	2.07	2.04	0.90	1.79	1.15
Yield (%)					
Methanol	2.86	3.91	3.60	3.83	8.10
Ethanol	5.00	6.41	3.97	6.41	9.92
1-Propanol	2.02	2.17	0.69	2.03	2.52
2-methyl-1-Propanol	0.24	0.24	0.08	0.29	0.19
1-Butanol	0.39	0.34	0.10	0.34	0.35

Bearing in mind that the oxidation on exposure to atmospheric air and calcination conditions could play an important role in the performance of the catalysts, a series of catalytic tests were performed to investigate the impact of promoter, GHSV, temperature and ratio of syngas on the CO hydrogenation over Co-MoS_2/K_2CO_3/clay/lubricant catalyst.

Table 3.2 shows the CO conversion (CO_2 free), mole percentage of gas and liquid product, alcohol selectivity and alcohol yield as a function of concentration of K_2CO_3, GHSV, temperature and syngas ratio.

Concentration of K_2CO_3

The impact of K_2CO_3 concentration on the reaction can be studied by comparing data of Run 2 and Run 3. With an increasing in K_2CO_3 concentration from 10% to 12.5%, CO conversion and selectivity towards methane showed slight drop. For higher hydrocarbons (C>2), the selectivity with higher potassium concentration was more than half of that obtained from catalyst with lower concentration. Figure 3.6 depicts the impact of concentration of K_2CO_3 on CO conversion, alcohol selectivity and alcohol yield. Generally there was increase in the alcohol selectivity as well as yield with the exception that in both cases C_4 alcohol remained almost the same.

The observed reaction results indicate that the role of K is supposed to slow down the hydrogenation of CO to hydrocarbons by blocking the active site for formation of higher hydrocarbons, simultaneously creating active site for the synthesis of alcohols. This is consistent with the finding of Iranmahbood *et al.* in the literature [9].

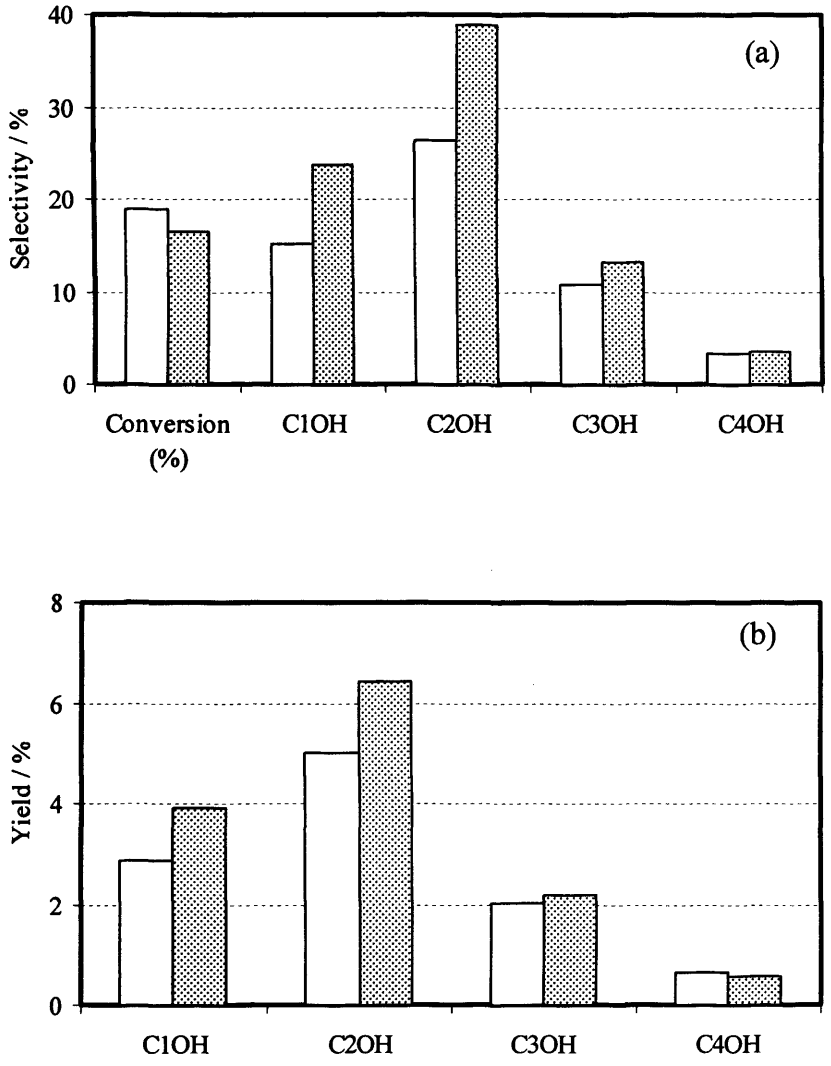

Figure 3.6 Impact of K_2CO_3 concentration on (a) CO conversion and alcohol selectivity; (b) alcohol yield; □ 10% K_2CO_3 ⁙ 12.5% K_2CO_3

GHSV

Catalyst with 12.5% K_2CO_3 was also evaluated as a function of GHSV at 580 K and 75 bar. Run 3 and Run 4 were the corresponding tests at GHSV of 1225 and 2450 h^{-1} respectively. The CO conversion, alcohol selectivity and yield are illustrated in Figure 3.7.

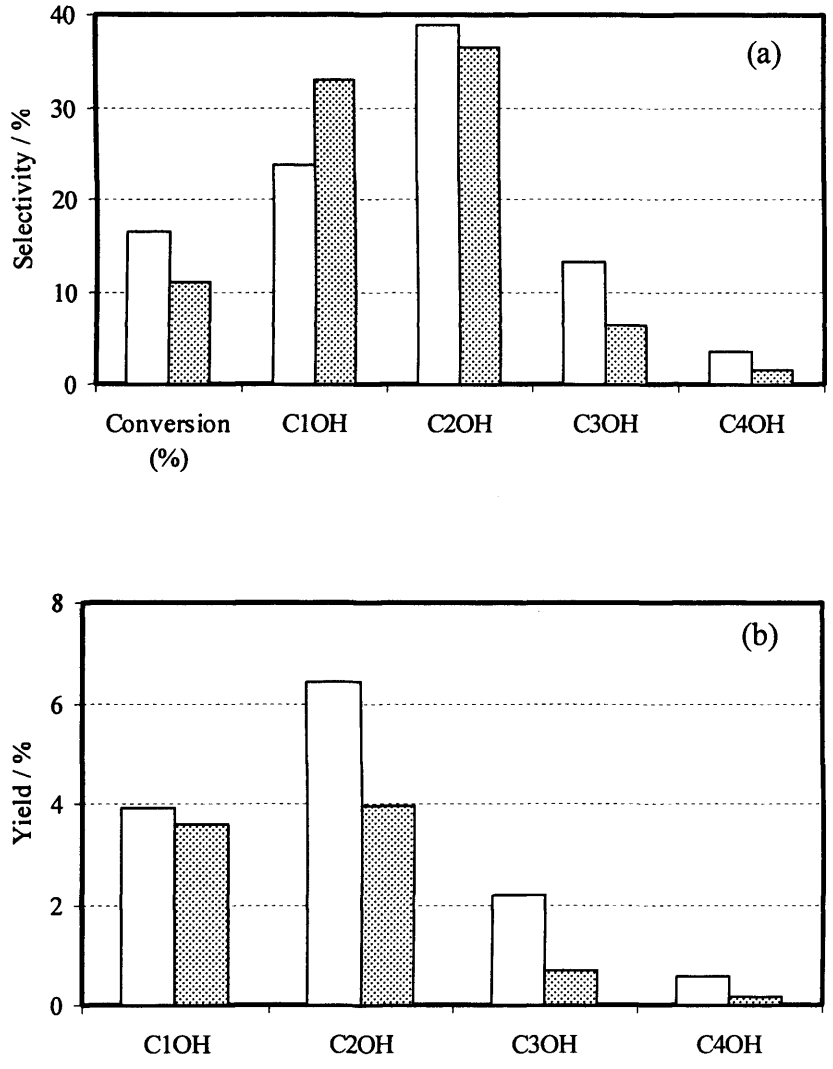

Figure 3.7 Impact of GHSV on (a) CO conversion and alcohol selectivity; (b) alcohol yield; □ GHSV=1225 ⁙ GHSV=2450

As GHSV doubled, the CO conversion was decreased from 17% to 11%. For hydrocarbons, both methane and higher hydrocarbons showed decreased selectivity. For alcohol products, methanol selectivity was increased whereas the C_{2+} alcohol selectivity was decreased. This finding is in agreement with the results obtained by Murchison and co-workers [32]. The yield for all alcohols showed decreased trend as GHSV doubled.

Temperature

The impact of temperature was tested at 580 K in Run 4 and at 603 K in Run 5 with GHSV at 2450 h^{-1}. An increase in reaction temperature led to an increase in CO conversion, selectivity for methane and higher hydrocarbons.

The impact of temperature on CO conversion, alcohol selectivity and yield is illustrated in Figure 3.8. Selectivity of methanol and ethanol was decreased with the increase in temperature. However, for C_3 and C_4 alcohols, it was noticed that both selectivities were increased with the temperature. The observed results were in general agreement with the trend reported by Iranmahboob [7]. They investigated production distribution on the same type of catalyst over temperature range from 563 – 593 K, with GHSV=1800 h^{-1} and 136 bar pressure. Their results show that with the increase in temperature, methanol composition was decreased over the whole range, and ethanol gave a maximum around 573 K, whereas the compositions of C_3 and C_4 alcohol kept increasing. This may indicate that for a specific fuel alcohol, different optimum temperature or even operation condition exists.

As for alcohol yield, there were increases for all the alcohols, which were mainly attributed to the significant increase in CO conversion.

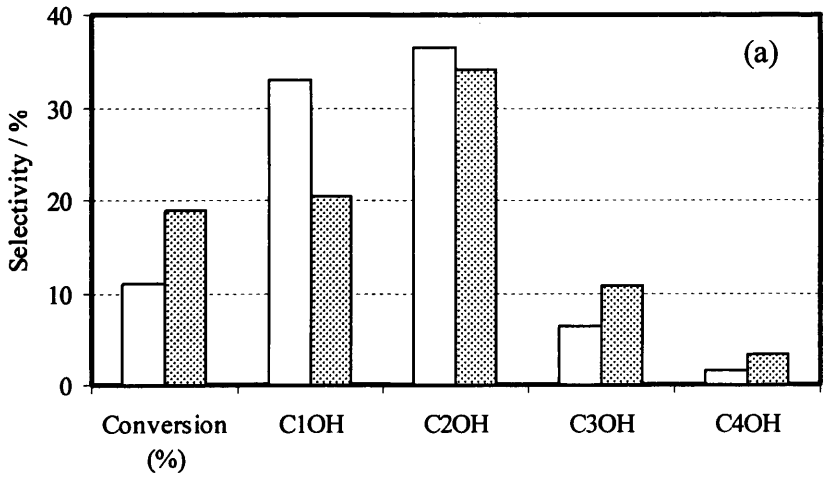

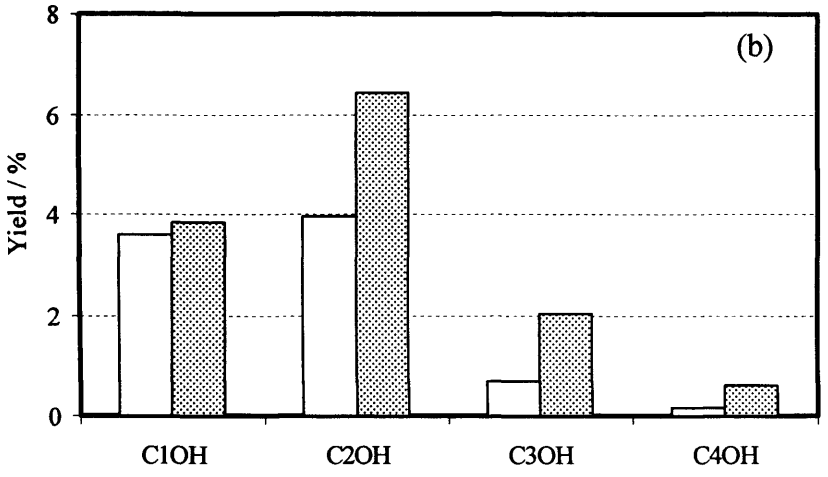

Figure 3.8 Impact of temperature on (a) CO conversion and alcohol selectivity; (b) alcohol yield; □ 580 K ⁙ 603 K

Syngas composition

For the FT synthesis, the stoichiometric number is dependent on the syngas composition or the ratio of H_2 to CO, which may have influence on the catalytic reaction. A syngas ratio of 2 (H_2/CO) was employed in Run 6 to study the impact of syngas ratio with Run 2 (H_2/CO=1) as reference. The reaction was carried out over catalyst with 10% K_2CO_3 at 580 K and 75 bar with GHSV = 1225 h^{-1}.

The increase in syngas ratio resulted in increased methane selectivity, whereas, decreased selectivity was observed for higher hydrocarbons.

The CO conversion, alcohol selectivity and yield are illustrated in Figure 3.9. When the syngas ratio doubled, the CO conversion was increased from 19% to 31%. Methanol, ethanol selectivity was also increased to different level. For C_3 and C_4 alcohols, there were slight drop in selectivity observed. Concerning the alcohol yield, the increase in syngas ratio led to increases in $C_1 - C_3$ alcohols, leaving unaffected the yield of C_4 alcohol. One possible explanation for the increased catalyst activity at higher syngas ratio in this study is that higher hydrogen partial pressure could

eliminate coke formation by side reactions, such as Boudouard reaction or methane decomposition.

Among the above tests, this test (Run 6) with a syngas ratio of 2 gave the highest alcohol yield. This result could be further improved by considering other reaction parameters as discussed before, e.g. the impact of K_2CO_3 concentration. A higher concentration of K_2CO_3, e.g. 12.5% with a syngas ratio of 2 may give improved results.

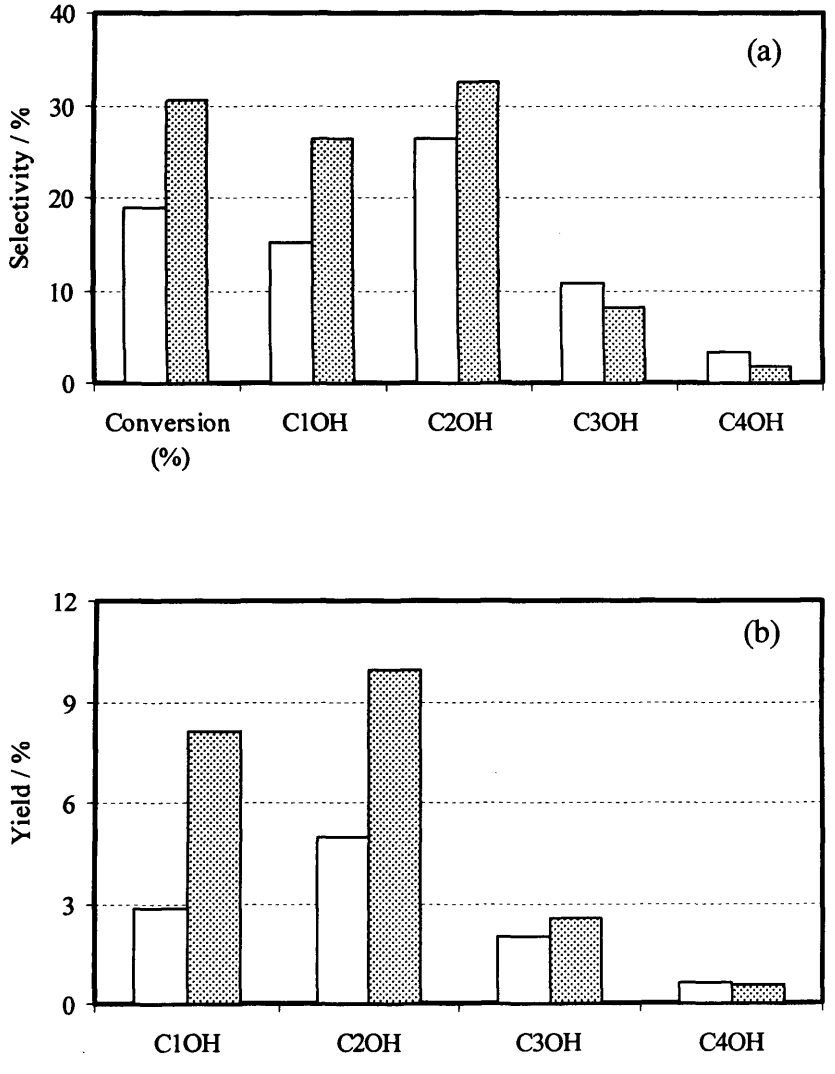

Figure 3.9 Impact of syngas composition on (a) CO conversion and alcohol selectivity; (b) alcohol yield; □ $H_2/CO = 1$ ⁙ $H_2/CO = 2$

Product distribution

The distribution of alcohol products were calculated according to the Anderson-Schulz-Flory (ASF) equation described in Chapter 1. The obtained ASF plots are shown in Figure 3.10.

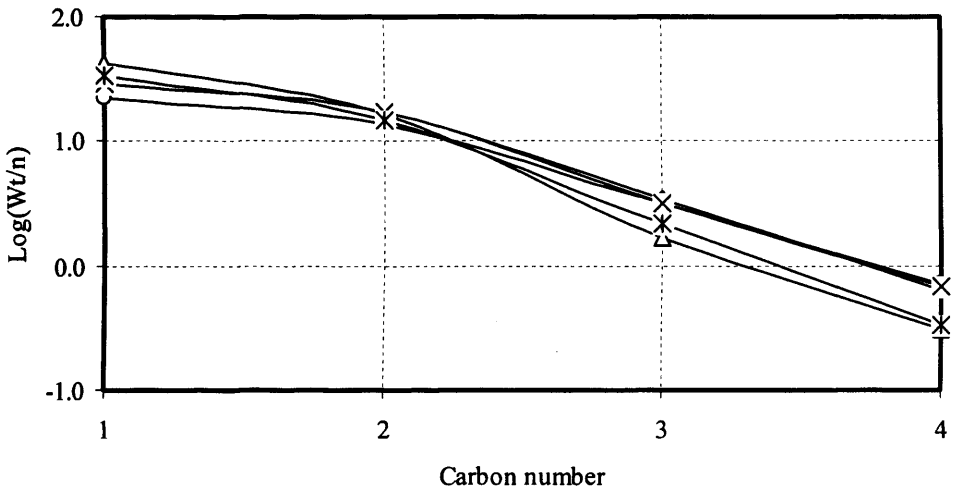

Figure 3.10 ASF plots of distribution for alcohol products in catalytic runs listed in Table 3.2. ○ Run 2; ◊ Run 3; Δ Run 4; × Run 5; * Run 6.

The above five catalytic runs (Run 2 – 6) show similar trend. In general, distributions of C_2 – C_4 alcohols are in straight lines, indicating that the formation of C_2 – C_4 alcohols follows the classical ASF distribution. The chain propagation factors are between 0.18 and 0.27. For methanol formation, however deviations were observed for all the above tests. This negative deviation was also reported by Xiang *et al.* on K/β-Mo_2C (K/Mo = 0.2) catalysts [33]. This deviation suggests that the production of methanol could be occurring at different active site from higher alcohols. Another possible explanation for this negative deviation from ASF distribution could be the loss of methanol into gas stream. Although a cold gas-liquid separator was used to collect liquid products (alcohols), it was noticed that trace amount of methanol was always detected in the gas phase analysis.

3.4 Results on Cu-Co mixed oxide catalyst system

3.4.1 Catalyst characterization

The analysis of metal content was performed by ICP-MS (Earth department, Cardiff University). The obtained ratio of metal components is: Cu/Co/Zn/Zr = 3/2/5/3.

3.4.1.1 BET surface area and X-ray diffraction results

The BET surface area of Cu-Co mixed oxide catalyst was 105 m^2/g.

X-ray diffraction measurement was also performed on the catalyst. It was found that the catalyst solid was essentially amorphous (Figure 3.11).

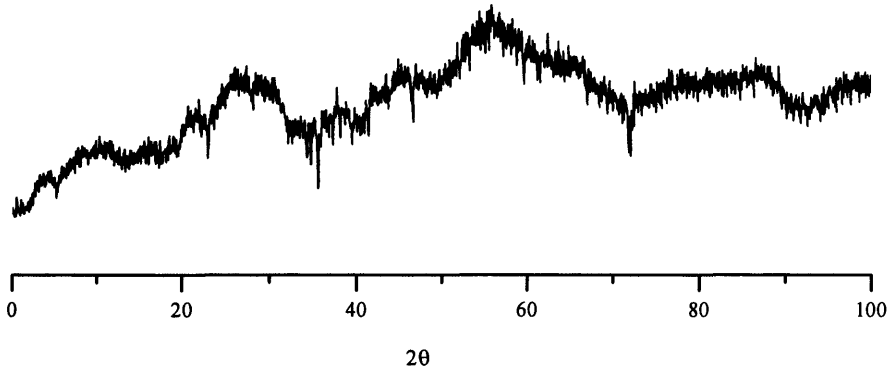

Figure 3.11 XRD patterns of Cu-Co mixed oxides

3.4.1.2 Temperature programmed reduction

The TPR profile for the Cu-Co mixed oxide catalyst is shown in Figure 3.12. There are two peaks observed over the investigated temperature range. The first peak is relatively sharp occurring over temperature range of 450 – 580 K. The peak could be assigned to the reduction of CuO. The second peak is small and flat occurring over

temperature range of 580 – 700 K. This peak may correspond to the reduction of Co_3O_4. A similar feature was observed by Baker and co-workers [26].

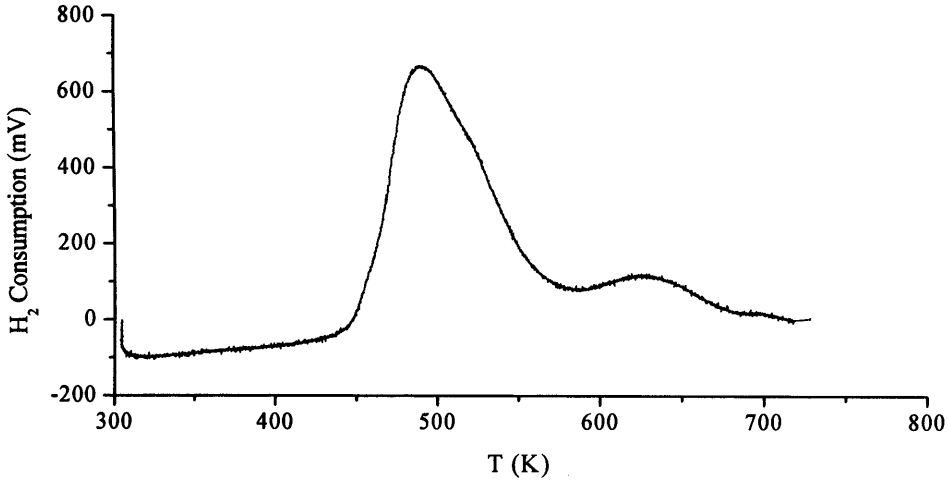

Figure 3.12 TPR profile for Cu-Co mixed oxide catalyst

3.4.2 Catalytic results

The present section deals with the influence of variables such as temperature, pressure and water addition on the results obtained in the catalytic experiments.

3.4.2.1 Effect of reaction temperature

A series of catalytic tests were carried out in the Lab reactor at 25 bar with a GHSV of 4200 h^{-1} over a range of 578 – 598 K to investigate the impact of temperature on the CO hydrogenation over Co-Cu mixed oxide catalyst. Table 3.3 shows the reaction condition and the obtained results. From Table 3.3, it was noticed that the increase in temperature led to an increase in methane selectivity, which is consistent with the thermodynamic statement that methane is the most thermodynamically stable product as explained in Chapter 1 of this thesis. The increase in temperature also led to a loss in olefinicity for the hydrocarbon products. The ratios of alkene to alkane at different temperature are illustrated in Figure 3.13.

Table 3.3 Impact of temperature on CO hydrogenation over Cu-Co mixed oxide catalyst

	Run 1	Run 2	Run 3
Temperature, K	578	588	598
Pressure, Bar	25	25	25
GHSV, h^{-1}	4200	4200	4200
Feed ratio, H_2/CO	1	1	1
Conversion of CO (exclusive CO_2), %	1.6	2.2	3.3
Products (mol%)			
CH_4	62.8	69.0	75.5
C_2H_4	5.46	3.87	3.42
C_2H_6	5.22	6.35	7.22
C_3H_6	4.16	3.48	3.44
C_3H_8	1.10	1.13	1.12
C_4H_8	1.44	1.02	0.98
C_4H_{10}	0.39	0.37	0.36
C_5H_{10}	0.70	0.46	0.43
C_5H_{12}	0.23	0.24	0.24
Methanol	11.4	8.12	3.91
Ethanol	4.36	2.75	1.35
1-Propanol	1.68	1.47	0.77
2-methyl-1-Propanol	0.61	1.23	0.96
1-Butanol	0.52	0.53	0.27
Carbon mole Selectivity (%)			
CH_4	43.3	48.2	52.7
$C_{>2}$	33.8	30.3	30.5
Methanol	7.83	5.68	2.73
Ethanol	6.01	3.85	1.88
1-Propanol	3.47	3.09	1.62
2-methyl-1-Propanol	1.69	3.44	2.69
1-Butanol	1.44	1.49	0.77
Yield (%)			
Methanol	0.12	0.13	0.09
Ethanol	0.10	0.09	0.06
1-Propanol	0.05	0.07	0.05
2-methyl-1-Propanol	0.03	0.08	0.09
1-Butanol	0.02	0.03	0.03

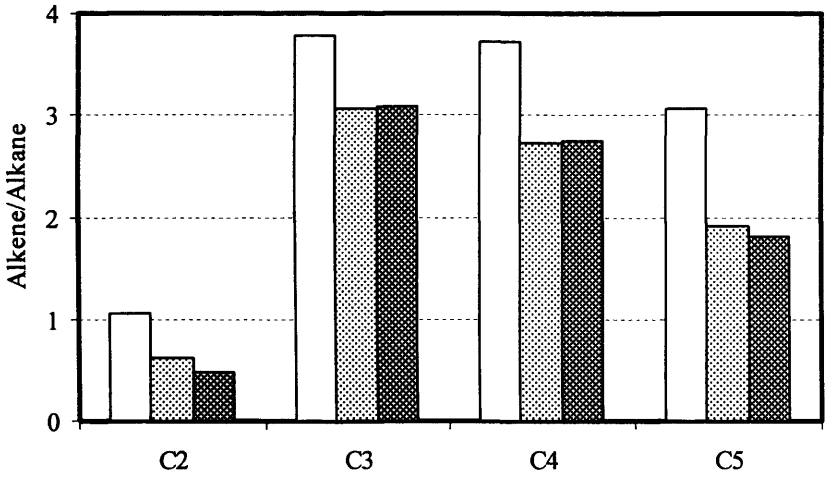

Figure 3.13 Olefinicity at different temperatures; □ 578 K; ⁙ 588 K; ▩ 598 K

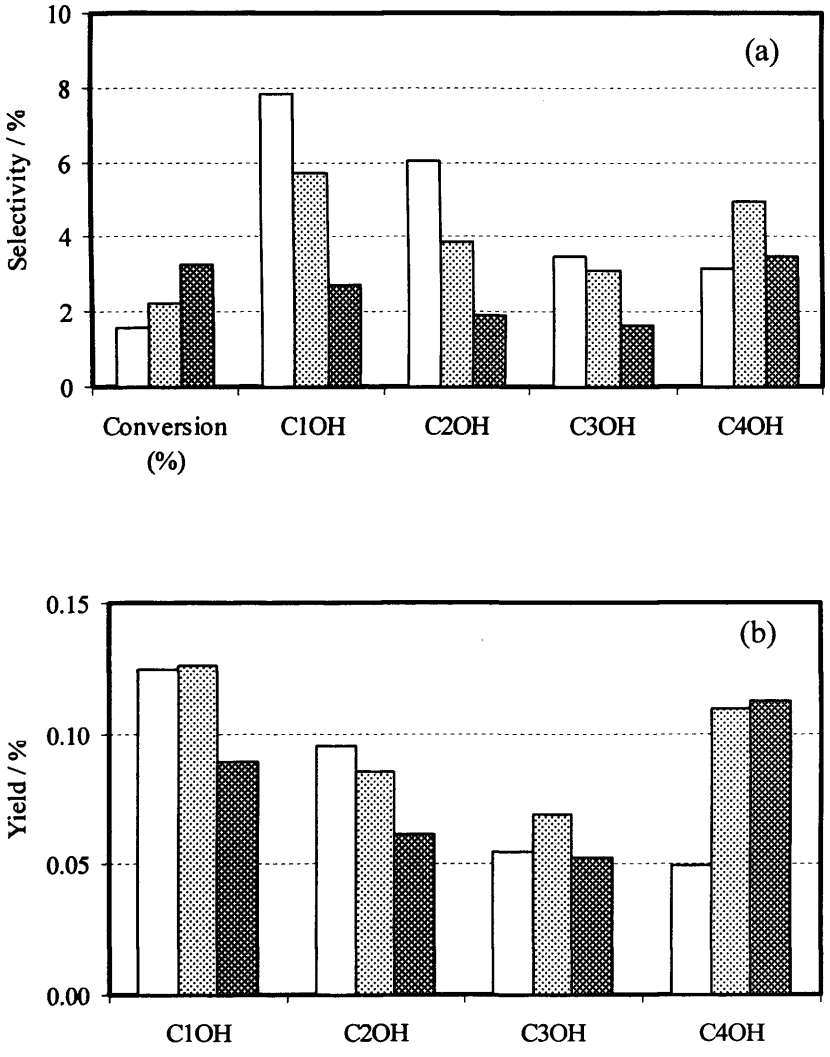

Figure 3.14 Impact of temperature on (a) CO conversion and alcohol selectivity; (b) alcohol yield; □ 578 K; ⁙ 588 K; ▩ 598 K

The data on CO conversion, alcohol selectivity and alcohol yields are further depicted in Figure 3.14. It was noticed that with the increase in temperature, there was an increase in CO activity however decreases were observed for the selectivity towards C_1 to C_3 alcohols. For C_4 alcohols, the highest selectivity was observed with temperature at 588 K. There was no clear trend for the alcohol yields over the investigated temperature range. Apparently, the formation of C_1 and C_2 alcohols prefers the lower temperature range, whereas higher temperatures were favored by the formation of C_3 and C_4 alcohols. This indicates that the formation of C_{1-2} and C_{3+} alcohols probably follows a different route. For alcohol synthesis, the reaction route involves two basic steps, i.e. linear addition and aldol condensation. The rate of linear addition was found slower than that of β-addition [34, 35]. This rate difference could be enhanced at higher reaction temperature, leading to increased formation of C_{3+} alcohols.

3.4.2.2 Effect of reaction pressure

Tests concerning the impact of pressure on the catalytic performance were carried out using the Micro reactor at 633 K with a GHSV of 12,000 h^{-1}. The reaction condition and the obtained results were tabulated in Table 3.4.

The results presented in Table 3.4 shows that the increase in the reaction pressure resulted in increases in conversion of carbon oxides however decreases in selectivities of methane and higher hydrocarbons.

Table 3.4 Impact of pressure on CO hydrogenation over Cu-Co mixed oxide catalyst

	Run 4	Run 5	Run 6
Temperature, K	633	633	633
Pressure, Bar	25	50	75
GHSV, h^{-1}	12000	12000	12000
Feed ratio, $H_2/CO/CO_2/N_2$	57/38/1/4	57/38/1/4	57/38/1/4
Conversion of CO/CO_2, %	4.6	6.5	9.1
Products (mol%)			
CH_4	74.8	74.3	47.0
C_2H_4	2.52	0.85	0.69
C_2H_6	7.78	8.41	5.01
C_3H_6	3.67	2.34	1.11
C_3H_8	1.83	1.95	1.27
C_4H_8	1.10	0.54	0.26
C_4H_{10}	0.79	0.65	0.39
C_5H_{10}	0.57	0.25	0.12
C_5H_{12}	0.57	0.37	0.21
Methanol	4.88	8.23	36.7
Ethanol	0.82	1.01	3.64
1-Propanol	0.26	0.37	1.27
2-methyl-1-Propanol	0.38	0.64	2.02
1-Butanol	0.08	0.09	0.38
Carbon mole Selectivity (%)			
CH_4	56.8	55.5	39.3
$C_{>2}$	38.3	29.3	19.1
Methanol	3.70	6.14	30.7
Ethanol	1.24	1.50	6.09
1-Propanol	0.59	0.83	3.20
2-methyl-1-Propanol	1.16	1.92	6.78
1-Butanol	0.24	0.26	1.26
Yield (%)			
Methanol	0.17	0.40	2.80
Ethanol	0.06	0.10	0.55
1-Propanol	0.03	0.05	0.29
2-methyl-1-Propanol	0.05	0.12	0.62
1-Butanol	0.01	0.02	0.11

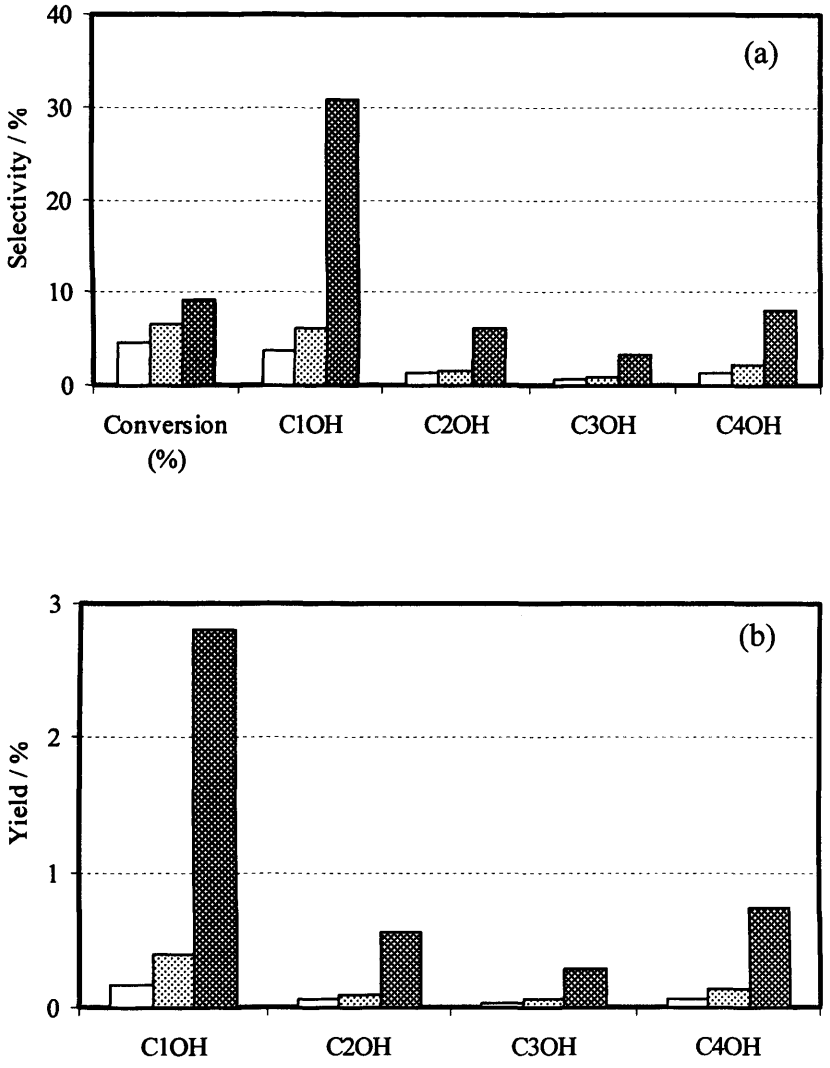

Figure 3.15 Impact of pressure on (a) CO conversion and alcohol selectivity; (b) alcohol yield; □ 25 bar; ▒ 50 bar; ▓ 75 bar

The conversion of carbon oxides, alcohol selectivity and alcohol yields are also presented in Figure 3.15. With the increase in pressure, there were increases in carbon oxide activity, alcohol selectivity and alcohol yield. Alcohol selectivity and alcohol yield were dramatically increased when 75 bar was employed in the catalytic test. This observation is in agreement with impact of pressure on different catalytic systems [10, 36].

One possible explanation for the difference between the impact of pressure on hydrocarbon selectivity and alcohol selectivity could be obtained by considering the

reaction pathway employed for these two types of products. The formation of alcohol may follow a reaction pathway involving non-dissociated CO (e.g. the CO insertion mechanism), whereas the formation of hydrocarbons may require dissociated CO (such as the carbide mechanism). The increase in reaction pressure could result in large amount of non-dissociated CO due to the limited active site of catalyst surface, consequently these non-dissociated CO led to the increased formation of alcohols. The real mechanism involved in hydrocarbon and alcohol synthesis is still not clear, hence this above explanation is purely speculative and may not represent the reason behind the observed catalytic results.

Product distribution

Figure 3.16 shows the ASF plot of the distribution of alcohol products for the tests over Cu-Co mixed oxide catalysts.

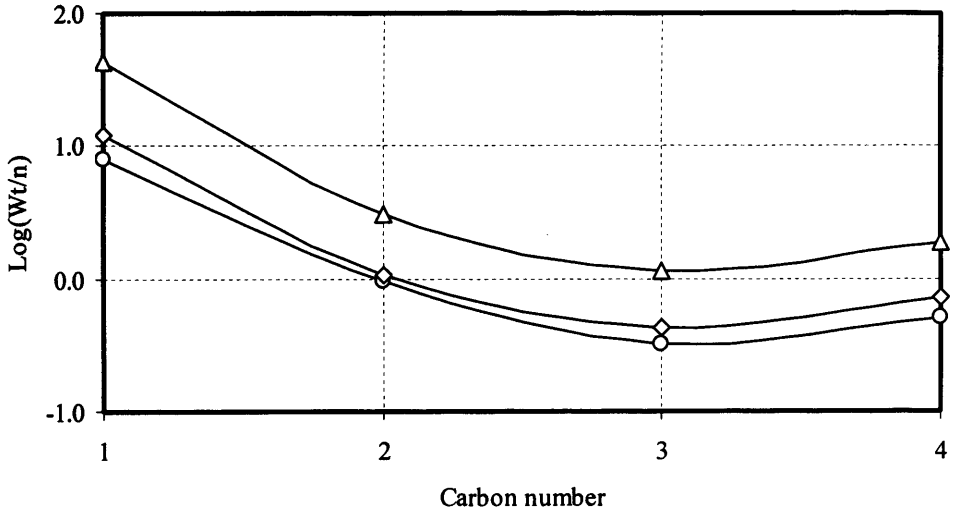

Figure 3.16 ASF plots of distribution for alcohol products in catalytic runs listed in Table 3.4. ○ Run 4; ◊ Run 5; Δ Run 6.

The above three catalytic tests (Run 4 – 6) show similar trend. Clear deviations from the ASF plot were observed for each catalytic test. The deviations mainly occur with the C_4 alcohols. From Table 3.4, it was noticed that the selectivity and yield of 2-methyl-1-propanol were particularly high, which contribute to the high weight fractions of the C_4 alcohols. A possible explanation is that for the investigated catalyst, the synthesis of linear alcohol and branched alcohol may occur at different active site.

3.4.2.3 Effect of water addition

With the purpose of investigating the effect of water on the CO hydrogenation to alcohols over Cu-Co mixed oxide catalysts, Run 7 was performed under the same reaction condition of Run 5 with the exception that water was added to the feed stream in Run 7. The reaction condition and obtained results are shown in Table 3.5.

The conversion of carbon oxides, selectivity of alcohols and yield of alcohols are presented in Figure 3.17. In the presence of water, the conversion of carbon oxides was increased, which partially was from the increased amount of CO_2 produced *via* the water gas shift reaction. It was also noticed that the addition of water lowers the selectivity and yield for methanol and ethanol. Decreases in both selectivity and yield were observed for methanol, whereas significant increases were obtained for ethanol. There was no C_{3+} alcohol observed in the presence of water.

A possible explanation for the increase in selectivity and yield for ethanol is that water may take part in the alcohol synthesis. Meanwhile, the absence of C_{3+} alcohol indicates that water could play another role in inhibiting the carbon chain growth.

Table 3.5 Impact of water addition on CO hydrogenation over Cu-Co mixed oxide catalyst

	Run 5	Run 7
Temperature, K	633	633
Pressure, Bar	50	50
GHSV, h^{-1}	12000	12000
Feed ratio, $H_2/CO/CO_2/N_2$	57/38/1/4	57/38/1/4
H_2O/Syngas	0	1
Conversion of CO/CO_2, %	6.5	10.2
Products (mol%)		
CH_4	74.3	74.7
C_2H_4	0.85	0.40
C_2H_6	8.41	7.17
C_3H_6	2.34	1.91
C_3H_8	1.95	3.55
C_4H_8	0.54	0.50
C_4H_{10}	0.65	1.70
C_5H_{10}	0.25	0.30
C_5H_{12}	0.37	1.06
Methanol	8.23	1.95
Ethanol	1.01	6.79
1-Propanol	0.37	0.00
2-methyl-1-Propanol	0.64	0.00
1-Butanol	0.09	0.00
Carbon mole Selectivity (%)		
CH_4	55.5	50.3
$C_{>2}$	29.3	31.8
Methanol	6.14	1.31
Ethanol	1.50	9.15
1-Propanol	0.83	0.00
2-methyl-1-Propanol	1.92	0.00
1-Butanol	0.26	0.00
Yield (%)		
Methanol	0.40	0.13
Ethanol	0.10	0.93
1-Propanol	0.05	0.00
2-methyl-1-Propanol	0.12	0.00
1-Butanol	0.02	0.00

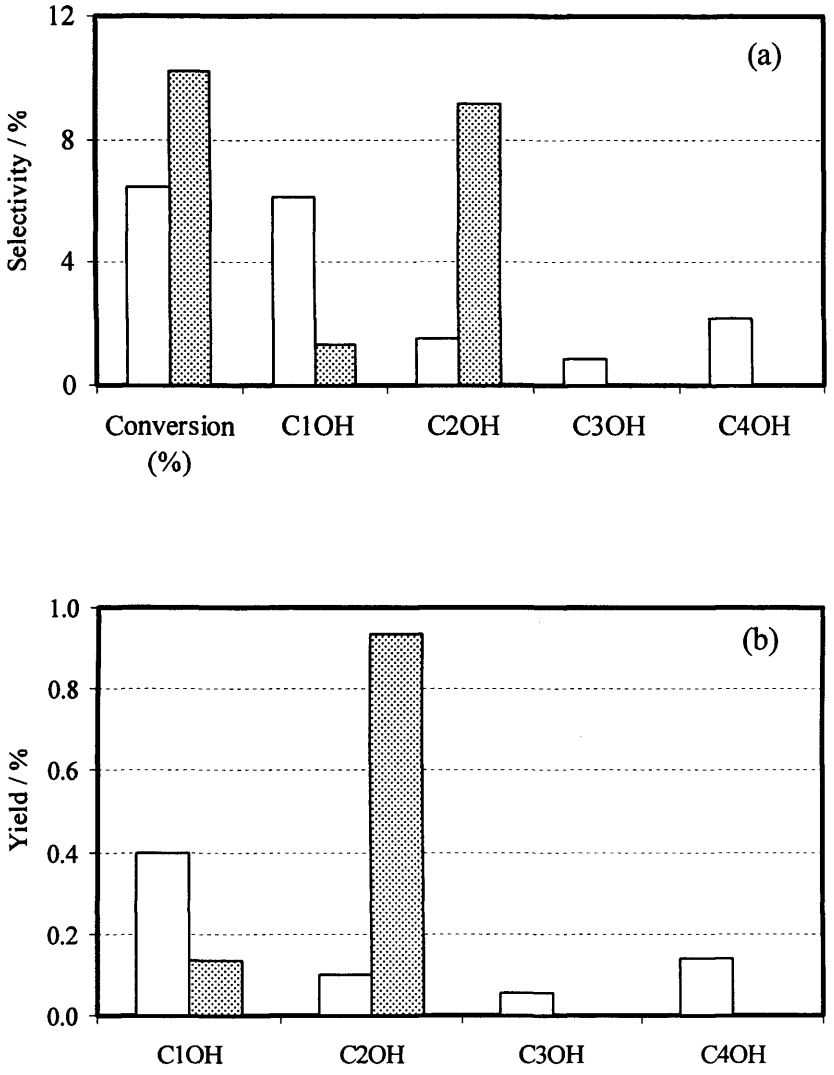

Figure 3.17 Impact of pressure on (a) CO conversion and alcohol selectivity; (b) alcohol yield □ without water addition; ⁙ with water addition

3.5 Conclusions

Two different catalyst systems, namely Co-MoS_2/K_2CO_3 based catalyst and the Cu-Co mixed oxides catalyst, were investigated under different reaction conditions in this study. For the Co-MoS_2/K_2CO_3 based catalyst, the experiment on catalyst aerial oxidation suggests that fresh catalyst is more active than old one. For catalysts calcined at different ramping rate, the experimental data shows that the use

of higher ramping rate could result in larger surface area which further facilitates the CO hydrogenation to higher alcohols. A series of catalytic tests concerning the effect of K_2CO_3 concentration, GHSV, temperature and feed composition were investigated. Among the investigated parameters/conditions, feed with syngas ratio of 2 gave the highest activity (30% CO conversion) and HA yield (methanol: 8%; HA: 13%) with an operation condition of 580 K, 75 bar and GHSV = 1225 h^{-1}. The obtained product distribution follows the ASF distribution with methanol having slight negative deviation.

For the Cu-Co mixed oxide catalyst, impact of temperature, pressure and water addition was investigated. The experimental data on temperature effect shows that for the temperature range of 578 – 598 K, C_1 and C_2 alcohol favor the lower temperature whereas C_3 and C_4 prefer the higher one. The results on pressure effect demonstrates that HAS favors higher pressure operation. The increase in alcohol yield was particularly dramatic for C_1 and C_4 alcohols. The result of water addition experiment shows that the presence of water gives improved catalyst activity and in particular enhanced ethanol selectivity and yield.

Since the above two catalyst systems belong to different HAS catalyst category, different catalytic reaction conditions (temperature, pressure, GHSV etc.) were chosen for each catalyst system. The obtained results suggest that Co-MoS_2/K_2CO_3 based catalyst gives higher activity, higher HAS selectivity and yield than that of the Cu-Co mixed oxides catalyst.

References

[1] Murchison, C.B.; Conway, M.M.; Stevens, R.R.; Quarderer, G.J., Proc. 9th Int. Congr. Catal., 2 (1988) 626

[2] Stevens, R. R., Eur. Patent 172431 (1986)

[3] Kinkade, N. E., Eur. Patents 0149255 and 0149256, (1985)

[4] Santiesteban, J.G.; Bogdan, C.E.; Herman, R.G.; Klier, K., Proc. 9th Int. Congr. Catal., 2 (1988) 561

[5] Youchang, X.; Naasz, B.M.; Somorjai, G.A., Applied Catalysis, 27 (1986) 233

[6] Iranmahboob, J.; Toghiani, H.; Hill, D.O.; Nadim, F., Fuel Processing Technology 79 (2002) 71

[7] Iranmahboob, J., Hill, D.O.; Toghiani, H., Appl. Catal. A: General 231 (2002) 99

[8] Iranmahboob, J., Hill, D.O.; Toghiani, H., Applied Surface Science 185 (2001) 72

[9] Iranmahboob, J.; Toghiani, H.; Hill, D.O., Appl. Catal. A: General 247 (2003) 207

[10] Xie, Y.; Naasz, B. M.; Somorjai, G. A., Appl. Catal, 27 (1986) 233

[11] Herman, G., in: Guczi, L., Ed., New Trends in CO Activation, Studies on Surface Science and Catalysis 64, Elsevier Science B.V., Amsterdam, 1991, p. 265

[12] Courty, P.; Durand, D.; Fruend, E.; Sugier, A., J. Mol. Catal., 17 (1982) 241

[13] Elliot, D.J.; Pennella, F., J. Catal., 102 (1986) 464

[14] Mouaddib, N.; Perrichon, V., Proc. 9th Int. Congr. Catal., 2 (1988) 521

[15] Farragher, A.L., Adv. Colloid Interf. Sci., 11 (1979) 3

[16] Topsøe, H.; Clausen, B.S.; Candia, R.; Wivel, C.; Morup, S., J. Catal., 68 (1981) 433

[17] Topsøe, H.; Clausen, B.S.; Topsøe, N.Y.; Pederson, E., Ind. Eng. Chem. Fundam., 25 (1986) 25

[18] Surgier, A.; Freund, E., US Patent 4122110, (1978)

[19] Surgier, A.; Courty, P.; Freund, E., US Patent 4257920, (1981)

[20] Courty, P.; Durand, D.; Freund, E.; Surgier, A., GB Patent 2118061, (1983)

[21] Courty, P.; Durand, D.; Surgier, A.; Freund, R., US Patent 4659742, (1987)

[22] Courty, P.; Chaumette, P.; Durand, D.; Verdon, C.,US Patent 4780481, (1988)

[23] Chaumette, P.; Courty, P.; Durand, D., Freund, E.; Grandvallet, P.; Travers, C., GB Patent 2158730, (1985)

[24] Courty, P.; Marcilly, C., in Poncelet, G.; Grange, P.; Jacobs, P. A., (Eds.) Preparation of Catalysts III, Elsevier, Amsterdam, 1983, 485

[25] Sugier, A.; Mikotenko, P.; Quang, D.V., in: 2nd, World Congress of Chemical Engineering, Montreal, October 1981

[26] Baker, J.E.; Burch, R.; Golunski, S.E., Appl. Catal., 53 (1989) 279

[27] Mahdavi, V.; Peyrovi, M.H., Catal. Commun. 7 (2006) 542

[28] Utz. B.R.; Cugini, A.V.; Frommell, E., in: Baker, R.T.K.; Murrell, L.L. (Eds.), Novel Materials in Heterogeneous Catalysis, American Chemical Society Symposium Series 437, 289 (1990) 404.

[29] Jacobsen, C.J.H.; Törnqvist, E.; Topsøe, H., Catal. Lett. 63 (1999) 179

[30] Woo, H.C.; Nam, I.; Lee, J.S.; Chung, J.S.; Kim, Y.G., J. Catal., 142 (1993) 672

[31] Iranmahboob, J., Hill, D.O., Catal. Lett., 78 (2002) 49

[32] Murchison, C.; Conway, M.; Steven, R.; Quarderer, G.J., in: Proc. 9th Int. Congr. On Catalyst, Vol. 2 (1988) 626

[33] Xiang, M.; Li, D.; Qi, H.; Li, W.; Zhong, B.; Sun, Y., Fuel 86 (2007) 1298

[34] Calverley, E.M.; Smith, K.J., J. Catal. 130 (1991) 616

[35] Calverley, E.M.; Smith, K.J., Ind. Eng. Chem. Res., 31 (1992) 792

[36] Slaa, J.C.; Ommen, J.G.; Ross, J.R.H., Catal. Today, 15 (1992) 129

Chapter 4 CO hydrogenation over Au containing catalysts

4.1 Introduction

Gold, when in its bulk state, is regarded as poorly active as a catalyst in heterogeneous catalytic reactions. This could be attributed to its fully occupied d-band and high ionization potential [1]. However the discovery in the 1979 that finely supported nanoparticles of gold could act as catalysts for reactions at low temperatures has stimulated considerable research effort on gold catalysts. Bond and co-workers [2] were amongst the first to demonstrate that very small gold particles supported on silica could give interesting catalytic performance for hydrogenation of butadiene. Subsequently, Hutchings and co-workers showed that Au/ZnO could be used for selective hydrogenation of α,β-unsaturated aldehydes [3]. Haruta and co-workers discovered that supported Au catalysts are very active for low temperature CO oxidation [4]. There have been excellent reviews on gold catalyzed oxidation,

hydrogenation and environmental related reactions [5-8]. A detailed review specified in hydrogenation was given by Claus [9].

Studies on gold containing catalyst used for carbon oxide hydrogenation are very limited [10, 11]. Baiker and co-workers investigated Au/ZrO_2 catalyst prepared by co-precipitation technique and proved that Au/ZrO_2 was active in methanol synthesis from CO_2 hydrogenation [12,13]. An initial study by Haruta and co-workers [11] reported that gold supported on ZnO and Fe_2O_3 could be used as a catalyst for carbon monoxide hydrogenation, and a small amount of methanol was observed.

As introduced in Chapter 1, higher alcohols or mixed alcohols have potential market value and are widely used as fuel additives in the petroleum industry. This chapter aims to extend the study of Haruta and co-workers [11], and explore the possibility of using gold containing catalysts in the synthesis of higher/mixed alcohols, particularly the role of gold in Au/ZnO and Au/Fe_2O_3 catalysts for the synthesis of higher/mixed alcohols.

4.2 Experimental

Catalysts used in this study were ZnO, 5 wt% Au/ZnO, Fe_2O_3 and 5 wt% Au/Fe_2O_3. They were prepared by co-precipitation or precipitation technique as detailed in Chapter 2. ZnO and 5%Au/ZnO catalysts were prepared by Mpela (University of Witwatersrand, South Africa). All the catalysts were evaluated in the Lab reactor described in Chapter 2. The typical catalyst test procedure is described below. The catalyst (ca. 0.2 gram) was pre-treated in the reactor with 1% H_2/N_2 (flow rate 10 ml/min) for 1 h at 523K under atmospheric pressure. After the catalyst bed was cooled to room temperature, syngas ($CO/H_2/N_2$=47.5/47.5/5, BOC UK) was introduced to the reaction system, followed by an increase in pressure to 25 bar by

using the back-pressure regulator. The reactor was then heated to 573K at which point the catalyst was evaluated for CO hydrogenation.

4.2.1 Characterization

The ZnO and 5% Au/ZnO catalysts were characterized by XRD and Raman techniques.

The XRD pattern of the 5% Au/ZnO catalyst was that of the oxide support (Figure 4.1). The reflections are labeled with the Miller indices which are characteristic of the hexagonal ZnO with a zincite structure. The similar pattern of 5% Au/ZnO and ZnO catalysts suggests that either the amount of Au on the sample is too low to be sufficient of providing distinct X-ray diffraction pattern of crystalline Au particles [14], or that the Au particle is too small to show diffraction peaks in the investigated catalysts.

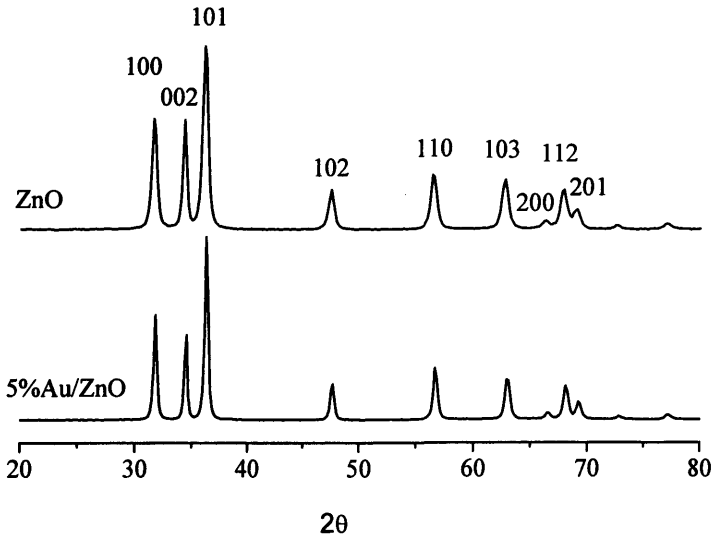

Figure 4.1 XRD pattern of ZnO and 5% Au/ZnO catalysts

The laser Raman spectra of the ZnO support and 5%Au/ZnO catalyst are presented in Figure 4.2. Unfortunately, significant fluorescence was observed for the ZnO support. For the Au/ZnO sample, the fluorescence was decreased and new bands at 3224 and 3472 cm^{-1} were observed. The bands were assigned to hydroxyl groups, which may be associated with the interface between the ZnO and the Au nanocrystal as they were absent in the ZnO support.

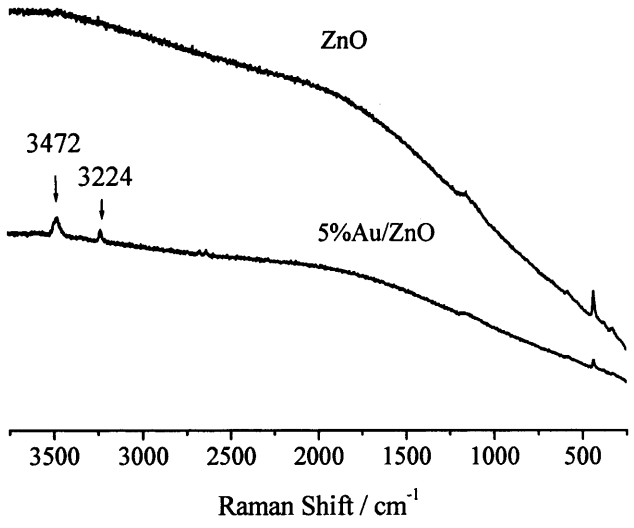

Figure 4.2 Laser Raman spectra of ZnO and 5% Au/ZnO catalysts

The Fe_2O_3 and 5%Au/ Fe_2O_3 catalysts were characterized by XRD technique.

The XRD pattern of Fe_2O_3 and 5% Au/Fe_2O_3 catalyst are essentially identical (Figure 4.3). The obtained diffraction lines are characteristic to the rhombohedral α-Fe_2O_3 with a hematite structure. The observed X-ray pattern suggests that either the amount of Au is too low or the Au particle size is too small to be detected within the experimental resolution.

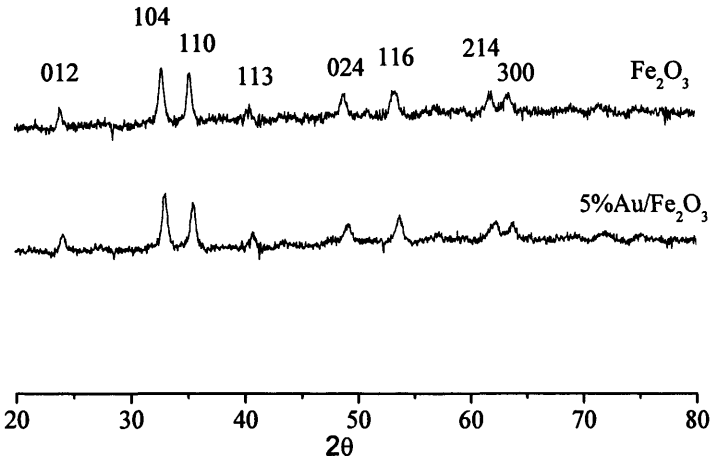

Figure 4.3 XRD pattern of Fe_2O_3 and 5% Au/Fe_2O_3 catalysts

4.3 Results

4.3.1 Au/ZnO catalyst

Two sets of experiments for CO hydrogenation were carried out over ZnO and 5%Au/ZnO. Table 4.1 shows CO conversion (CO_2 free), gas and liquid product composition and selectivity obtained over these two catalysts. The catalytic results show that both materials had a rather low conversion in CO hydrogenation. Gold supported catalysts gave a CO conversion of 2.2% which was approximately 25% of that observed for zinc oxide alone. It was also noticed that gold supported catalyst did not synthesize liquid hydrocarbons ($C_{>5}$).

Table 4.1 CO hydrogenation results of ZnO and 5% AuZnO catalysts

	Run 1	Run 2
Catalysts	ZnO	5%AuZnO
Reaction temperature, K	573	573
Pressure	25	25
Feed ratio, H_2/CO	1	1
Conversion of CO (exclusive CO_2), %	9.2	2.2
Products (mol%)		
CH_4	27.0	44.1
C_2H_4	12.3	11.0
C_2H_6	3.61	6.24
C_3H_6	11.2	13.1
C_3H_8	1.62	2.05
C_4H_8	6.17	7.05
C_4H_{10}	1.19	1.62
C_5H_{10}	3.36	3.96
C_5H_{12}	0.67	1.00
$C_{>5}$	24.2	0.00
Methanol	7.16	7.19
Ethanol	1.18	2.08
2-Propanol	0.06	0.04
1-Propanol	0.19	0.46
1-Butanol	0.05	0.13
Carbon mole Selectivity (%)		
CH_4	7.16	22.1
$C_{>2}$	84.6	69.8
Methanol	1.90	3.61
Ethanol	0.62	2.09
2-Propanol	0.05	0.06
1-Propanol	0.20	0.92
1-Butanol	0.06	0.27

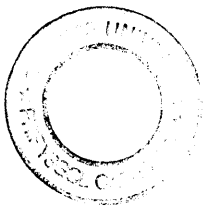

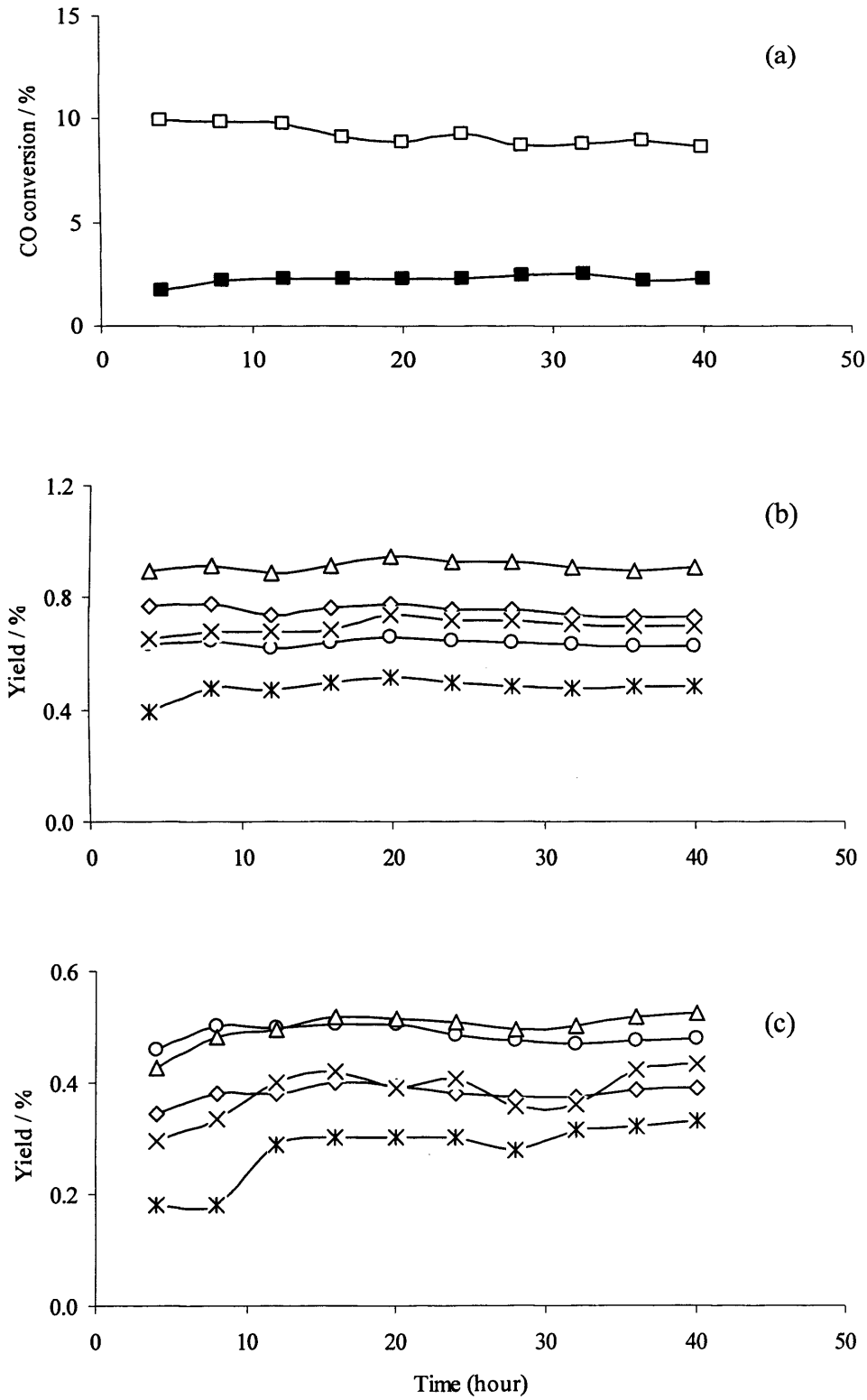

Figure 4.4 Gas phase time online data of CO hydrogenation over ZnO and 5%Au/ZnO catalysts (a) CO conversion: □ ZnO, ■ 5%Au/ZnO catalysts; (b) hydrocarbon yield over ZnO catalyst; (c) hydrocarbon yield over 5%Au/ZnO catalyst. ○ C_1; ◊ C_2; Δ C_3; × C_4; * C_5

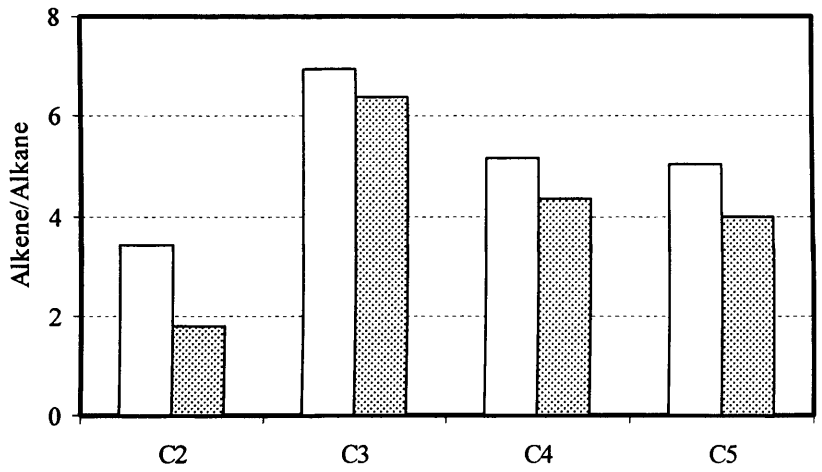

Figure 4.5 Ratio of alkene/alkane produced by CO hydrogenation over ZnO (□) and 5%Au/ZnO (▨) catalysts

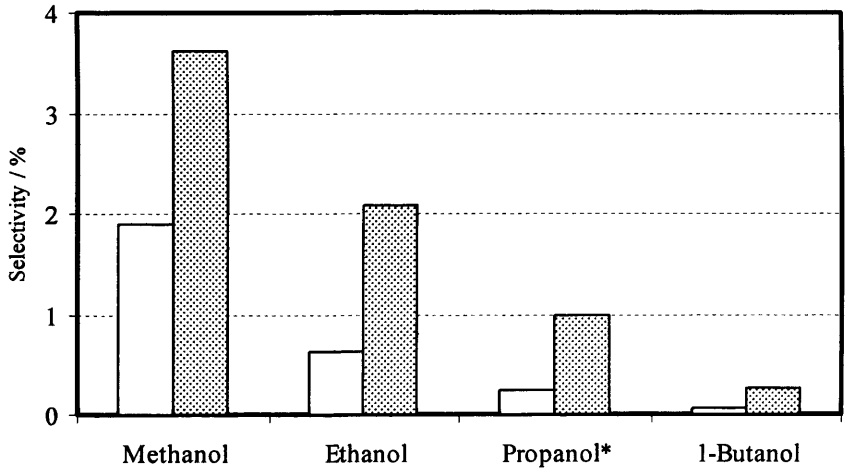

Figure 4.6 Alcohol selectivity by CO hydrogenation over ZnO (□) and 5%Au/ZnO (▨) catalysts (* 1-propanol and 2-propanol)

Figure 4.4 illustrates the CO conversion, gas phase hydrocarbon yield for the hydrogenation of CO at various times on stream for these two catalysts. Both catalytic systems show quite stable CO conversion during the entire run. Due to the low alcohol selectivity observed for both systems, CO conversion and hydrocarbon yield displayed a similar trend in the time on stream data. Upon the addition of gold, the obtained hydrocarbon yields show different levels of decrease. This decrease could be partially responsible for the decrease in the catalytic activity.

For C_2 to C_5 higher hydrocarbons, the ratios of alkene and alkane were studied for comparative purposes over ZnO and Au/ZnO catalysts respectively. It was noted that with the addition of gold, there was a decrease in the ratio of alkene/alkane (Figure 4.5). This indicates there was a reduction in the olefinicity for all the C_2-C_5 hydrocarbons. It may suggest that gold takes part in the hydrocarbon synthesis in a negative manner by blocking the active site for the formation of alkane and alkene, to different levels. This difference could be linked to the activity of gold in hydrogenation of the initially produced alkene further to alkane [9].

Figure 4.6 presents the effect of gold addition to zinc oxide on the alcohol selectivity. Although both catalytic systems gave rather low selectivity and yield of alcohols, it is clear that the selectivity of all the alcohols increased upon addition of gold to the zinc oxide support. It was also noticed that the ratio of higher alcohols to methanol was almost doubled.

The results of experiments performed over catalysts Au/ZnO and ZnO allow us to study the role of gold in CO hydrogenation.

It is known that ZnO alone is a methanol synthesis catalyst [15-17]. However, the impurities (for example, alkaline residues) introduced to the catalyst during the preparation accelerate side reactions including higher alcohol synthesis and

hydrocarbon synthesis [16]. In this study, the support and the gold catalysts were prepared in a similar way, which enables us to investigate the function of gold over the supported catalysts.

The observed results suggest that the presence of Au may play two roles in CO hydrogenation. One role is to suppress the activity of the catalyst for the production of hydrocarbons typically higher hydrocarbons. This could be achieved by blocking the active site for hydrocarbon synthesis. The other role is to shift the selectivity towards higher alcohols, which may be realized either by blocking the active site for methanol synthesis or by creating new site for higher alcohol synthesis.

4.3.2 Au/Fe_2O_3 catalyst

Two experiments of CO hydrogenation were carried out to examine the effect of Au on the Fischer Tropsch synthesis with Fe_2O_3 as support material. Table 4.2 lists the reaction condition, CO conversion (CO_2 free) and product distributions of CO hydrogenation over Fe_2O_3 and 5% Au/Fe_2O_3 catalysts. The obtained results show that both catalysts were moderately active in CO hydrogenation at the tested conditions. Compared with test on iron oxide alone, there was a 25% drop in the observed conversion over gold supported catalyst.

Table 4.2 CO hydrogenation results of Fe_2O_3 and 5%Au/Fe_2O_3 catalysts

	Run 3	Run4
Catalysts	Fe_2O_3	5%AuFe_2O_3
Reaction temperature, K	573	573
Pressure	25	25
Feed ratio, H_2/CO	1	1
Conversion of CO (exclusive CO_2), %	29.6	22.0
Products (mol%)		
CH_4	31.7	37.7
C_2H_4	13.7	3.59
C_2H_6	5.87	11.9
C_3H_6	14.6	9.26
C_3H_8	2.02	6.28
C_4H_8	6.91	3.02
C_4H_{10}	1.21	4.37
C_5H_{10}	3.09	1.34
C_5H_{12}	0.63	3.36
$C_{>5}$	16. 6	16.7
Methanol	0.38	0.92
Ethanol	3.01	1.30
2-Propanol	0.04	0.00
1-Propanol	0.24	0.19
1-Butanol	0.07	0.07
Carbon mole Selectivity (%)		
CH_4	9.76	11.2
$C_{>2}$	87.9	79.5
Methanol	0.12	0.28
Ethanol	1.86	0.77
2-Propanol	0.04	0.00
1-Propanol	0.30	0.23
1-Butanol	0.09	0.09

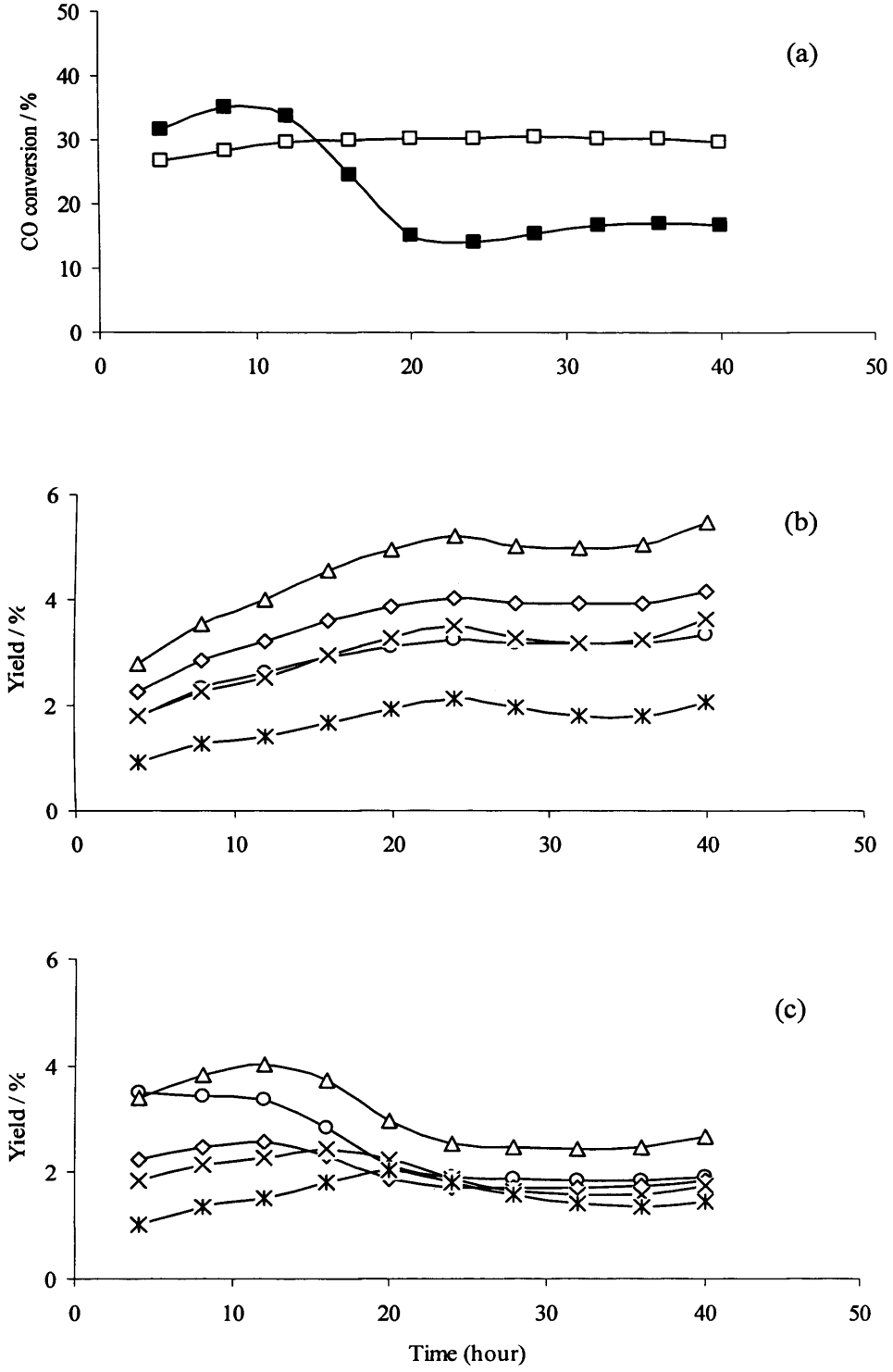

Figure 4.7 Gas phase time online data of CO hydrogenation over Fe_2O_3 and 5%Au/Fe_2O_3 catalysts (a) CO conversion: □ Fe_2O_3, ■ 5%Au/ Fe_2O_3 catalysts; (b) hydrocarbon yield over Fe_2O_3 catalyst; (c) hydrocarbon yield over 5%Au/ Fe_2O_3 catalyst. ○ C_1; ◊ C_2; Δ C_3; × C_4; * C_5

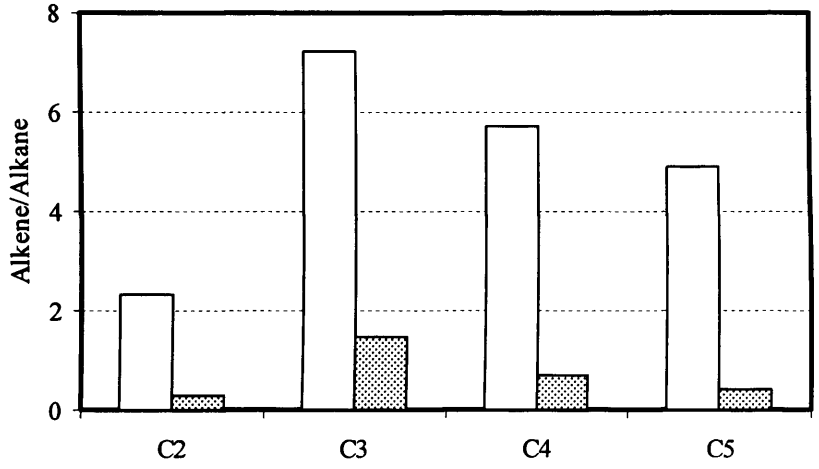

Figure 4.8 Ratio of alkene/alkane produced by CO hydrogenation over Fe_2O_3 (□) and 5%Au/ Fe_2O_3 (▨) catalysts

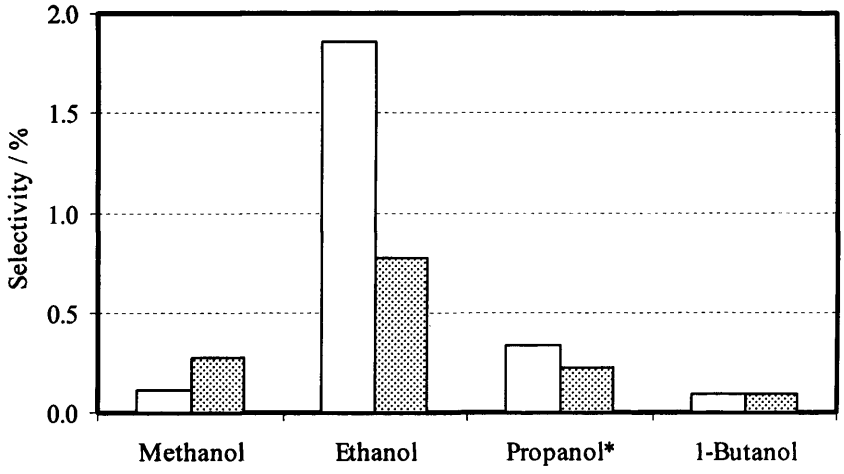

Figure 4.9 Alcohol selectivity by CO hydrogenation over Fe_2O_3 (□) and 5%Au/ Fe_2O_3 (▨) catalysts (*1-propanol and 2-propanol)

Figure 4.7 illustrates the time-on-stream data which includes CO conversion and gaseous hydrocarbon yield for CO hydrogenation over Fe_2O_3 and Au/Fe_2O_3 catalysts. Different from the results observed for zinc containing catalysts, it took circa 20 hours for both iron containing catalytic systems to reach steady states (stable conversion and hydrocarbon yields). For each catalyst, different trend was observed to reach its steady state. For Fe_2O_3 catalyst, both conversion and hydrocarbon yield increased gradually until they became stable. However, for Au/Fe_2O_3 catalyst, both conversion and hydrocarbon yield increased slightly in the first 10 h and then dropped rapidly until after 20 h when they reached a steady state displaying a 'Z' shaped curve.

This 'Z' shaped curve observed over Au/Fe_2O_3 catalyst was different from other tested materials. The reason remains unclear to us at the moment. Since this behavior was only observed over Au/Fe_2O_3 catalyst, it is very likely linked with the interaction between gold and its support.

Similar to the results obtained on zinc containing catalysts, upon addition of gold to the support, there was a decrease in the yields of all the gaseous hydrocarbons and the ratios of alkene to alkane decreased (Figure 4.8).

Figure 4.9 presents the effect of gold addition to iron oxide on the alcohol selectivity. Different from the results observed for Au/ZnO catalyst, upon addition of gold to iron oxide, there was a decrease in higher alcohol selectivity, accompanied by a slight increase in the selectivity toward methanol.

4.4 Discussion

There are a few features observed when comparing the results obtained for the above pair of catalysts. CO hydrogenation performed over Fe_2O_3 and Au/Fe_2O_3

materials gave much higher conversions (29.6% and 22% respectively) than those of ZnO and Au/ZnO materials (9.2% and 2.2% respectively). This indicates that activity of the tested materials was very closely linked with the oxidic supports, e.g. Fe_2O_3 and ZnO. In the presence of gold, both zinc containing and iron containing catalysts show a decreased conversion, which may suggest that gold play a similar role in blocking active sites for CO hydrogenation. In general, the catalytic data show that alcohol selectivity and yield are quite low. An improved reactor rig, such as the micro reactor used in previous test is needed to check the possibility of using gold supported material for industrial application.

There is an interesting observation of the function of gold in alcohol synthesis. From the selectivity data, especially for the liquid analysis, the addition of gold to ZnO suppressed the higher hydrocarbon formation and shifted the alcohol to higher alcohol side; whereas for iron containing catalysts, the opposite trend was observed. The reverse effect of addition of gold could be related to the interaction of gold with support. ZnO and Fe_2O_3 are two types of support sharing several different characteristics in nature, which mainly includes reducibility and acidity/basicity. ZnO is quite stable and basic, while Fe_2O_3 was slightly acidic and reported of being reduced to Fe_3O_4 after the reduction and reaction [10]. Although it is not clear which properties of support is the key factor in higher alcohol synthesis. It is clear that gold may play a role in tuning the alcohol distribution.

More work is needed to investigate the interaction between gold and metal oxides by using different supports (e.g. ZrO_2, SiO_2, TiO_2). Presumably the surface areas of supports are different and so dispersion of gold will be different. The tuning function could also be further investigated by doping gold to well-studied alcohol synthesis catalysts (e.g. Dow catalysts).

4.5 Conclusions

Gold containing catalysts were studied for CO hydrogenation to investigate the possibility of using gold as a higher alcohol synthesis catalyst. Alcohols including methanol, ethanol, 1-propanol, 2-propanol and 1-butanol have been synthesized at 573K and 25 bar over supported Au catalysts. The obtained results, particularly for the Au/ZnO catalyst, are interesting and suggest that Au could play a role in the synthesis of mixed alcohols: (1) by suppressing the side hydrocarbon synthesis reaction and (2) shifting the product selectivity towards higher alcohols. This initial study demonstrates that supported gold catalyst typically Au/ZnO material can be the catalyst of choice for mixed alcohol synthesis by carbon monoxide hydrogenation. Clearly, more supports are needed to be tested to figure out the main characteristic of support responsible for the positive interaction with gold in higher alcohol synthesis.

References

[1] Haruta, M.; CATTECH, 6 (3) (2002)

[2] Sermon, P.A.; Bond, G.C.; Wells, P.B.; J. Chem. Soc., Faraday Trans. 1, 75 (1979) 385

[3] Bailie, J. E.; Hutchings, G. J.; Chem. Commun.,1999, 2151

[4] Haruta, M.; Kobayashi, T.; Sano, H.; Yamada, N.; Chem. Lett., 4 (1987) 405

[5] Bond, G.C.; Thompson, D.T.; Catal. Rev.-Sci. Eng., 41 (1999) 319

[6] Bond, G.C.; Thompson, D.T.; Gold Bull., 33 (2000) 41

[7] Hutchings, G.J.; Catal. Today, 100 (2005) 55

[8] Haruta, M.; Catal. Today, 36 (1997) 153

[9] Claus, P; Appl. Catal. A 291 (2005) 222

[10] Sakuri, H; Tsubota, S; Haruta, M; Appl. Catal. 102 (1993)125

[11] Sakurai, H.; Haruta, M., Appl. Catal. A, 127(1995) 93

[12] Baiker, A; Kilo, M; Maciejewski, M; Menzi, S; and Wokaun, A; Stud. Surf. Sci. Catal., 75 (1993) 1257

[13] Koeppel, R.A.; Baiker, A; Schild, C; and Wokaun, A; J. Chem. Soc., Faraday Trans., 87 (1991) 2821

[14] Bailie, J. E.; Abdullah, H. A.; Anderson, J. A.; Rochester, C. H.; Richardson, N. V.; Hodge, N.; Zhang, J.; Burrows, A.; Kiely, C. J.; and Hutchings, G. J.; Phys. Chem. Chem. Phys., 3(2001) 4113

[15] Wilmer, H.; Kurtz, M.; Klementiev, K.V.; Tkachenko, O.P.; Grunert, W.; Hinrichsen, O.; Birkner, A.; Rabe, S.; Merz, K.; Driess, M.; Woll, C. and Muhler, M.; Phys.Chem.Chem.Phys., 5 (2003) 4736

[16] Bridger, G.W.; Spencer, M.S.; 'Methanol Synthesis' in Catalysis Handbook ed. by Twigg, V.M.1989

[17] Hoflund, G.B. and Epling, W.S.; Catal. Lett. 45(1997) 135

Chapter 5 Combined Steam Reforming and Fischer Tropsch synthesis

5.1 Introduction

The syngas used for the Fischer Tropsch (FT) reaction can be generated from three main resources, namely coal, natural gas and biomass. With its rich reserves and almost negative price due to new regulations of flaring, natural gas related technologies have received much more attention. Among all the technologies developed, steam reforming of methane is the most well developed process due to its advantage of being able to treat sufficient quantities of natural gas and produce syngas at an acceptable rate.

For a typical FT plant, a capital cost calculation was given by Choi and co-workers [1]. Up to 66% of the total cost goes to syngas manufacture process. Among the rest, 2/3 of the investment is used for FT synthesis including syngas compression and recycle, reaction system, recovery of hydrogen and hydrocarbons; and 1/3 is for product grade-up. The distribution of capital cost suggests that reduction of expenses in syngas generation is more beneficial than the other two steps for an FT process.

There are two main reactions (equations 5.1 and 5.2) involved in steam reforming process.

$$CH_4 + H_2O = CO + 3H_2 \qquad \Delta H^{\ominus}_{298} = 206 \text{ kJ·mol}^{-1} \tag{5.1}$$

$$CH_4 + 2H_2O = CO_2 + 4H_2 \qquad \Delta H^{\ominus}_{298} = 163.8 \text{ kJ·mol}^{-1} \tag{5.2}$$

The above reactions are endothermic and the process is industrially operated over relatively high temperature range (1073-1273K) and at atmospheric pressure. Such high temperature operation needs special tubular reformer which is normally made of expensive high Ni-Cr alloy steel. Additionally, a large amount of energy is required for steam generation and the plant operation is capital intensive. Furthermore, the syngas produced has a composition of H_2/CO = 3 at high temperature, or even greater when a lower temperature is employed, which is not ideal for many down stream processes (e.g. ammonia, DME, methanol and FT). The syngas ratio normally is adjusted by the removal of the excess hydrogen. The amount of carbon monoxide can be adjusted *via* the water gas shift reaction and subsequent removal of the carbon dioxide. Hydrogen and carbon dioxide can be removed by using membrane separation and amine stripping respectively, which contributes to another portion of the high operation cost.

There are growing interests arising from chemical engineering and/or catalyst development aspects in steam reforming and FT related process trying to explore new routes for the generation and utilization of syngas. Numbers of inventions [2-6] have been patented on integration of the syngas generation process with FT synthesis: CO_2 was directly passed into FT reactor without separation; H_2 rich stream after FT reactor was reutilized in combustion channel to provide heat for the reforming; water produced from FT was recycled to reforming process. A typical common point about

these patented integration processes is that more than one reactor, operated at different reaction conditions, is required.

Combined Steam Reforming and Fisher Tropsch (CRAFT) process carried out in a single fixed bed reactor was reported by Hutchings and co-workers [7]. Higher hydrocarbons, mainly C_2, C_3 and C_4 alkanes were synthesized directly from methane and steam, but in very small amount and for very short catalyst time. The present study is aimed to extend this CRAFT study from higher hydrocarbon synthesis to alcohols synthesis to check the possibility of synthesizing alcohol from methane and steam using one single reactor.

Firstly, this chapter describes the concept of the CRAFT and the associated thermodynamic analysis. The experimental procedure is then presented, followed by characterization of catalysts. Afterwards, as a preliminary study, catalytic tests on the effect of water on FT systems over a series of Ru/single oxide are reported. Finally, the results of CRAFT tests over Ru/ZrO_2 material are presented and discussed.

5.2 CRAFT concept

The core of the CRAFT concept is that both steam reforming and FT synthesis are carried out in a single reactor over the same catalyst without separation of syngas from methane and steam. The simplified process is illustrated in Figure 5.1.

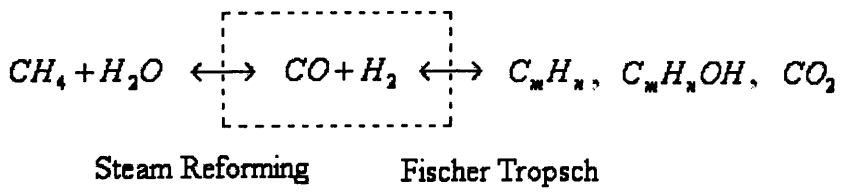

Figure 5.1 simple illustration of the CRAFT process

The process can be treated as higher hydrocarbons and alcohols being directly synthesized from methane and steam. Considering cost cutting related with product separation and grade-up, potential implication of the CRAFT process would be phenomenal. It may also shed light on the combination of different processes.

5.2.1 Thermodynamic and kinetic analysis of the CRAFT to synthesize alcohols

For the CRAFT reaction, typical net reaction types can be simplified as:

$$CH_4 + H_2O \rightarrow hydrocarbons / alcohols + H_2 \quad (5.3)$$

$$CH_4 + H_2O \rightarrow hydrocarbons / alcohols + H_2 + CO_2 \quad (5.4)$$

The calculated standard free Gibbs energies of reaction per carbon of the produced alcohols as function of temperature are shown in Figure 5.2. Thermodynamic data used for the calculation are obtained from the book by Stull *et al* [8].

In general, no matter which reaction proceeds following equations (5.3) and (5.4) shown above, values of ΔrG^{θ} for C_{1-4} alcohols are always positive over the range from 300K to 1000K. In the case of methanol, the equilibrium constants for reaction equation (5.3) and (5.4) at 633 K are calculated as $1.56*10^{-10}$ and $2.56*10^{-14}$. Such low equilibrium constants indicate that extremely low yield of alcohol is to be expected for the CRAFT process. It also suggests that it would be rather difficult for the alcohol synthesis directly from methane and steam to be achieved under thermodynamic control.

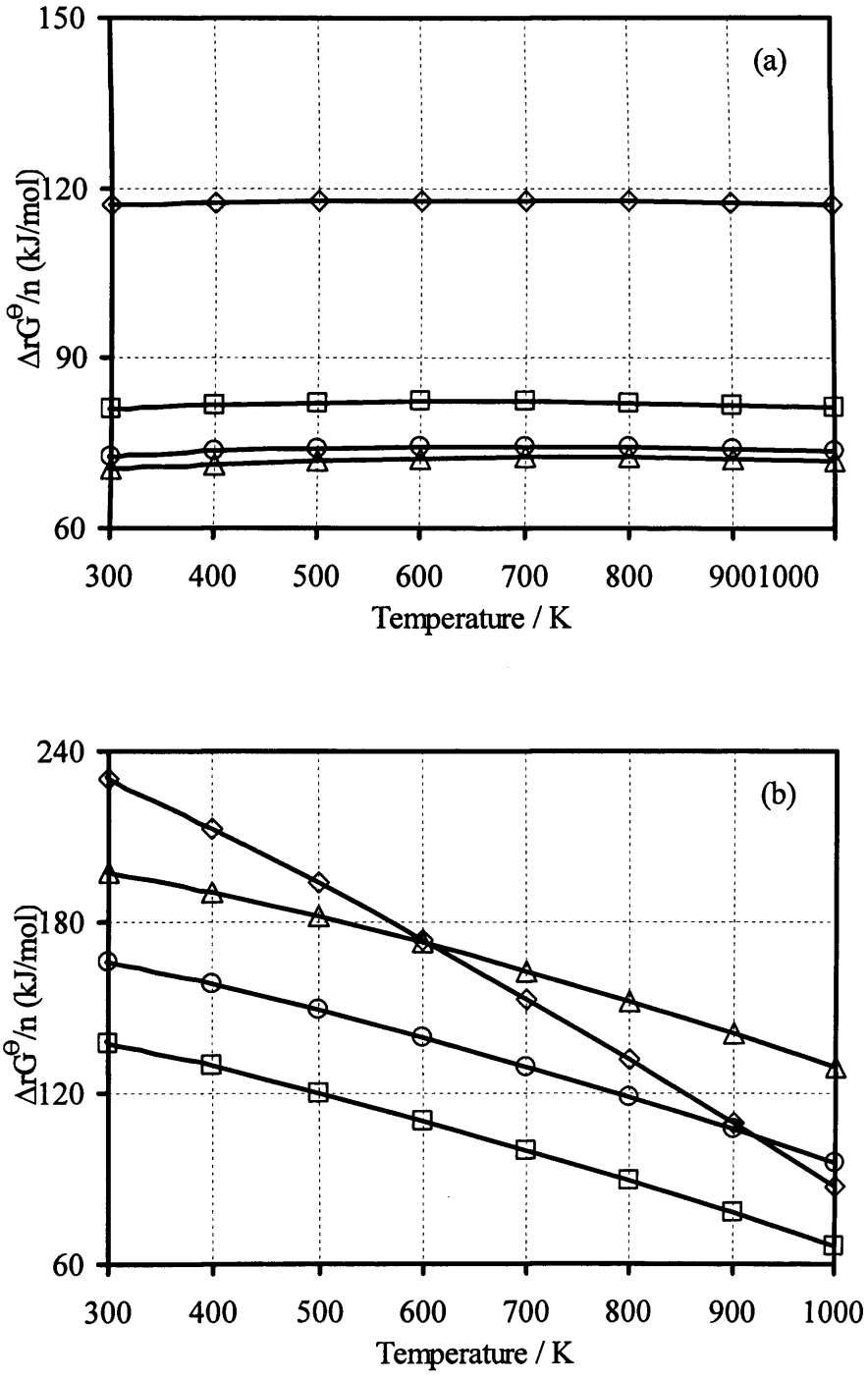

Figure 5.2 Standard free Gibbs energies of reaction per carbon of the product for (a) reaction type [5.3] and (b) reaction type [5.4] as function of temperature. ◊ Methanol; □ Ethanol; ○ 1-Propanol; Δ 1-Butanol.

Due to the very different kinetic characteristics of the steam reforming and the FT synthesis, kinetic analysis suggests that the combined process could be feasible. A simple kinetic description for the CRAFT process was given by Johns [9]. The combined reaction could be considered as consecutive reaction as below, where k_1 is the rate constant of the steam reforming and k_2 is the rate constant of the FT synthesis.

$$A \xrightarrow{k_1} B \xrightarrow{k_2} C$$

It is known that the rate of the FT synthesis is far greater than that of the steam reforming, i.e. $k_2 >> k_1$. This suggests that syngas ([B]) produced by the steam reforming could be removed rapidly by the FT reaction, driving the steam reforming equilibrium to the right ([C]). The obtained kinetic model is illustrated in Figure 5.3.

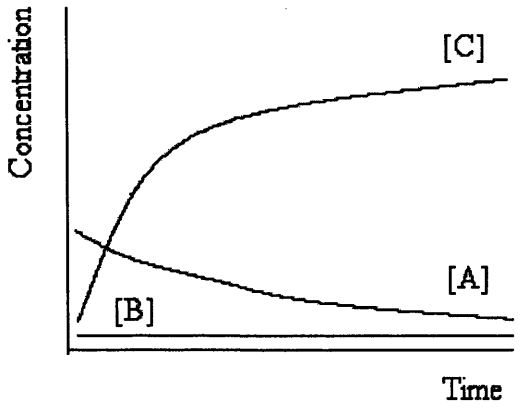

Figure 5.3 Simple kinetic plot for the CRAFT process [ref. 9].

5.2.2 Low temperature steam reforming

Due to the very different nature of the steam reforming reaction and the FT synthesis, e.g. endothermic and exothermic; volume/moles expansion and contraction, the primary consideration of combining these two processes in a single reactor should be choosing an intermediate operation condition.

The steam reforming reaction is usually carried out at high temperature and under thermodynamic control, whereas the FT synthesis is performed at low temperature range and under kinetic control (Chapter 1). Among all the FT synthesis products, methane is the most thermodynamically favorable component. With an increase in reaction temperature, methane/methanation becomes to dominate the FT synthesis. In this sense, the operation condition for CRAFT falls into a low temperature steam reforming and relatively high temperature FT synthesis regime. A temperature range of 550 – 650 K was selected to investigate the CRAFT process.

Research articles on low temperature steam reforming are very limited. Jun and co-workers investigated hydrogen production for fuel cells through methane reforming at low temperatures and demonstrated that Ni/Ce-ZrO_2/θ-Al_2O_3 catalyst shows very high activity and equilibrium CH_4 conversion at temperatures from 673 to 923 K [10]. Matsumura and co-workers [11] reported that nickel supported on zirconia is the most effective in methane steam reforming under reaction condition at 773 K and H_2O/CH_4 = 2 (mol) among supports such as silica, γ-alumina and zirconia, giving a methane conversion of 25.5%. Methane steam reforming over Ce-ZrO_2 supported noble metal catalysts at low temperature was investigated by Kusakabe and co-workers [12]. They reported that the highest activity was obtained over $Rh/Ce_{0.15}Zr_{0.85}O_2$ catalyst with a methane conversion of 28.1% at 773 K.

For CRAFT reaction, the desired temperature range is 550 – 650 K, which is lower than the above literature reported. Considering that steam reforming reaction is thermodynamically controlled process, an equilibrium calculation was performed using equilibrium constants data provided by Twigg [13]. The methane equilibrium conversion under reaction condition of 1 atm pressure and steam/methane = 1 is shown in Figure 5.4.

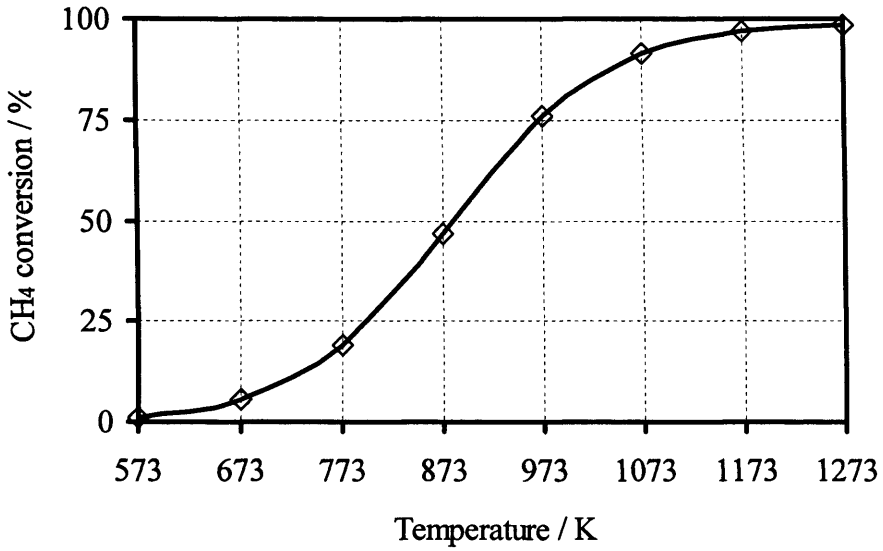

Figure 5.4 Equilibrium methane conversion of steam reforming (1 atm, steam/methane =1)

From Figure 5.4, it can be seen that the equilibrium conversion of methane from 573 – 673 K is ca. 1- 6% under the employed reaction condition, which suggests a very low concentration of syngas (CO and hydrogen) to be obtained. The low conversion also indicates that large amount of unconverted methane and steam exists in the reaction stream, which may have influence on the down stream FT process. The methane conversion can be increased by employing higher ratio of steam to methane; however, this again could result in large amount of unconverted steam.

Apart from the high concentrations of methane and steam/water, high values of H_2/CO and CO_2/CO resulted from low temperature steam reforming [13] are not preferred by the down stream – the FT synthesis, which has to be considered in the CRAFT process as well.

Possible side reactions that could be associated with the CRAFT process were given by Hutchings and co-workers [7]. They also reported the dependence of

standard free Gibbs energies of reaction as function of temperature. Table 5.1 lists these reactions which may occur to different level in the CRAFT process.

Table 5.1 Possible reactions associated with the CRAFT process

Process	Equation	
Dry reforming of methane	$CH_4 + CO_2 \leftrightarrow 2H_2 + 2CO$	(5.5)
Water gas shift	$CO + H_2O \leftrightarrow CO_2 + H_2$	(5.6)
Methane decomposition	$CH_4 \leftrightarrow C + 2H_2$	(5.7)
Boudouard reaction	$2CO \leftrightarrow C + CO_2$	(5.8)
CO reduction	$CO + H_2 \leftrightarrow C + H_2O$	(5.9)
Methanation	$CO + 3H_2 \leftrightarrow CH_4 + H_2O$	(5.10)

Taking into consideration the above brief analysis, answers to these two key factors are crucial for the CRAFT concept: (1) Does steam reforming reaction proceed at low temperature range, e.g. 550 – 650 K? (2) What is the impact of high concentrations of water/steam and methane on the FT synthesis?

5.3 Catalyst design

5.3.1 The active metal

A catalyst suitable for the CRAFT process has to be active for both the FT synthesis and the low temperature steam reforming reaction at the same time.

For the FT synthesis, the catalyst needs to be active with very low concentration of syngas and meanwhile resistant to high concentrations of methane and water.

Ru containing catalyst was chosen for the CRAFT test in the work for higher hydrocarbon synthesis by Hutchings and co-workers [7]. They compared the kinetics of the FT reaction on different catalysts, typically rate expressions for Ni, Co, Fe and Ru containing catalysts, and they concluded that Ru containing catalyst was the

catalyst for the CRAFT study mainly attributed to its negative order of reaction with respect to CO.

Ru catalyst is also a good choice for the low temperature steam reforming reaction. It is known that normally Ni or the noble metals such as Ru, Rh, Pt, Pd, Ir are used as active metals for the steam reforming reaction. Ni and Ru are potentially active even at low temperature, e.g. 673 K with a proper reaction condition employed [14]. Ni is the most commonly used due to its low cost. However, the noble metals are found to be more resistant to coking than nickel even when low steam-to-carbon ratio is employed [14].

Taking consideration of both the catalyst activity at low temperature and the resistance to coking, Ru catalyst becomes a potential strong candidate for the CRAFT process.

5.3.2 The catalyst support

The influence of support on the FT synthesis or on the steam reforming reaction can not be ignored. The catalyst support usually is used to disperse the active metal. The main function of support is to control the dispersion of the active metal, by which improving or altering the catalyst activity and selectivity. Support is also used to improve the resistance of catalyst to coking and sintering.

Supports such as Al_2O_3, SiO_2 and MnO were chosen by Hutchings and co-workers in the CRAFT test for higher hydrocarbon synthesis [7]. In this study, criteria considered for choosing supports is focused on its function on (1) alcohol synthesis, and (2) low temperature steam reforming.

A series of metal oxides with different acidity/basicity and reducibility were chosen as supports for the investigation of alcohol synthesis *via* the CRAFT reaction.

The metal oxides are MgO, MoO_3, TiO_2 and ZrO_2. Material MgO is strongly basic [15], whereas TiO_2 and ZrO_2 are amphoteric, containing both acid and base sites [16]. The acidity of these supports follows a decreasing order [17, 18]:

$$MoO_3 > TiO_2 > ZrO_2 > MgO$$

Supports MoO_3, TiO_2 and ZrO_2 also have different redox properties. The reduction behavior of Ru supported catalysts was measured using TPR (Temperature Programmed Reduction) technique. Results are shown in section 5.6.4 of this chapter.

According to literature data, it is known that these materials showed good activity in both alcohol synthesis [17, 19] as well as the methane steam reforming [20, 21].

5.4 Effect of water addition on the FT synthesis

In the FT synthesis, water is produced along with hydrocarbons and/or oxygenates. Over cobalt based catalysts, oxygen atoms in carbon oxides are mainly removed in the form of H_2O [22]. With water concentration approaching to a certain level, its presence could have influence on the activity and selectivity of catalyst in the FT reaction. The product distribution of the FT reaction could be modified with the addition of water. One way of water involved in the FT reaction is *via* the water gas shift reaction (equation shown in Table 5.1). The water gas shift reaction is mildly exothermic ($\Delta H^{\ominus}_{298}$ = - 41.1 $kJ \cdot mol^{-1}$) and the reaction thus is favored by low temperatures.

The effect of water addition has been widely investigated over iron and cobalt catalysts. For iron based catalysts, it is commonly accepted that water may re-oxidize the catalysts [23, 24].

The effect of water addition for cobalt catalysts is much more complicated. Hilmen *et al.* reported that Co/Al_2O_3 and $CoRe/Al_2O_3$ catalysts deactivated when water was added during the FT synthesis [25]. Li *et al.* studied Pt promoted Co/Al_2O_3 and found that at high space velocity, the catalyst exposed to low water partial pressure exhibited stable activity [26]. Similar observation was obtained over Ru promoted Co/TiO_2 catalysts by the same authors [27]. They also reported that over Co/SiO_2 catalyst, the addition of water over a short term in the range of 5-25% has positive effect on the conversion, however long term and larger amount of water resulted in a severe catalyst deactivation [28].

Investigations over Ru containing catalyst are however limited. Claeys and co-workers studied the effect of water addition over Ru/SiO_2 catalyst, and they found that water addition led to an improved chain growth and lower methane selectivity [29]. Similar observation was reported with increased C_{5+} selectivity and decreased methane formation by Kim [30].

The above studies concerning the addition of water are mainly focused on the hydrocarbon synthesis. Studies devoted to water effect on the alcohol synthesis are very scarce. Klier *et al.* investigated water injection experiment over Cu/ZrO_2 catalyst in the synthesis of oxygenates from syngas, and they found a continuous decrease in the productivity of methanol with water addition [31]. Vedage and co-workers studied water addition over Cu/ZnO catalyst and reported that small amount of water could enhance methanol yields [32, 33]. To the best of our knowledge, there have been no published reports on water addition in alcohol synthesis over Ru containing catalysts.

As pointed out in last section, under the CRAFT reaction condition there could be large amount of unconverted water/steam which is considerably higher than that

produced along with hydrocarbon/alcohol synthesis. This suggests that the effect of water could not be ignored in the CRAFT reaction.

In this study, as an important preliminary test for the CRAFT reaction, the impact of water on the alcohol synthesis was investigated over Ru containing catalyst.

5.5 Experimental

Catalysts used in this study were Ru/MgO, Ru/MoO_3, Ru/TiO_2 and Ru/ZrO_2 with a content of 3 wt% ruthenium. They were prepared by impregnation technique as detailed in Chapter 2. The catalytic tests were performed in the Micro reactor described in Chapter 2. Typical catalyst test procedure is as below. The catalyst bed consisted of 2 ml Ru/single oxide, diluted with 3 ml SiC. The catalyst was reduced in the reactor with pure H_2 (99.999%, BOC UK, flow rate 50 ml/min) overnight at 673K under atmospheric pressure. After the catalyst bed was cooled to reaction temperature (633K), the H_2 feed was replaced by the relevant reactant gas (syngas and/or methane). Reactant gases used in this study were syngas ($CO/H_2/N_2$ = 47.5/47.5/5, BOC UK) and methane (CH_4/N_2 = 95.04/4.96, BOC UK). Water was directed to the system using an HPLC pump. Water was heated up and mixed with gaseous feed in the top zone of the reactor. The majority of the FT tests were carried out at atmospheric pressure with a GHSV of 3000 h^{-1} unless otherwise indicated. All the tests involving steam reforming process were performed at atmospheric pressure with a GHSV of 6000 h^{-1}.

5.6 Catalyst Characterization

5.6.1 BET surface area measurement

The surface areas of all the Ru/single oxide catalysts were measured using BET method, which are shown in Table 5.2.

Table 5.2 Surface areas of the Ru/single oxide catalysts measured with the BET method

Catalyst	BET surface area (m^2/g)
Ru/MgO	53
Ru/MoO_3	1.4
Ru/TiO_2	11
Ru/ZrO_2	6

5.6.2 X-ray diffraction results

Both Ru/single oxide and oxide support were characterized by powder X-ray diffraction (XRD) technique.

XRD patterns of all Ru/single oxide catalysts are those of the oxide supports. Figure 5.5 presents the diffraction pattern of the Ru/single oxide materials. The absence of reflections ascribable to Ru compounds indicates that the size of Ru crystallite is very small. The results obtained indicate that the phase of MgO is cubic. The reflection lines of Ru/MoO_3 and MoO_3 samples belong to orthorhombic MoO_3. The samples consist of TiO_2 show characteristic peaks of anatase titania. For ZrO_2 and Ru/ZrO_2 solids, diffraction peaks correspond to monoclinic ZrO_2. The 2θ value and miller indices of all the samples are shown in Table 5.3.

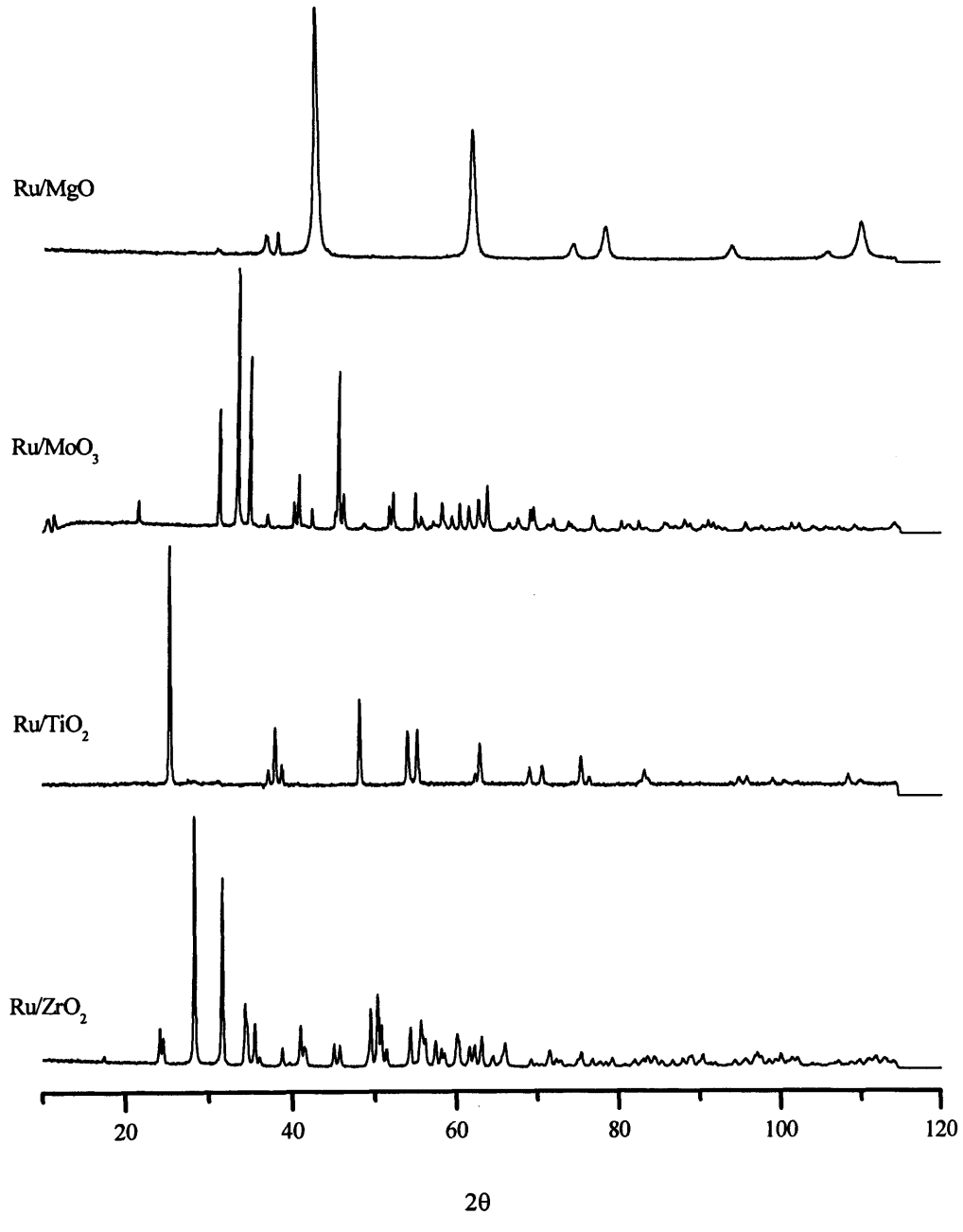

Figure 5.5 XRD patterns of Ru/single oxide catalysts

Table 5.3 XRD 2θ value and miller indices of the Ru/single oxide catalysts

Solid	2θ	Miller indices	2θ	Miller indices	2θ	Miller indices	2θ	Miller indices
Ru/MgO	37	1 1 1	62	2 2 0	79	2 2 2	106	3 3 1
	43	2 0 0	75	3 1 1	94	4 0 0	109	4 2 0
Ru/MoO_3	13	0 2 0	33.7	1 1 1	45.7	2 0 0	53	2 1 1
	23	1 1 0	35	0 4 1	46	2 1 0	54	2 2 1
	25	0 4 0	38.5	1 3 1	49	0 0 2	55	1 1 2
	27	0 2 1	38.9	0 6 0	50	2 3 0	56	0 4 2
	30	1 3 0	40	1 5 0	51.5	1 7 0	58	1 8 0
	33.1	1 0 1	42	1 4 1	52	1 6 1	58.8	0 8 1
Ru/TiO_2	25	1 0 1	38.5	1 1 2	55	2 1 1	69	1 1 6
	37	1 0 3	48	2 0 0	62.1	2 1 3	70	2 2 0
	37.8	0 0 4	54	1 0 5	62.6	2 0 4	75	2 1 5
Ru/ZrO_2	24	1 1 0	35	0 0 2	44.8	2 1 1	51	-1 2 2
	24.4	0 1 1	36	-2 0 1	45.5	-2 0 2	54	0 0 3
	28	-1 1 1	38.5	1 2 0	49	2 2 0	55	3 1 0
	31	1 1 1	41	-1 1 2	50.1	0 2 2		
	34	0 2 0	41.4	-1 2 1	50.6	-2 2 1		

5.6.3 Raman spectroscopy measurement

Ru/single oxide and oxide support were characterized by the Raman spectroscopy technique. There were no Raman peaks observed for the MgO and Ru/MgO materials. Raman spectra of other materials are presented in Figure 5.6. Raman spectra of Ru/single oxide show a significantly reduced intensity compared with that of the support itself. For Ru/ZrO_2 solid, it is difficult to observe Raman peak. The decreasing intensity in Raman spectra may suggest that the support was scattered by clusters consisting of Ru compounds, e.g. Ru oxide.

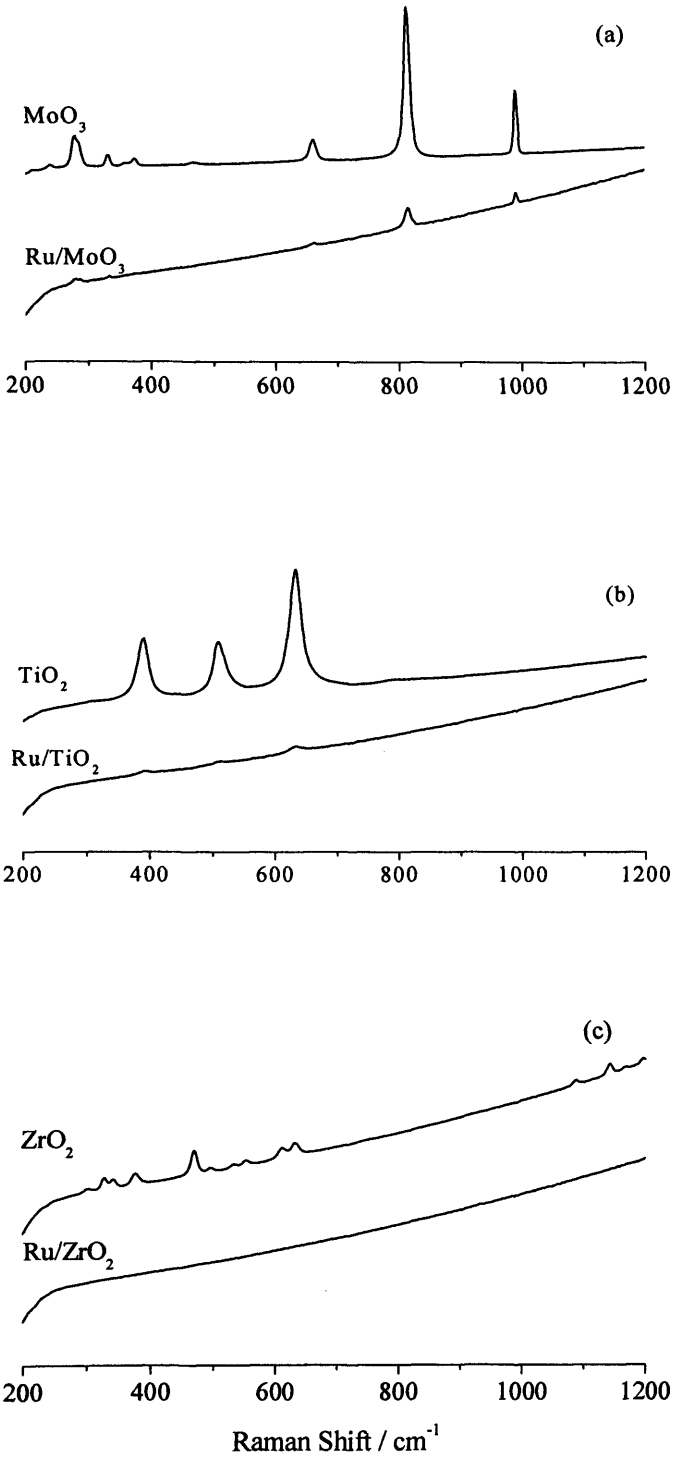

Figure 5.6 Raman spectra of materials (a) MoO_3 and Ru/MoO_3; (b) TiO_2 and Ru/TiO_2; (c) ZrO_2 and Ru/ZrO_2

5.6.4 Temperature programmed reduction

Temperature programmed reduction (TPR) technique was used to study the effect of pretreatment / hydrogen reduction on the Ru/oxide catalysts. The TPR profiles for the catalysts are shown in Figure 5.7.

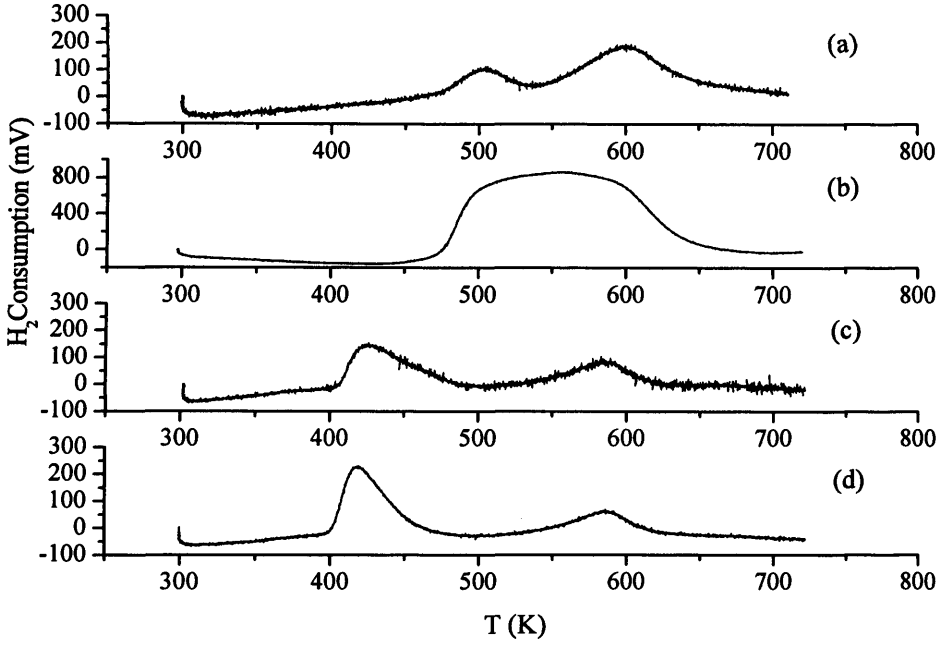

Figure 5.7 TPR profiles for catalysts (a) Ru/MgO; (b) Ru/MoO_3; (c) Ru/TiO_2 and (d) Ru/ZrO_2

Except for Ru/MoO_3 material with only one peak observed, all the other catalysts displayed two peaks in the TPR profile. Very similar profiles were obtained with Ru/TiO_2 and Ru/ZrO_2 materials. For both materials, hydrogen consumption occurred over ca. 400-500K and 500-650K ranges. In the case of Ru/MgO catalyst, the two peaks shifted to 450-550K and 550-700K ranges. The peak shift observed in the case of Ru/MgO material, towards higher temperature range could be due to a strengthening of Ru-O bond.

For Ru/TiO_2, Ru/ZrO_2 and Ru/MgO materials, these two peaks were assigned to the reduction of Ru oxide [34-38]. It was noticed that in the above referred papers

there are some variations of the exact position of these peaks, which may essentially due to different catalyst precursors, different catalyst preparation method and/or different TPR analysis (e.g. heating rate). RuO_2 was considered as the appropriate Ru species responsible for the hydrogen consumption, as RuO_4 was not present due to its instability [37]. The double peak observed could be explained by particle size [34]. Juan and co-workers suggested that particles with smaller size could be completely oxidized during the calcination process, however for particles with larger size, the oxidation was only partial [34]. Based on this hypothesis, the same author suggested that the peak at high temperature range could be assigned to the reduction of smaller particles, and the one at low temperature range to the reduction of larger particles. Another explanation for the double peak could be the existence of two different types of oxygen, of which one is easily reducible surface oxygen and the other one is bulk oxygen. If this is true, the first peak could be assigned to the reduction of the surface oxygen, and the second one could be the bulk oxygen.

In the case of Ru/MoO_3 material, there was only one broad peak observed over the range of 450-700K. This hydrogen consumption was due to the reduction of Ru oxide considering that reduction of MoO_3 starts at approximately 750K [34, 39].

From the above TPR profiles, it was noticed that the hydrogen consumption over Ru/MoO_3 material was significantly higher than the other three materials, suggesting an enhanced reduction behavior for Ru/MoO_3 material. For Ru/TiO_2 and Ru/ZrO_2 materials, there was a variation on the amount of hydrogen consumed, with Ru/ZrO_2 material being slightly higher. The obtained results suggest the following order of degree of reduction assuming all catalyst start with same amout of RuO_2:

$$\frac{Ru}{MoO_3} > \frac{Ru}{ZrO_2} > \frac{Ru}{MgO}, \frac{Ru}{TiO_2}$$

It is important to note that the TPR measurements and the activation of the catalyst were performed at different conditions (e.g. heating rate, holding time, composition of the reducing gas). It is for this reason that the TPR profile only provides general information about the effect of activation on the tested materials.

5.7 Effect of water on alcohol synthesis over Ru/Single oxide catalysts

This section presents the impact of water on the CO hydrogenation over Ru/single oxide catalysts. The results are tabulated in Table 5.4. The catalysts are denoted Ru/X in Table 5.4, where X is the metal in the oxide support, for example, Ru/MgO is Ru/Mg. Catalytic runs 1-4 are the tests performed without addition of water, whereas runs 5-8 are the corresponding ones tested in the presence of water. Due to the limitation of the current reaction rig (chapter 2), all the liquid products and unconverted water were collected in the liquid gas separator. The presence of dominant fraction of water makes accurate quantification of produced alcohol difficult. Therefore, the alcohols produced were only qualified using an off-line GC in this section, and in section 5.8 they were roughly classified into different levels according to the intensity of the FID signal.

CO conversion

From Table 5.4, it can be seen that the addition of water led to an increase in the CO conversion for all the tested materials, with Ru/MgO being the most dramatic. Time on stream data of CO conversion was depicted in Figure 5.8 for the above Runs. Clearly, the increase in CO conversion was mainly due to an increase in CO_2 production. This suggests that water gas shift reaction can hardly be ignored in CO hydrogenation over tested Ru/single oxide catalysts with the addition of water, which

is consistent with the literature findings on water gas shift reaction over Ru supported catalysts [18, 40-42].

Table 5.4 CO hydrogenation over Ru/single oxide catalysts with/without water addition (total reactor analysis)

	Run1	Run2	Run3	Run4	Run5	Run6	Run7	Run8
Catalysts*	Ru/Mg	Ru/Mo	Ru/Ti	Ru/Zr	Ru/Mg	Ru/Mo	Ru/Ti	Ru/Zr
Temperature, K	633	633	633	633	633	633	633	633
Pressure, atm	1	1	1	1	1	1	1	1
Syngas ratio, H_2/CO	1	1	1	1	1	1	1	1
H_2O/Syngas	-	-	-	-	2/3	2/3	2/3	2/3
CO conversion, %	2.2	49.8	2.8	3.9	35.1	68.0	8.5	8.1
Gas Phase C mole Selectivity (%)								
CO_2	31.6	32.6	35.2	30.6	78.5	80.2	51.6	86.0
CH_4	16.7	45.2	33.8	24.9	3.3	1.7	9.6	2.5
C_2H_4	15.1	0.06	9.5	18.9	0.13	0.01	1.4	0.65
C_2H_6	5.2	15.6	8.3	2.6	0.39	0.62	1.4	0.26
C_3H_6	15.2	0.03	8.9	3.9	0.12	0.00	0.70	0.26
C_3H_8	1.1	3.4	1.2	0.3	0.04	0.16	0.05	0.01
C_4H_8	2.1	0.24	1.3	2.7	0.02	0.02		0.02
C_4H_{10}	2.8	0.48	1.4	1.6	0.02	0.03		0.02
C_5H_{10}		0.16		0.9				
C_5H_{12}		0.12		1.8				
Liquid Phase**								
Methanol		+					+	+
Ethanol		+					+	

* Mg, Mo, Ti, Zr in the catalysts refer to its oxides

** lack of accurate quantification, using '+' represents small amount

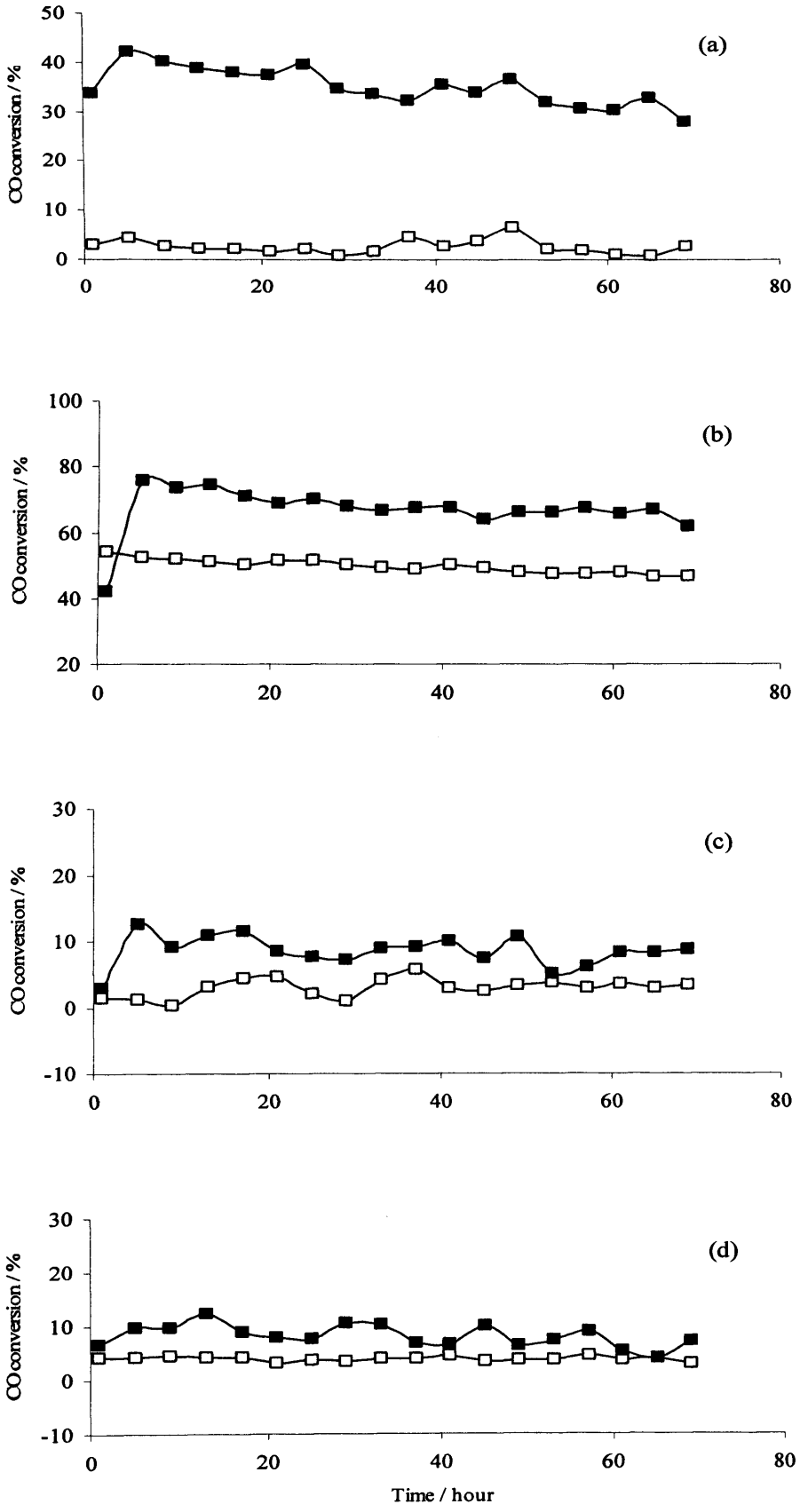

Figure 5.8 Stream on time data of CO conversion over (a) Ru/MgO (b) Ru/MoO_3 (c) Ru/TiO_2 and (d) Ru/ZrO_2 without (-□-) and with (-■-) water addition (for catalytic tests in Table 5.4)

Hydrocarbon synthesis

For the synthesis of hydrocarbons, it is known that Ru supported on oxide shows higher activity in CO hydrogenation when the oxide has acidic character than that of basic one [43-45]. The trend of CO activity towards hydrocarbons in Runs 1 – 4 is:

$$\frac{Ru}{MoO_3} > \frac{Ru}{ZrO_2} > \frac{Ru}{TiO_2} > \frac{Ru}{MgO}$$

which is almost identical to the trend of acidity of the support with the exception between Ru/ZrO_2 and Ru/TiO_2 materials.

The addition of water resulted in a sharp decrease in the selectivity to all the products (except CO_2) as can be seen in Table 5.4. The yields of all the hydrocarbons were calculated and it was found that generally there was a decrease in the yields with the addition of water. The time on stream data of C_{2+} hydrocarbons is presented in Figure 5.9. Clearly, it can see that the addition of water inhibited hydrocarbon chain growth to different level. In the case of Ru/MoO_3, there was no $C_{\geq 3}$ hydrocarbon synthesized in the presence of water after the 1st hour of reaction. For Ru/TiO_2 and Ru/ZrO_2 catalysts, the inhibition started with C_3H_8 after reaction running for approximately 25 and 15 hours respectively.

The decrease in hydrocarbon yield shown in Figure 5.9 however was not reflected in the corresponding CO conversion in Figure 5.8. This could be mainly due to the very low hydrocarbon yield compared with other products (mainly CO_2).

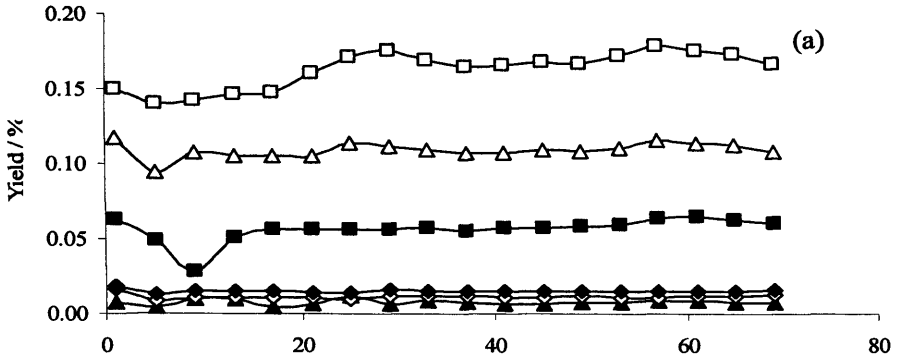
(a)
Yield / %
0.20
0.15
0.10
0.05
0.00
0
20
40
60
80

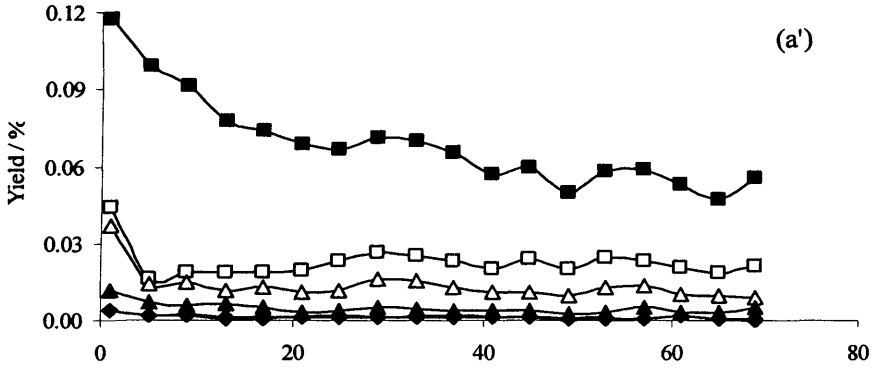
(a')
Yield / %
0.12
0.09
0.06
0.03
0.00
0
20
40
60
80

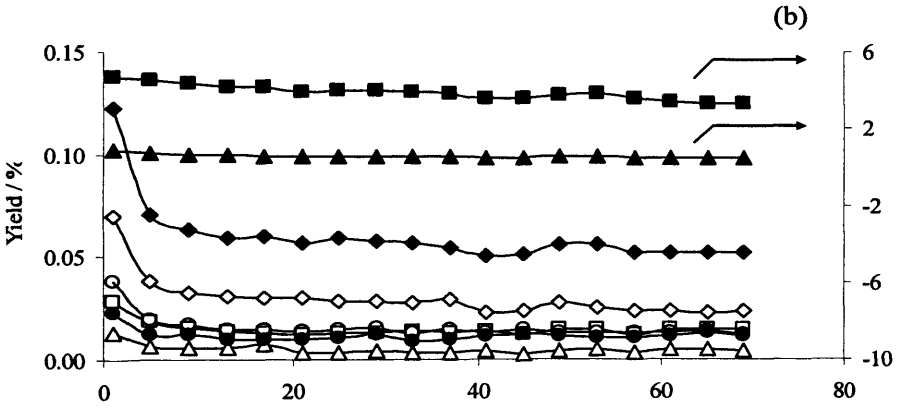
(b)
Yield / %
0.15
0.10
0.05
0.00
6
2
-2
-6
-10
0
20
40
60
80

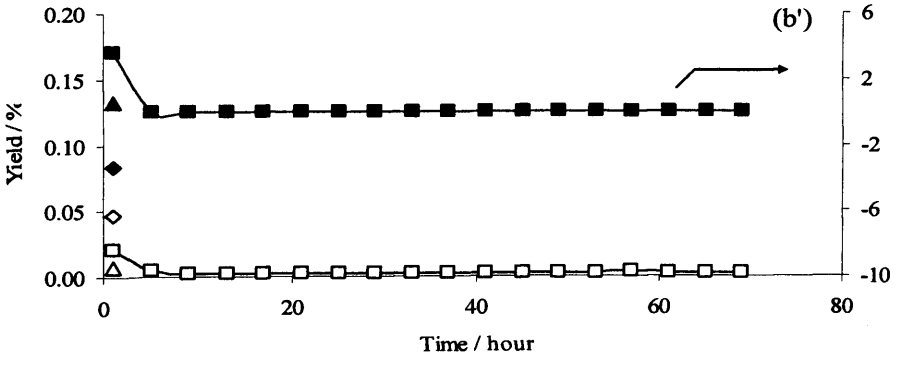
(b')
Yield / %
0.20
0.15
0.10
0.05
0.00
6
2
-2
-6
-10
0
20
40
60
80
Time / hour

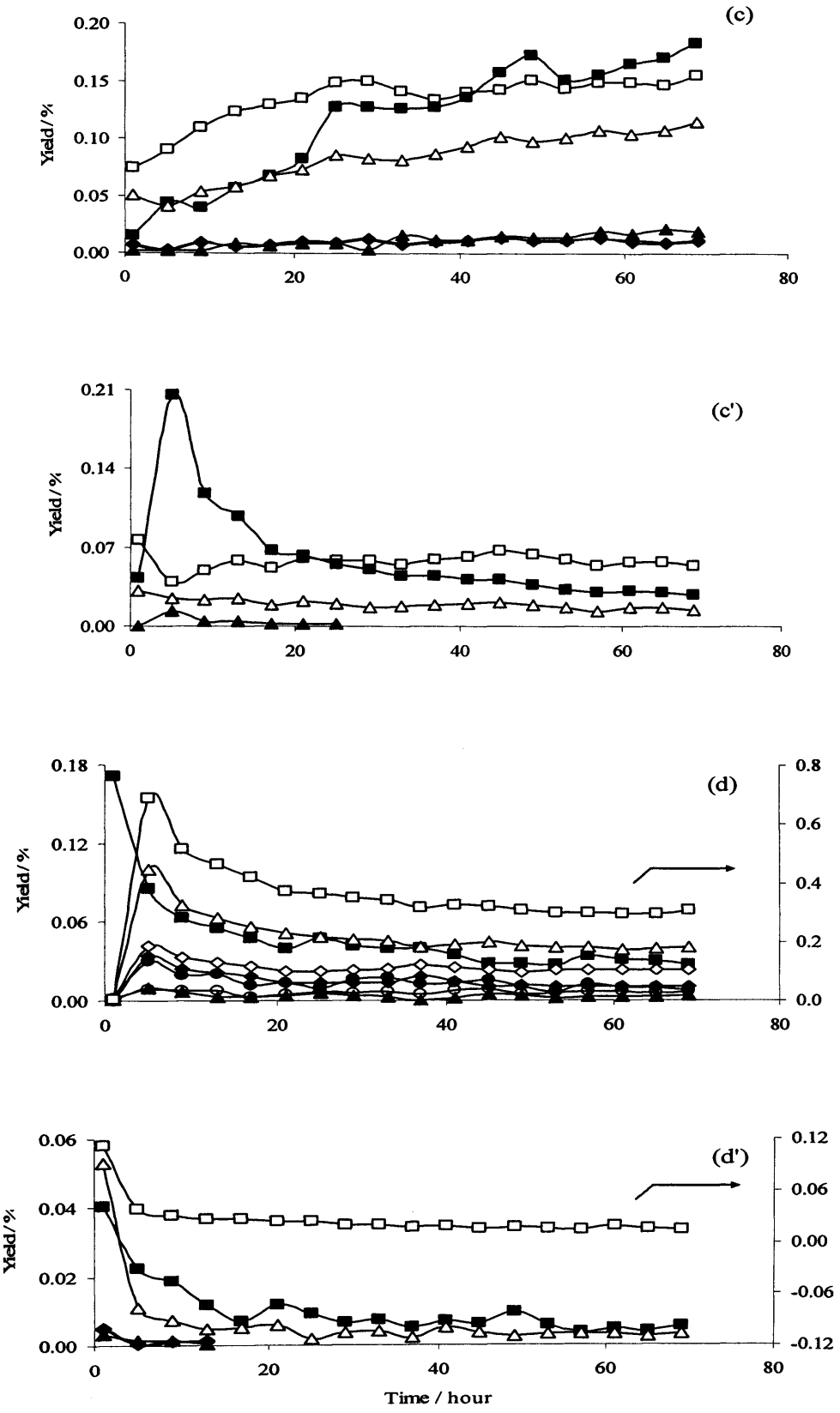

Figure 5.9 Formation of C_{2+} hydrocarbons from syngas for catalytic tests in Table 5.4 over (a) Ru/MgO (b) Ru/MoO_3 (c) Ru/TiO_2 and (d) Ru/ZrO_2 without addition of water; (a'), (b'), (c') and (d') are the corresponding ones with addition of water; □ C_2H_4; ■ C_2H_6; Δ C_3H_6; ▲C_3H_8; ◊ C_4H_8; ♦ C_4H_{10}; ○ C_5H_{10} and ● C_5H_{12}.

Alcohol synthesis

The results obtained on Runs 1 – 4 suggests that the alcohol synthesis is closely related to different support employed. For Ru/MgO, Ru/TiO_2 and Ru/ZrO_2 catalysts, there was no alcohol synthesized from syngas in the absence of water. Since alcohol synthesis favors higher pressure and lower temperature, the absence of alcohol in Run1, Run3 and Run4 could be due to the unfavorable reaction condition (high temperature and atmospheric pressure) employed. Ru/MoO_3 is the only catalyst capable of synthesizing alcohol under the used reaction conditions. This excellent catalytic activity of Ru/MoO_3 is consistent with the findings by Josefina and co-workers [17]. Josefina *et al.* investigated the CO hydrogenation over a series of ruthenium supported catalysts under a condition of 513K and circa 50 bar, and they found that the selectivity towards alcohols were higher when MoO_3 used as support than those of ZrO_2 and TiO_2. With MoO_3 being the most easily reducible oxide, which was confirmed by their TGA (Thermo-gravimetric Analysis) and XPS (X-ray Photoelectron Spectroscopy) study, the same authors suggested that the selectivity towards oxygenates seems to be linked to the reducibility of the metal oxide supports. In this study, although the TPR profile of Ru/MoO_3 did not show reduction of MoO_3 support as observed by the above authors, the highest hydrogen consumption among all the catalysts suggests that the superior catalytic activity of Ru/MoO_3 could be very likely related to its enhanced reduction behavior.

Another possibility to account for the extraordinary catalytic activity of Ru/MoO_3 could be attributed to the strong acidity of the oxide support, with MoO_3 being the most acidic one among all the supports.

It was also noticed that Ru/MoO_3 material has the smallest BET surface area as shown in Table 5.2. It is known that for catalysts with similar chemical properties,

the one with lower surface area exhibits poorer catalytic activity. In this case, the observed catalytic results over different catalysts can hardly be simply related with the BET surface area; or the BET surface area did not play a major role in the alcohol synthesis.

Therefore, the catalytic activity of Ru supported catalysts in the absence of water could be very likely related to the reduction behavior of the catalyst as well as the acid/base property of the oxide support.

The impact of water addition on alcohol synthesis can be obtained by comparing the results of Run 1 – 4 and Run 5 – 8 in Table 5.4. As can be seen from the results of Run 1 and Run 5, there was no alcohol synthesized over Ru/MgO catalyst, suggesting that water addition did not result in significant effect on alcohol synthesis. For Ru/MoO_3 catalyst, methanol and ethanol were synthesized in the absence of water, however there was no alcohol observed when water was introduced into the reaction system. Contrary to the results for Ru/MoO_3 catalyst, there was no alcohol obtained over Ru/TiO_2 and Ru/ZrO_2 in the absence of water; however in the presence of water, methanol and ethanol were synthesized over Ru/TiO_2 catalyst, whereas methanol over Ru/ZrO_2 catalyst.

The results obtained over Ru/MoO_3, Ru/TiO_2 and Ru/ZrO_2 materials are intriguing.

One possible explanation for the loss of activity in CO hydrogenation could be related to the oxidation property of water. Water, as an oxidizing agent, its presence could change the reduction behavior of the above catalysts. During the reduction/activation procedure, Ru containing catalysts essentially goes through chemical reaction as below:

$$\frac{1}{2}RuO_2 + H_2 = \frac{1}{2}Ru + H_2O \qquad (5.11)$$

Its equilibrium constants are $7.3*10^{13}$ at 400 K and $4.7*10^{8}$ at 700 K respectively [46]. Such high equilibrium constants indicate that oxidation of metallic Ru by water to its oxidation state (e.g. RuO_2) is thermodynamically unfavorable. However, the oxidation by water may be possible with the assistance of an acidic environment. If this hypothesis is true, for Ru/MoO_3 catalyst with strong acidic property, water could easily re-oxidize Ru into its oxidation state which may responsible for the loss in CO hydrogenation activity. For Ru/TiO_2 and Ru/ZrO_2 materials, the amphoteric nature of TiO_2 and ZrO_2 may only suffer limited consequence of oxidation here. The oxidation could be related to interactions between Ru and oxide supports. Catalyst Ru/TiO_2 is well known for the phenomena of strong metal support interaction (SMSI) [47], it was found that Ru/TiO_2 catalyst was highly resistant towards oxidation in a study of partial oxidation of methane [48].

Ru/TiO_2 and Ru/ZrO_2 materials showed improved activity in alcohol synthesis when water was added to the system. Independently to their possible resistance to water oxidation, thermodynamic analysis on CO hydrogenation in the presence of water may provide another explanation. The calculated standard free Gibbs energies of reaction per carbon of the produced alcohols as function of temperature are shown in Figure 5.10. By comparing with Figure 1.2 in Chapter 1, the value of ΔrG^{θ} suggests that CO hydrogenation in the presence of water is much favorable than that without water addition.

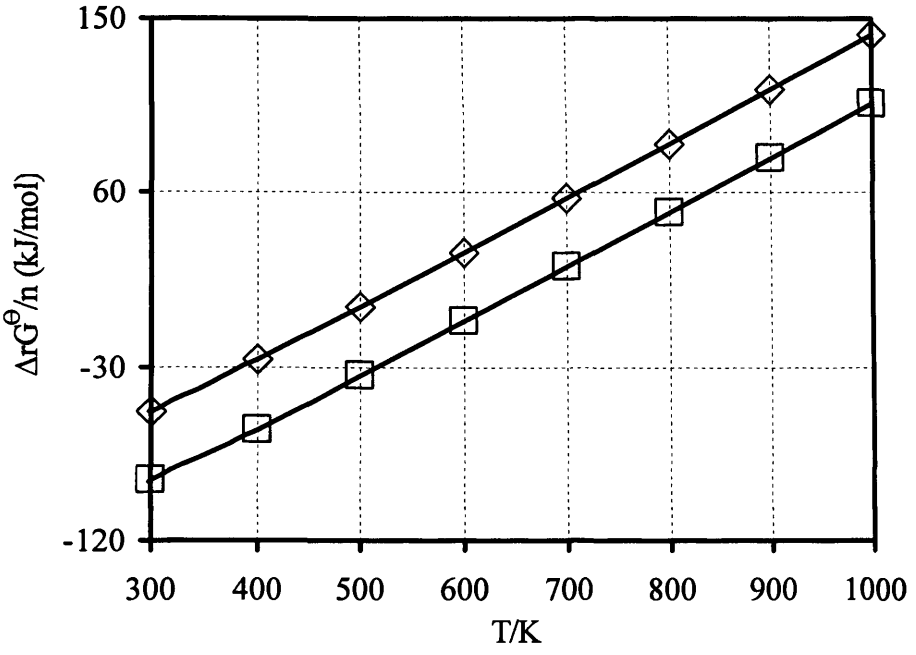

Figure 5.10 Standard free Gibbs energies of reaction per carbon of the product as function of temperature (for CO hydrogenation with consumption of water, original data used for calculation from ref. 8). ◊ Methanol; □ Ethanol.

The observed impact of water on alcohol synthesis could also be a result of different reaction pathway involved for different catalysts. Similar observations were reported in the literature on ZrO_2 and ZnO materials [49, 50]. Their studies by TPD/TPDE showed that adsorbed water is required for ZrO_2 to obtain methanol, whereas its absence is required on ZnO materials. The above authors proposed a reaction model for this observation (Figure 5.11).

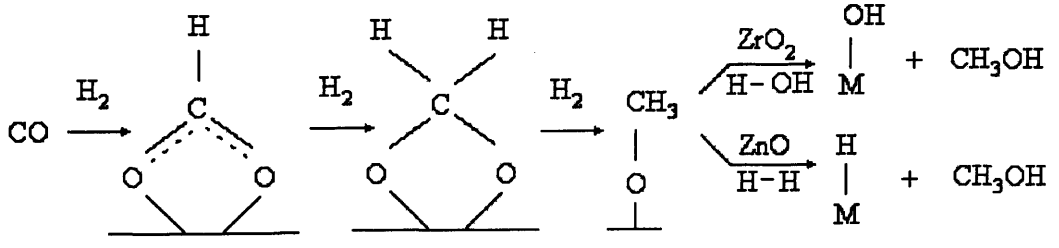

Figure 5.11 Proposed reaction path on ZrO_2 and ZnO catalysts [ref. 49].

The findings in this study strengthened this model with Ru/ZrO_2 and Ru/TiO_2 materials favoring water addition whereas Ru/MoO_3 catalyst prefers the absence of water. Unfortunately, catalytic reactions on metal oxides alone were not investigated in this study. Bearing this in mind, it is difficult to conclude that the impact of water on alcohol synthesis was mainly coming from the metal oxide alone or the Ru/single oxide. Nevertheless, in both cases the results indicate that water may take part in the alcohol synthesis.

Certainly, the above interpretations of the catalytic results are speculative, and were conducted by only considering acidity/basicity, and/or reduction behavior of the catalyst and the interaction between metal and support, other factors such as particle size, metal dispersion etc. may have different level of influence on the catalytic behavior as well. Unfortunately the characterization data of the present study are insufficient to fully understand the detailed surface science and the intrinsic reaction pathway involved. However, as an important preliminary test for the CRAFT reaction, the results obtained over Ru/TiO_2 and Ru/ZrO_2 demonstrate that alcohol could be synthesized in the presence of water at least up to a mole level of 2 to 3 (H_2O/syngas), which is a key finding for the CRAFT test.

5.8 Catalytic results over Ru/ZrO_2 catalyst

Encouraged by the results obtained over Ru/TiO_2 and Ru/ZrO_2 materials of CO hydrogenation in the presence of water, several tests were carried out. The tests were CO hydrogenation under high concentrations of methane and water, and the CRAFT reaction directly from methane and water. Ru/ZrO_2 material was chosen as a model catalyst here.

Table 5.5 CO hydrogenation and CRAFT tests[a]

Test	Feed	Reaction condition		Conversion	Gaseous product(wt%)[b]					Liquid product (wt%)[c]				
		T/K	P/Bar	(%)	H_2	CO	CO_2	CH_4	C_{2+}	methanol	ethanol	1-propanol	2-methyl-1-propanol	1-butanol
I	syngas	673	20	14.2[d]			61.6	22.1	15.2	2.6	1.8	0.35	0.47	0.23
II	syngas	633	1	3.9[d]			61.1	18.1	20.1					
III	syngas : H_2O (3:2)	633	1	8.1[d]			98.5	1.05	0.45	++++				
IV	methane : syngas : H_2O (9:1:3.3)	633	1	48.7[d]/1.8[e]	5.3		94.6		0.04	++				
V	methane : H_2O (3:1)	633	1	0.1[e]	11.9	42.9	43.1			+				

a. catalyst: Ru/ZrO_2

b. normalized weight distribution of gaseous products

c. normalized weight distribution of liquid products, if lack of accurate quantification, using '+' represents 1 unit of small amount

d. CO conversion

e. CH_4 conversion

The obtained results are listed in Table 5.5. For the sake of comparison, results on the standard CO hydrogenation and water addition test were also included. There are five tests over Ru/ZrO_2 catalyst: (I) CO hydrogenation at high temperature and pressure; (II) CO hydrogenation at low temperature and pressure; (III) CO hydrogenation with the addition of water; (IV) CO hydrogenation under high concentrations of methane and water; and (V) CRAFT reaction with methane and water.

It is known that alcohol synthesis is favored by low temperature and high pressure conditions. In order to establish potential product distribution, Test I and II are CO hydrogenations carried out at 673 K and 20 bar, and 633 K and 1 bar respectively. Data from Test I demonstrates that the selected catalyst, namely Ru/ZrO_2 is an FT catalyst capable of synthesizing alcohols. However, test performed at 633 K and 1 bar did not synthesize any liquid product. Results obtained for these two tests show a drop in CO conversion from 14.2% to 3.9%, which was accompanied by a shift of selectivity in gas phase from methane to higher hydrocarbons.

Test III and IV are two steps trying to simulate CRAFT reaction. It is expected that under the CRAFT reaction conditions there would be large amount of unconverted steam and methane in the system. For this reason, it is necessary to investigate catalyst behavior for CO hydrogenation with the addition of water and further diluted with methane.

Results of Test III show that with the addition of water, the CO conversion increased from 3.9% in Test II to 8.1% in Test III. As explained in section 5.7, this was mainly due to an enhancement in CO_2 production. Higher hydrocarbons including C_2 to C_4 alkanes and alkenes were observed. However C_3 and C_4 hydrocarbon products were obtained only in the initial 15 hours. Small amounts of methanol were

synthesized. The results suggest that when water was added to the feed, (1) water gas shift reaction occurs to a significant level at the expense of FT synthesis towards higher hydrocarbons; (2) water was involved in CO hydrogenation typically to alcohol, which may shed light on the intrinsic mechanism of FT synthesis.

Data of Test IV shows that 48.7% CO conversion and 1.8% CH_4 conversion were achieved under the specified reaction conditions. For gaseous product, higher hydrocarbons including C_2H_4, C_2H_6 and C_3H_6 were observed only for the initial 4 hours which is much shorter than the 15 hours observed in Test III. This may be due to the high concentration of methane which diluted the other components. Alternatively, it may suggest that addition of methane accelerate the chain termination process to a higher level. GC analysis of liquid phase shows that methanol was synthesized however much less than that of obtained Test III in quantity by comparing the intensity of the FID signal.

The meaning of results of Test IV is signi ficant. Firstly it answered that question on low temperature steam reforming. The obtained results demonstrated that steam reforming reaction does proceed at low temperature over selected catalyst, e.g. Ru/ZrO_2. Secondly, the results also show that the Ru/ZrO_2 catalyst is capable of catalyzing both the FT synthesis and steam reforming reactions to a certain level under the same reaction conditions. Last but more importantly, it proves that alcohols, typically methanol, can be produced from syngas which is highly diluted in methane and in the presence of water albeit in small amounts.

Test V was an extension of Test IV with the purpose of investigating CRAFT concept in alcohol synthesis. An average of 0.1% CH_4 conversion was obtained. Online GC spectra showed that H_2, CO and CO_2 were the main gaseous products. Ethane was also observed however which was proved to be the impurity in the feed.

For the liquid analysis, methanol was detected. GC spectrum of the obtained liquid products is shown in Figure 5.12. There are two peaks which were assigned to methane and methanol respectively. The observation of methane in the liquid analysis was a result of small amount of unconverted methane dissolved in the liquid product. For methanol, it can see that intensity of the signal is very low. The main reason could be that methane conversion to methanol in the CRAFT reaction is very low, which was shown in the section of thermodynamic analysis. Another reason is that the produced methanol was highly diluted in large amount of unconverted water.

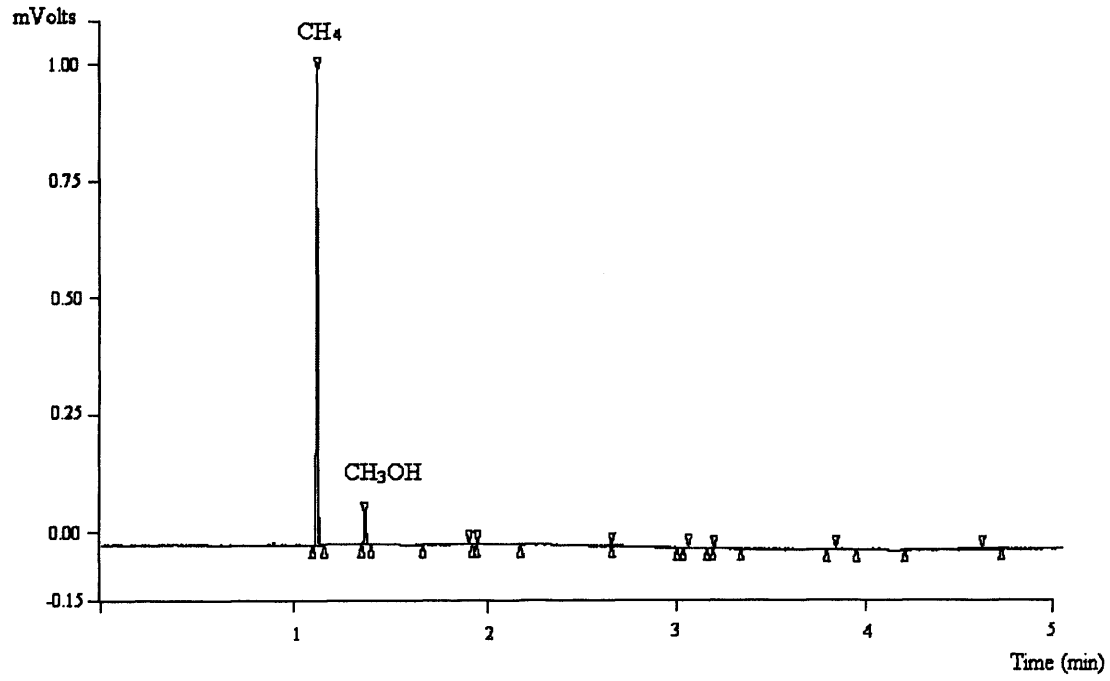

Figure 5.12 GC trace of liquid analysis of Test V (in Table 5.5)

Series of tests aimed to check the reproducibility of methanol from methane and water were performed. It was found that steam reforming over Ru/ZrO_2 in the current catalytic rig is very process sensitive. The way in which the catalysts were treated and the way that water was fed to the reaction system are two factors identified

of having a significant influence on the catalytic behavior. As a consequence, parameters responsible for the production of methanol directly from methane and water have not yet been fully identified.

Results of Test V and tests of reproducibility check show that methanol can be synthesized from methane and water however the reaction is very process sensitive. This sensitivity may indicate that the reaction might proceed through a non-stable state which unfortunately is not clear to us at this stage.

5.9 Conclusions

Thermodynamic analysis of the CRAFT reaction for alcohol synthesis – alcohol directly synthesized from methane and water – shows that the reaction has extremely small equilibrium constants and consequently very low conversion. It seems that alcohol synthesis by the CRAFT process is thermodynamically unfavorable. However, the apparent thermodynamic limitation could be overcome by appropriate kinetic control.

Design of catalyst for the CRAFT reaction was based on previous study and meanwhile taking consideration of alcohol synthesis. Materials containing Ru active metal and metal supports with different acidity and reducibility were chosen for the CRAFT reaction.

Since the CRAFT reaction essentially includes two kinds of reactions, specific requirement must be satisfied for each type of reactions, e.g. low temperature steam reforming and the FT alcohol synthesis.

In the case of low temperature steam reforming, Thermodynamic analysis of low temperature steam reforming was carried out and the obtained results suggest that circa 1-6% conversion could be achieved over 573 – 673 K. In a later catalytic

reaction performed on Ru/ZrO_2 material, it was demonstrated that low temperature steam reforming was possible under the investigated reaction conditions, giving a conversion of circa 1.8%.

For the FT synthesis, effect of catalyst support on standard FT reaction was firstly studied. MoO_3 was found to be the most active support for alcohol synthesis. Experiments aimed to study the impact of water addition on alcohol synthesis were subsequently carried out. With the addition of water, Ru/MoO_3 catalyst lost the activity for alcohol synthesis. On the contrary, positive effect was found for Ru/TiO_2 and Ru/ZrO_2 materials. The results suggest that water could take part in the alcohol synthesis.

The CRAFT and its related tests were carried out on Ru/ZrO_2 material. Very small amount of methanol was synthesized directly from methane and water. The reproducibility of the CRAFT test was not good. It was found out that the reaction was very process sensitive. Results of a close simulation of the CRAFT reaction (e.g. CO hydrogenation under high concentrations of methane and water) demonstrate that both steam reforming and the FT alcohol synthesis can be performed over the same catalyst in the same reactor although alcohol yield at this point is low.

References

[1] Choi, G.N.; Kramer, S.J.; Tam, S.T.; Fox, J.M., Design/economics of a natural gas based Fischer-Tropsch plant, in *Spring National Meeting*, American Institute of Chemical Engineers, Houston, 1996

[2] Hardman, S., Woodfin, W.T., Ruhl, R.C., EU patent 0516441A1

[3] Hensman, J.R., WO 2004/103896 A1

[4] Bowe, M.J., WO 2004/078642 A1

[5] Abbott, P., Edward, J., McKenna, M., WO 2004/096952 A1

[6] Bowe, M.J., WO 2005/090521 A1

[7] Johns, M., Collier, P., Spencer, M.S., Alderson, T., Hutchings, G.J., Catal. Lett. 90 (2003) 187

[8] Stull, D.R.; Westrum, E.F.; Sinke, G.C., The Chemical Thermodynamics of Organic Compounds (Wiley, New York, 1969).

[9] Johns, M., PhD Thesis, Cardiff University, 2002

[10] Liu, Z.; Jun, K.; Roh, H.; Park, S., Journal of Power Sources 111 (2002) 283

[11] Matsumura, Y.; Nakamori, T., Appl. Catal. A 258 (2004) 107

[12] Kusakabe, K.; Sotowa, K.; Eda, T.; Iwamoto, Y., Fuel Processing Technology 86 (2004) 319

[13] Twigg, M.V., Catalyst Handbook (2^{nd} edition); Wolfe Publishing Ltd, 1989

[14] Rostrup-Nielsen, J.R.; Sehested, J.; Nørskov, J.K., Adv. Catal. 47 (2002) 65

[15] Tanabe, K., in: Proceedings in the Ninth International Congress on Catalysis, Phillips, M.J.; Terman, M. (Eds.), Ottawa, Canada, 1988 p.85

[16] Tanabe, K., Solid Acids and Bases, Academic Press, New York, 1970 p. 47

[17] Josefina, P.M.; Muriel, D.; Yann, H.; Anne, G.; Lucien, L.; Ginette, L.; Mireya, G.; Luisa, C.M.; Geoffery, B., Appl. Catal. A 274 (2004) 295

[18] Utaka, T.; Okanishi, T.; Takeguchi, T.; Kikuchi, R.; Eguchi, K., Appl. Catal. A 245 (2003) 343

[19] Bossi, A.; Garbassi, F.; Petrini, G., J.Chem. Soc., Faraday Trans. 1., 78 (1982) 1029

[20] Hegarty, M.E.S.; O'Connor, A.M.; Ross, J.R.H., Catal. Today 42 (1998) 225

[21] Qin, D.; Lapszewicz, J.; Jiang X., J. Catal. 159 (1996) 140

[22] Krishnamoorthy, S.; Tu, M.; Ojeda, M.P.; Pinna, D.; Iglesia, E., J. Catal. 211 (2002) 422

[23] Anderson, R.B. In Catalysis; Emmet, P.H., Ed.; Reinhold Publishing Corp. New York, 1956; Vol.4, pp247-283

[24] Dry, M.E. Appl. Catal., A 138 (1996) 319

[25] Hilmen, A.M., Schanke, D., Hanssen, K.F., Holmen, A., Appl. Catal. A 186 (1999) 169

[26] Li, J.; Zhan, X.; Zhang, Y.; Jacobs, G., Das, T., Davis, B.H., Appl. Catal. A 228 (2002) 203

[27] Li, J.; Jacobs, G., Das, T., Davis, B.H., Appl. Catal. A 233 (2002) 255

[28] Li, J.; Jacobs, G., Das, T., Zhang, Y.; Davis, B.H., Appl. Catal. A 236 (2002) 67

[29] Claeys, M.; van Steen, E., Catal. Today 71 (2002) 419

[30] Kim, C.J., US Patent 5227407 (1993)

[31] Klier, K.; Herman, R.G.; Beretta, A.; Burcham, M.A.; Sun, Q.; Cai, Y.; Roy, B., Oxygenates *via* synthesis gas, final technical report, 1/1/1995-09/30/1996

[32] Vedage, G.A.; Pitchai, R.; Herman, R.G.; Klier, K., Proc.8th Intern.Congr.Catal. 1984a, II, 47

[33] Vedage, G.A.; Pitchai, R.; Herman, R.G.; Klier, K., Preprint, Div.Fuel.Chem., ACS 29 (1984b) 196

[34] Juan, A.; Damiani, D.E., J. Catal. 137 (1992) 77

[35] Coq, B.; Kumbhar, P.S.; Moreau, C.; Moreau, P.; Figueras, F., J.Phys. Chem. 98 (1994) 10180

[36] Betancourt, P.; Rives, A.; Hubaut, R.; Scott, C.E.; Goldwasser, J., Appl. Catal. A 170 (1998) 307

[37] Li, D.; Ichikuni, N.; Shimazu, S.; Uematsu, T., Appl. Catal. A 180 (1999) 227

[38] Perkas, N.; Zhong, Z.; Chen, L.; Besson, M.; Gedanken, A., Catal. Lett. 103 (2005) 9

[39] Matsuda, T.; Uozumi, S.; Takahashi, N., Phys. Chem. Chem. Phys. 6 (2004) 665

[40] Panagiotopoulou, P; Kondarides, D.I., J. Catal. 225 (2004) 327

[41] Panagiotopoulou, P; Kondarides, D.I., Catal. Today 112 (2006) 49

[42] Basińska, A.; Kępiński, L.; Domka, F., Appl. Catal. A 183 (1999) 143

[43] Gupta, N.M.; Londhe, V.P.; Kamble, V.S., J. Catal. 169 (1997) 423

[44] Asakura, K.; Iwasawa, Y., J. Chem. Soc., Faraday Trans. 86 (1990) 2657

[45] Ishihara, T.; Harada, K.; Eguchi, K.; Arai, H., J. Catal. 136 (1992) 161

[46] Anderson, R.B., The Fischer Tropsch Synthesis, Academic Press, Inc., 1984

[47] Diebold, U., Surface Science Reports 48 (2003) 53

[48] Elmasides, C.; Verykios, X.E., J. Catal., 203 (2001) 477

[49] He, M.-Y.; White, J.M., J. Mol. Catal., 30 (1985) 415

[50] He, M.-Y.; Ekerdt, J.G., J. Catal., 90 (1984) 17

Chapter 6 Conclusions

6.1 Introduction

The experimental work in this thesis was aimed at investigating the synthesis of alcohols from carbon monoxide and hydrogen *via* a modified Fischer Tropsch (FT) reaction. The investigation was divided into three different categories. The first category is the CO hydrogenation over two well-known catalyst systems, namely Co-MoS_2/K_2CO_3 based catalyst and the Cu-Co mixed oxides catalyst for the alcohol synthesis. The second category is concerning the alcohol synthesis by CO hydrogenation over gold supported catalyst which was discovered active in the FT reaction only recently. The last category was aimed to check the feasibility of combining steam reforming reaction and the FT reaction (CRAFT) together for alcohol synthesis.

Chapter 3, 4 and 5 detailed the results related to the different categories explained above. The present chapter shows the conclusions that can be extracted by examination of such results.

6.2 Conclusions on Co-MoS_2 based catalyst and the Cu-Co mixed oxides catalyst

6.2.1 Co-MoS_2 based catalyst

The study on CO hydrogenation over Co-MoS_2 based catalyst provided information about the catalyst and the effect of reaction parameters on the higher alcohol (HA) synthesis. The main findings related with this catalyst are summarized below.

It was found that Co-MoS_2 based catalyst became deactivated on aerial oxidation which could be facilitated by the presence of K_2CO_3, clay and lubricant. The finding suggests that the sulfide level of the investigated catalyst is essential for the CO hydrogenation to hydrocarbons and alcohols.

A rapid temperature ramping rate during the catalyst calcinations gave increased CO activity and increased alcohol yields. This increase could be attributed to the increased surface area obtained with higher ramping rate.

A series of catalytic tests was aimed to find an optimal reaction condition by studying the effect of K_2CO_3 concentration, GHSV, temperature and feed composition. The studies on potassium content show that the catalyst with higher K_2CO_3 concentration (12.5%) gave decreased CO conversion and hydrocarbon yields, however increased alcohol yields were obtained at the same time. The results suggest that the role of potassium is probably to slow down the hydrogenation of CO to hydrocarbons by blocking the active site for formation of higher hydrocarbons, simultaneously creating active site for the synthesis of alcohols. Concerning the effect of GHSV, the obtained results show that higher GHSV gave decreased hydrocarbon and C_{2+} alcohol selectivities whereas increased methanol selectivity was observed. The experimental data on reaction temperature shows that an increase in reaction

temperature resulted in decreased selectivities for methanol and ethanol. At the same time, increased C_3 and C_4 alcohols selectivities was observed. The results on temperature effect indicate that an optimum reaction temperature range may exist for each specific fuel alcohol. The effect of feed composition (with different syngas ratios) on the alcohol synthesis was also investigated. The experimental data shows that higher syngas ratio (H_2/CO = 2) gave increased activity and C_1 – C_3 alcohol yields. This is considered to be due to the higher hydrogen partial pressure which could eliminate coke formation by side reactions, such as boudouard reaction or methane decomposition. The highest HA yield (13%) was achieved at an operating condition of 580 K, 75 bar, GHSV = 1225 h^{-1} and H_2/CO = 2. This result could be further improved by more intensive tests.

For Co-MoS_2 based catalyst, it was found that the product distribution follows the Anderson-Schulz-Flory (ASF) distribution with methanol having slight deviation. A possible explanation for the deviation could be the loss of methanol into gas phase. Another possible explanation could be that different active sites may exist for methanol and higher alcohol synthesis.

6.2.2 Cu-Co mixed oxides catalyst

The effect of temperature, pressure and water addition was investigated over Cu-Co mixed oxides catalyst.

The investigation on temperature effect shows that the increase in temperature led to an increase in methane selectivity and a loss in olefinicity for hydrocarbon products. For alcohol products, it was found that the formation C_1 and C_2 alcohol prefers the lower temperature range, whereas the formation of C_3 and C_4 alcohols

were favored by higher temperatures. This is considered to be due to different route followed by the formation of C_{1-2} and C_{3+} alcohols.

The experimental data detailed on the effect of pressure on the CO hydrogenation over Cu-Co mixed oxides catalyst shows that higher carbon oxide activity, alcohol selectivity and alcohol yield were obtained with higher system pressure.

For the Cu-Co mixed oxides catalyst, the CO hydrogenation in the presence of water resulted in improved catalyst activity and in particular enhanced ethanol selectivity and yield. This enhancement suggests that water may take part in the alcohol synthesis.

6.3 Conclusions on gold containing catalysts

Two support materials, ZnO and Fe_2O_3 were used in the investigation of the function of gold in the CO hydrogenation for alcohol synthesis.

The experimental data obtained on ZnO and Au/ZnO catalysts shows that the addition of gold resulted in decreased CO activity and hydrocarbon selectivity. However, the alcohol selectivity and yield were found increased with the introduction of gold. The alcohol distribution was found to shift towards higher alcohol side when ZnO was used as support. It was concluded that when ZnO was used as support, gold play a role in tuning the alcohol synthesis by shifting the product selectivity towards higher alcohols. When Fe_2O_3 was used as support, the addition of gold led to decreased CO activity and hydrocarbon selectivity, which is similar to the results on ZnO used as support. However, for alcohol synthesis, the addition of gold led to increased methanol selectivity and decreased selectivity towards higher alcohols. It is thus concluded that the function of gold is closely related with the support employed.

Future work using other different supports, e.g. ZrO_2, SiO_2 and TiO_2, are needed to understand the interaction between gold and support materials. Gold also could be doped to Co-MoS_2 and Cu-Co mixed oxides catalysts to further investigate the tuning function of gold.

6.4 Conclusions on the CRAFT process

A thermodynamic analysis of the CRAFT process to synthesize alcohols shows that the combined reaction has very low equilibrium constant and consequently low conversion. This thermodynamic limitation could be overcome by appropriate kinetic control [1].

Two primary reactions involved in the CRAFT process, namely low temperature steam reforming and the FT alcohol synthesis were analyzed over Ru supported catalysts respectively. It was demonstrated that low temperature steam reforming was possible under the investigated reaction conditions, giving a conversion of circa 1.8%. For the FT synthesis, effect of catalyst support (MgO, MoO_3, TiO_2 and ZrO_2) and the impact of water addition on alcohol synthesis were carried out. Solid MoO_3 was found to be the most active support for alcohol synthesis under the studied reaction condition (633 K, 1atm, GHSV=3000 h^{-1}) without water addition. In the case of other materials used as supports, no alcohol was obtained under the above mentioned experimental condition. The extraordinary catalytic activity of Ru/MoO_3 could be linked to its enhanced reduction behavior and the strong acidity of the oxide support. Upon addition of water, it was found that Ru/MoO_3 material lost the activity of CO hydrogenation very fast. However, positive effect was observed for Ru/TiO_2 and Ru/ZrO_2 materials with the addition of water. The results suggest that water could take part in the alcohol synthesis.

The CRAFT test over Ru/ZrO_2 gave very small amount of methanol however the reaction suffer reproducibility problem. It was found out that the reaction was very process sensitive. Results of a close simulation of the CRAFT reaction (e.g. CO hydrogenation under high concentrations of methane and water) demonstrate that both steam reforming and the FT alcohol synthesis can be performed over the same catalyst in the same reactor.

References

[1] Johns, M., Collier, P., Spencer, M.S., Alderson, T., Hutchings, G.J., Catal. Lett. 90 (2003) 187

Appendix Calculations for Catalytic Reaction

This section describes the way of calculations for catalytic reactions obtained in Chapter 3, 4 and 5.

(1) Calculation of CO conversion, CO (CO_2 free) conversion, Selectivity and Yield:

$$\text{CO conversion (\%)} = \frac{CO(moles)_{converted}}{CO(moles)_{in}} * 100$$

$$\text{CO (CO_2 free) conversion (\%)} = \frac{CO(moles)_{converted} - CO_2(moles)_{produced}}{CO(moles)_{in}} * 100$$

$$\text{Carbon mole selectivity (\%)} = \frac{Carbon(moles)_{product(i)}}{CO(moles)_{converted}} * 100$$

$$\text{Yield (\%)} = \frac{Carbon(moles)_{product(i)}}{CO(moles)_{in}} * 100$$

(2) Carbon balance calculation

This is a sample calculation for carbon balance analysis.

Reaction condition data:

Room temperature	295 K
Reaction temperature	580 K
Reaction pressure	75 Bar
Volume of catalyst	4.8 ml
Feed (H_2/CO/N_2)	47.5/47.5/5
Flow rate of syngas	100 ml/min
Reaction time	60 hours

Calculation of carbon balance:

$$\text{At room temperature: 1 mole} = \frac{22.4 * 295}{273} = 24.2 \text{ (liter)}$$

Feed in molar rate = (100 ml/min) * (1 liter/1000ml) *(1 mole/24.2 liter) * (60 min/hour)

= 0.25 mole/hour

CO molar rate = (0.25 mole/hour)*0.475= 0.12 mole/hour

Carbon mole (in) = CO mole in (total) = 0.12 mole/hour * 60 hour

= 7.0 mole

For gas phase product, the concentration (v%) of component i at time j (j = 1-60) can be obtained from GC analysis. The flow rate at time j (j = 1-60) of effluent out gas can be calculated using internal standard (N_2). With these two parameters known, the molar rate of component i at time j can be obtained. For example, at time 17 hour, the concentration of CO is 45.1% and the calculated flow rate (out) is 89.3 ml/min, the molar rate of CO at time 17 hour can be obtained as below.

Molar rate of component CO = 45.1% * (89.3 ml/min)*(60 min/hour)

*(1liter/1000ml) *(1 mole/24.2liter)

= 0.10 mole/hour

The molar rate of other components at 17 hours can be calculated in a similar way. The volume percentage of each components and the obtained molar rate at 17 hours is listed in Table A1.

Table A1 Gas phase data based on GC at time 17 hour time on stream

Component	Vol %	Mole / hour
CO	45.1	0.10
CO_2	3.02	0.01
CH_4	0.497	1.1e-03
C_2H_4	0.014	3.08e-05
C_2H_6	0.067	1.47e-04
C_3H_6	0.027	5.96e-05
C_3H_8	0.025	5.48e-05
C_4H_8	0.003	6.66e-06
C_4H_{10}	0.016	3.49e-05

For liquid phase product, composition of the liquid can be obtained from GC. With the total weight known (for example weight of total liquid collected = 21.06 g), the moles of each component can be calculated. The weight percentage and the calculated moles are listed in Table A2.

Table A2 Liquid phase weight percentage and calculated moles

Alcohol	wt %	wt	mole
Methanol	48.2	10.1	0.32
Ethanol	35.6	7.51	0.16
1-Propanol	7.31	1.54	0.03
1-Butanol	1.19	0.25	0.003

With the moles of gas product and liquid product known, the total moles of carbon out of system can be calculated.

$$\text{Carbon mole (out)} = \sum_{j=1}^{60} CO(mole)_{out} + \sum_{j=1}^{60} CO_2(mole) +$$

$$\sum_{j=1}^{60} CH_4(mole) + 2^* \sum_{j=1}^{60} C_2H_4(mole) +$$

$$2^* \sum_{j=1}^{60} C_2H_6(mole) + 3^* \sum_{j=1}^{60} C_3H_6(mole) +$$

$$3^* \sum_{j=1}^{60} C_3H_8(mole) + \ldots + CH_3OH\ (\text{mole}) +$$

$$2^*\ C_2H_5OH\ (\text{mole}) + 3^*\ C_3H_7OH\ (\text{mole}) + \ldots$$

$$= 6.9 \text{ mole}$$

$$\text{Error percentage} = \frac{Carbon(in) - Carbon(out)}{Carbon(in)} * 100\%$$

$$= \frac{7.0 - 6.9}{7.0} * 100\% = 1.4\%$$